

The Pennsylvania State University

The Graduate School

College of Engineering

**CONTACT ACTIVATION OF HUMAN PLASMA
COAGULATION**

A Thesis in

Bioengineering

by

Rui Zhuo

Submitted in Partial Fulfillment
of the Requirements
for the Degree of

Doctor of Philosophy

December 2006

The thesis of Rui Zhuo was reviewed and approved* by the following:

Erwin A. Vogler
Associate Professor of Material Science and Engineering
Thesis Advisor
Chair of Committee

William O. Hancock
Assistant Professor of Bioengineering

Christopher A. Siedlecki
Associate Professor of Surgery and Bioengineering

James P. Runt
Professor of Polymer Sciences

Herbert H. Lipowsky
Professor and Chairman of Bioengineering

*Signatures are on file in the Graduate School

ABSTRACT

Development of fully hemocompatible materials remains a substantially unrealized objective of applied biomaterials. Unfavorable cell-and-protein interactions with biomaterial surfaces that lead to thrombus formation are major obstacles that modern surface engineering seeks to overcome. Future advances in the surface-engineering of blood-contacting biomaterials are critically dependent on a detailed understanding of how blood interacts with artificial materials at a molecular level. Research summarized in this thesis is aimed at such a molecular understanding and seeks to establish structure-property relationships linking material characteristics such as surface chemistry/energy with the propensity to activate blood coagulation.

Blood-plasma coagulation occurs through a series of linked zymogen-enzyme conversions collectively known as the plasma coagulation cascade. The so-called intrinsic pathway of this cascade becomes activated when plasma contacts artificial material surfaces. As a consequence, all known cardiovascular biomaterials activate blood coagulation to a measurable extent. Previous research (corroborated by this thesis work) demonstrated that the propensity to activate plasma coagulation scales as an exponential-like function of surface energy, with low catalytic potential observed for hydrophobic (poorly water wettable, low surface energy) materials and much higher activation for hydrophilic (fully water wettable, high surface energy) materials. This thesis work further shows that the relationship between surface energy and contact activation holds only in the presence of plasma proteins, providing an important insight into the biochemical mechanism of plasma coagulation.

Blood factor XII (FXII, Hageman factor) is central to contact activation. The intrinsic pathway of coagulation is potentiated by conversion of the zymogen FXII into the enzyme form, FXIIa, through a surface-mediated reaction termed autoactivation. It is shown herein that autoactivation occurs with equal efficiency at hydrophilic and hydrophobic surfaces in neat-buffer solution but that autoactivation rate and yield is substantially attenuated at hydrophobic surfaces in the presence of plasma proteins. Thus it is concluded that FXII activation in the presence of plasma proteins leads to *an apparent specificity* for hydrophilic surfaces that is actually due to a relative diminution of the FXII→FXIIa reaction at hydrophobic surfaces. It is further concluded that contact activation of blood FXII in neat-buffer solution is not specific for anionic hydrophilic procoagulants as proposed by the accepted biochemistry of surface activation. These findings may lead to a new paradigm for the interpretation of hemocompatibility that can guide development of advanced hemocompatible biomaterials.

TABLE OF CONTENTS

LIST OF FIGURES	vii
LIST OF TABLES	ix
ACKNOWLEDGEMENTS	x
 Chapter 1 Introduction	 1
1.1 Biomaterials and Biocompatibility	1
1.2 Blood-Contact Biomaterials	3
1.3 Blood and Blood Coagulation Cascade	3
1.4 Contact Activation Complex	8
1.5 References	15
 Chapter 2 Materials and Methods	 1
2.1 Materials	22
2.1.1 General Reagents	22
2.1.2 Human Platelet Poor Plasma	23
2.1.3 Human Platelet Poor FXII Deficient Plasma and FXI Deficient Plasma	24
2.1.4 Plasma Proteins	25
2.1.5 Procoagulants	25
2.1.5.1 Clean and Silanized Glass Beads	25
2.1.5.2 SiO _x C _y	26
2.1.5.3 Pyrolytic carbon	30
2.2 Methods	31
2.2.1 Coagulation-Time Assays	31
2.2.2 Multiple Activation of Plasma Coagulation	32
2.2.3 Mathematical Methods of Thrombin Titration	33
2.2.4 Pyrolytic Carbon	35
2.2.5 Surface Activation of Activation of FXII in Neat-Buffer Solution and Plasma	36
2.2.6 FXI Hydrolysis by Surface Activated FXII	40
2.2.7 Chromogenic Assay	41
2.3 References	42
 Chapter 3 Procoagulant Stimulus Processing by the Intrinsic Pathway of Blood Plasma Coagulation	 44
3.1 Introduction	45

3.2 Thrombin Titration of Human Plasma.....	48
3.3 Surface Area Titration (SAT) of Human Plasma	51
3.4 Retention of Procoagulant Catalytic Potential.....	58
3.5 Discussion.....	60
3.6 Summary.....	64
3.7 References.....	66
 Chapter 4 Silicon Oxycarbide Glasses for Blood-Contact Applications	 71
4.1 Introduction.....	71
4.2 SiO _x C _y Glasses.....	75
4.3 Plasma Activation.....	77
4.4 Discussion.....	81
4.5 Summary.....	82
4.6 References.....	83
 Chapter 5 Contact Activation of Blood Factor XII.....	 86
5.1 Introduction.....	87
5.2 Surface Activation of FXII in Neat-Buffer Solution and Plasma.....	89
5.3 FXI Hydrolysis by Surface Activated FXII.....	92
5.4 Steady-State Surface Activation of FXII in Neat-Buffer Solution and a Protein Mixture.....	95
5.5 FXII Activation Rate in Plasma.....	97
5.6 Discussion.....	101
5.7 Summary.....	105
5.8 References.....	107
 Chapter 6 Practical Application of a Chromogenic FXIIa Assay	 111
6.1 Introduction.....	112
6.2 FXIIa Titration of Human Plasma	113
6.3 Chromogenic Assay for FXIIa in Buffer Solution	115
6.4 Correlation Between Plasma Coagulation and Chromogenic Rate Assay	120
6.5 Discussion.....	123
6.6 Summary.....	125
6.7 References.....	126
 Chapter 7 Conclusions and Future Work.....	 129
7.1 Silicon Oxycarbide Glasses for Blood-Contact Applications	130
7.2 Thrombin production in plasma by surface contact	131
7.3 Contact Activation of Blood Factor XII	132
7.4 Future Work.....	133
7.5 References.....	135

LIST OF FIGURES

Fig. 1.1 : Sketch of the plasma coagulation cascade emphasizing serial linkage of intrinsic and extrinsic pathways.....	7
Fig. 1.2 : Schematic representation of surface-dependent assembly of molecules responsible for contact activation.	9
Fig. 1.3 : Activation of FXII to 1. α -FXIIa and 2. β -FXIIa.	11
Fig. 1.4 : Propensity to contact activate the intrinsic pathway of blood plasma coagulation as a function of procoagulant surface energy.....	13
Fig. 2.1 : Schematic experimental outline for detection of FXIIa produced by contact with procoagulant surfaces.....	37
Fig. 2.2 : Schematic experimental outline for detection of FXIa produced by hydrolysis of FXI by products of FXII activation.	39
Fig. 3.1 : (A) Thrombin titrations (TT) plotted on a $\log_{10}[T^o]$ axis.....	50
(B) TT on $1/[T^o]$ coordinates consistent with Eq 2.2 of Method and Materials.....	50
Fig. 3.2 : Surface area titration with glass beads bearing different surface chemistries plotting observed coagulation time CT as a function of procoagulant surface area per mL test solution.	52
Fig. 3.3 : Representative thrombin titration curves in the presence of varying surface area of fully-water-wettable glass procoagulants.....	55
Fig. 3.4 : Bolus thrombin concentration Θ produced by varying surface area of glass-sphere procoagulants with different surface chemistries.	56
Fig. 3.5 : Procoagulant catalytic potential derived from SAT and COT coagulation assays scaled as a function of procoagulant surface energy expressed as water adhesion tension.....	57
Fig. 3.6 : Coagulation time (CT , min) of plasma in a single clean glass tube used in multiple coagulation assays.	60
Fig. 4.1 X-ray diffraction pattern of the SiOxCy glasses prepared by pyrolysis of polysilsequioxanes.....	76
Fig. 4.2 : Coagulation of human blood plasma coagulation induced by contact with variable surface area of SiOxCy glass powders compared to hydrophilic	

(water-wettable) SiOx glass, hydrophobic silanized SiOx glass, and pyrolytic carbon).....	79
Fig. 4.3: K_{act}^{SAT} versus (surface) oxygen content for the various SiOxCy and reference samples.....	80
Fig. 5.1: Schematic experimental outline for detection of FXIIa produced by contact with procoagulant surfaces.....	91
Fig. 5.2: FXIa produced by hydrolysis of FXI by products of FXII activation (30 min. incubation).....	93
Fig. 5.3: Rate of FXIa hydrolysis by products of FXII activation.....	94
Fig. 5.4: FXII autoactivation in neat buffer solution optionally containing 8 mg/mL of 5 proteins unrelated to the plasma coagulation cascade.	97
Fig. 5.5: FXII activation kinetics by hydrophilic (Panel A) and hydrophobic (Panel B) procoagulants (150 mm ² nominal surface area) in plasma supplemented with exogenous spikes of FXII.....	99
Fig. 5.6: Rate and net production of FXIIa as a function of [FXII] expressed in multiples of physiologic concentration.....	100
Fig. 6.1: FXIIa titration of normal platelet-poor plasma (PPP, squares) and FXII-depleted plasma (12dPPP, triangles).	114
Fig. 6.2: Slope of the FXIIa titration curve for FXII-depleted plasma.	115
Fig. 6.3: Color development kinetics for a chromogenic FXIIa assay performed in neat-buffer solutions of FXII.....	117
Fig. 6.4: Color-development rate systematically increases to a maximum rate V_{max} at swamping [FXII] > 10 µg/mL.	118
Fig. 6.5: Linear correlation between V_{max} and [FXIIa].....	119
Fig. 6.6: Linear correlation between plasma-coagulation-time and chromogenic-rate assays for FXIIa.....	121
Fig. 6.7: Plot of residuals about the fitted correlation line of Fig. 6.6.....	122

LIST OF TABLES

Table 1.1: Plasma Coagulation Factors	5
Table 2.1: Polysilsequioxane Prepolymers Used in Preparation of SiOxCy Glasses	28
Table 2.2: SiOxCy Glass Surface Composition Compared to SiOx Controls.....	30
Table 4.1: Procoagulant Activity of SiOx and SiOxCy Glasses.....	74
Table 5.1: Contact Activation of FXII by 30 min. Incubation with Hydrophilic and Hydrophobic Procoagulants.....	90
Table 5.2: Maximum steady-state FXIIa yield and Initial Rate of FXII production ...	96

ACKNOWLEDGEMENTS

With a deep sense of gratitude, I would like to thank my advisor Professor Erwin A. Vogler, for his continuous support during my Ph. D. study. He was always there to listen and to give advice. He is not only a great scientist with deep vision but also and most importantly a kind person. He taught me the way to solve a research problem and also showed me the need to be persistent to accomplish any goal. His wide knowledge and logical way of thinking have always been of great value for me. Without his encouragement and constant guidance, I could not have finished this dissertation.

My special thanks go to Dr. Christopher A. Siedlecki, for the help extended to me when I approached him and the valuable suggestions that he gave me during the whole course of research.

I am deeply grateful to my other committee members, Dr. William Hancock, who always asked me good questions, and Dr. James P. Runt, who gave insightful comments on my work.

I feel a deep sense of gratitude for Dr. Herbert H. Lipowsky who monitored my work and took effort in reading and providing me with valuable comments.

The episode of acknowledgement would not be completed without the mention of all my labmates for the help and friendship they gave me: Xiaomei Liu, Anu Krishnan, Paul Cha , Ravi Dhurjati , Florily Ariola , Naris Barnthip and Hyeran Noh.

Last but not least, I need to thank my family: my parents, Kechun Zhuo and Qin Wang, for educating me and unconditional support and encouragement. My husband,

Heng Yan, for the moral support he provided throughout my research work and the delicious meal he cooked for me during my dissertation writing.

Chapter 1

Introduction

1.1 Biomaterials and Biocompatibility

Biomaterials are “non viable materials used in medical devices intended to interact with biological systems” [1]. Biomaterials can be either synthetic or natural materials. Metals, ceramics, polymers, and composites thereof are used in high volumes in a wide variety of medical devices spanning sterile disposables to implanted materials.

Biomaterial applications can be traced back to antiquity. For example, gold strands were used as tissue sutures for hernia repairs as early as 1000 BC. Silver, gold and gemstones have been in widespread use in dental applications for centuries. The earliest written record of an application of metal in a surgical procedure dates from the year of 1565, but implants were not generally successful until the advent of aseptic surgical technique in the 1860’s [2].

By the mid-nineteenth century, biomaterials had become an important aspect of human healthcare, enabling a wide array of medical devices. In the 1900’s, synthetic plastics came into widespread medical use, supplementing a variety of metallic alloys and ceramics. The first metal prosthesis fabricated from Vitallium alloy was produced in

1938 and 1939 by Bives Willes and Bursch [2]. This prosthesis was used until 1960 when it was realized that corrosion products were detrimental to implant efficacy. In the early 1970's, ceramics such as alumina and zirconia were found to have excellent biocompatibility, especially as orthopedic implants. Biologically active or bioactive materials such as bioglass and hydroxyapatite developed by Hench (1971) [3] and Jarcho (~1970s) [4] greatly improved integration of these ceramics with bone tissue.

Clearly, over the past 30 years, significant scientific and technological advances have occurred in the field of biomaterials as a direct result of a collaboration among medical doctors, scientists, and engineers. Biomaterials enjoy a very significant socioeconomic impact. It has been estimated that approximately 20 million individuals have some sort of implanted medical device. Costs associated with prostheses and organ replacement therapies exceed \$300 billion U.S. dollars per year and comprise nearly 8% of total health-care spending worldwide [2].

Success in biomaterial end use depends on the compatibility of the material with the host. This so-called 'biocompatibility' is "the ability of a material to perform with an appropriate host response in a specific application" [1]. From this definition it is clear that biocompatibility is a measure of success in end use that has a different meaning for different applications. Therefore, biocompatibility is not an absolute material property and no single material is biocompatible in all medical application. This thesis focuses on material compatibility with blood, frequently termed "hemocompatibility".

1.2 Blood-Contacting Biomaterials

A complex network of biochemical and cellular interactions has evolved to maintain the integrity of the vascular system. This hemostatic system is designed to stop bleeding from localized injuries by blood clotting, on the one hand, yet not extend beyond the general region of the injury in a manner that would compromise blood flow elsewhere. This same clotting produces adverse responses when blood comes into contact with artificial surfaces. Indeed, formation of blood clots, or thrombus, on artificial materials is the most significant barrier to the development of blood-contacting biomaterials.

Thrombosis is a pathologic process in which platelets aggregate and/or a fibrin clot forms on the surface of blood-contacting biomaterials [7]. A fundamental biomaterials surface science goal is to develop non-thrombogenic materials for use in a broad range of cardiovascular devices. Despite more than 30 years of focused research, this goal has not been achieved [8]. Hence, the cellular and molecular basis of thrombosis remains an important area of investigation [9-11].

1.3 Blood and Blood Coagulation Cascade

The average human being contains five liters of blood of which 55% (by volume) is the fluid phase known as plasma and 45% is the “formed elements” (cells). Plasma is a pale yellow, viscous fluid comprised of 90% water, 8% plasma proteins, 1.1% organic substances and 0.9% inorganic ions. Three types of proteins dominate the plasma

proteome: serum albumin (60%), serum globulin (36%), and fibrinogen. Most of these proteins are produced by the liver, except serum globulin. Globulins can be further divided into three main groups: alpha-, beta- and gamma globulin. Gamma globulins are antibodies produced by the body immune system to fight infection. Fibrinogen, an important protein in blood coagulation, and approximately 490 proteins identified to date complete the plasma proteome.

In a healthy individual, blood circulates in the body as liquid. When there is a vascular injury, however, blood is required to form a clot rapidly in order to prevent hemorrhage. When endothelium is damaged, platelets adhere to the subendothelium and activation of the blood coagulation cascade produces fibrin, which forms a mesh over the platelet plug, sealing the injury site and preventing blood loss [13]. The ability of blood to clot must be carefully regulated because abnormal clotting leads to life-threatening thrombotic complications [13]. Hence blood coagulation is an important part of the human host defense mechanism.

Plasma coagulates through a complex cascade of self-amplifying enzyme reactions conversions that ultimately lead to conversion of fibrinogen to a fibrin clot [14, 15]. This 'plasma coagulation cascade' converts a series of blood factors (zymogens) to active enzymes. The sequential enzyme-amplifier nature of the cascade was first proposed by Davie and Ratnoff in 1960s [14, 15]. Plasma coagulation is an essential aspect of thrombus formation, which involves platelets as well, since artificial materials are known to activate the intrinsic pathway of the cascade.

Fig. 1.1 shows sketch of the plasma coagulation cascade emphasizing serial linkage of intrinsic and extrinsic pathways. Although the notion of separated "intrinsic"

and "extrinsic" pathways served as a useful model for coagulation for many years but more recent evidence reveals that the pathways are, in fact, highly interconnected, forming a redundant system to protect integrity of the vascular system.

Table 1.1: Molecular Weight and Plasma Concentration of Plasma Coagulation Factors

Factor	Molecular Weight	Plasma Concentration (µg/ml)
Fibrinogen	330,000	3000
Prothrombin	72,000	100
Factor V	300,000	10
Factor VII	50,000	0.5
Factor VIII	300,000	0.1
Factor IX	56,000	5
Factor X	56,000	10
Factor XI	160,000	5
Factor XIII	320,000	30
Factor XII	76,000	30
Prekallikrein	82,000	40
HMWK	108,000	100

The extrinsic pathway is initiated by release of tissue factor (TF) from the injury site. Upon vascular injury, cells expressing membrane-bound tissue factor are exposed to

plasma and bind to factor VII. This binding leads to the formation of TF-VIIa complex which triggers the extrinsic coagulation cascade [7].

The intrinsic pathway is initiated when blood comes into contact with a procoagulant surface resulting in the activation of factor XII to factor XIIa [16-24]. The term 'procoagulant' is used in this thesis to denote any material or enzyme that triggers the intrinsic pathway. The intrinsic pathway is the is directly responsible for material-contact coagulation [25]. The intrinsic pathway can be triggered when factor XII, prekallikrein (PK), and high-molecular weight kininogen (HMWK) bind to artificial surfaces. Once bound, reciprocal activation of FXII and prekallikrein occurs. Factor XIIa further triggers coagulation via the sequential activation of factors XI, IX, X, and II (prothrombin).

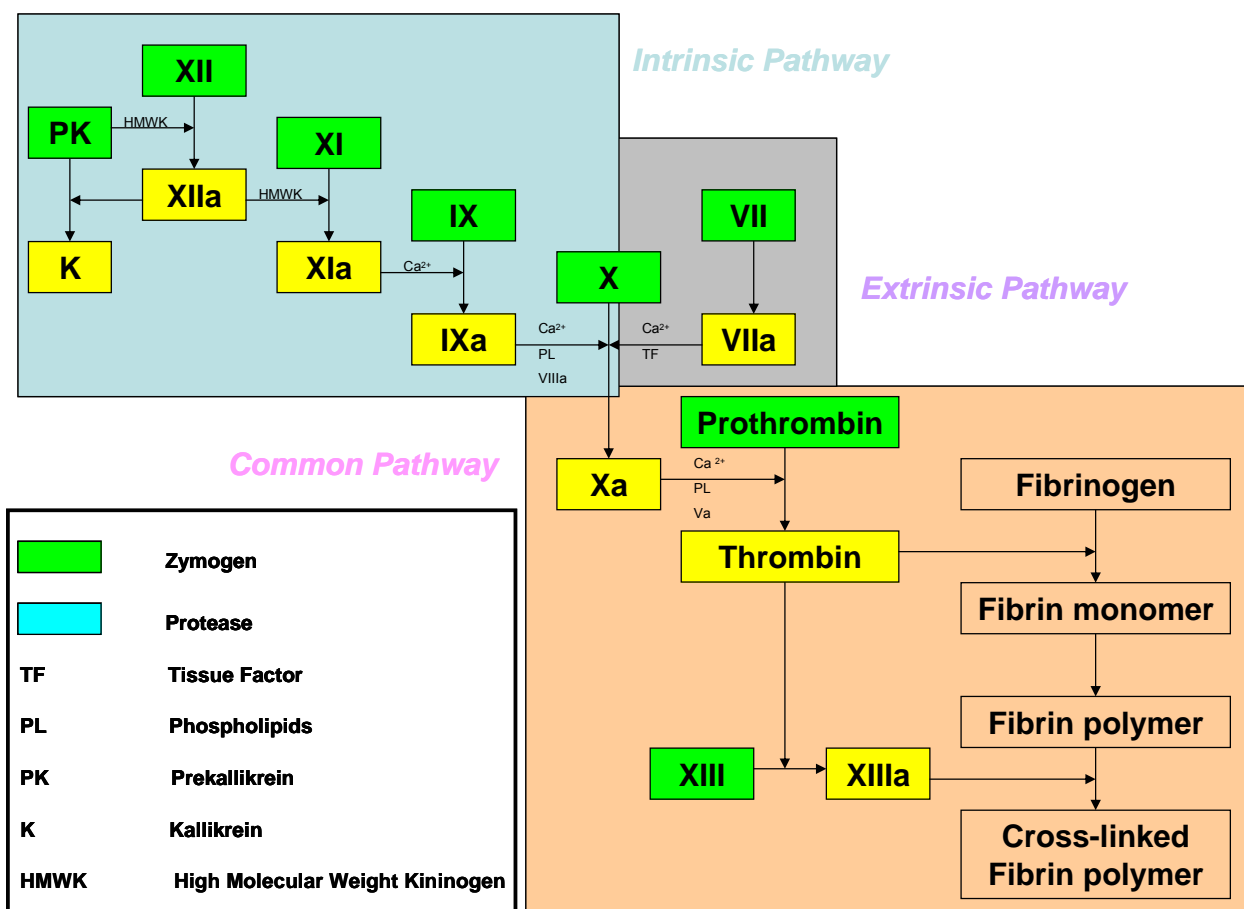


Fig. 1.1: Sketch of the plasma coagulation cascade emphasizing serial linkage of intrinsic and extrinsic pathways [26].

1.4 Contact Activation Complex

Normal blood quickly clots when it comes into contact with some foreign surfaces [13]. The initial steps in intrinsic pathway are known as contact activation reactions because they are triggered by surface contact. This contact activation complex consists of four proteins: FXII, FXI, plasma prekallikrein, and high molecular weight kininogen. [27].

The contact activation complex proteins have important roles in coagulation, fibrinolysis, thrombin-induced platelet activation, cell adhesion and angiogenesis [28]. These proteins were first identified as coagulation proteins because patients deficient in these proteins had abnormal activated partial thromboplastin times. It has been suggested that inherited or acquired deficiencies of these proteins may be risk factors for thrombosis [18, 23, 29, 30].

After FXII is activated to FXIIa, FXIIa can convert surface-bound PK and FXI to kallikrein and FXIa respectively. Kallikrein, in turn, activates surface-associated FXII to FXIIa [31]. This forms a positive feedback loop that serves to amplify the rapid mutual activation of FXII and PK. HMWK serves as a cofactor in the contact complex. It enhances the contact activation by binding FXI and PK to the surface [32], and it also enhances the activation of FXII by kallikrein. The exact biochemistry of FXII activation by material contact remains an unsolved mystery of significance to this thesis. Several hypotheses that have been proposed [22, 30, 33, 34] for contact activation. Needless to say, a better understanding of contact activation complex would greatly assist the design of biomaterials with improved hemocompatibility.

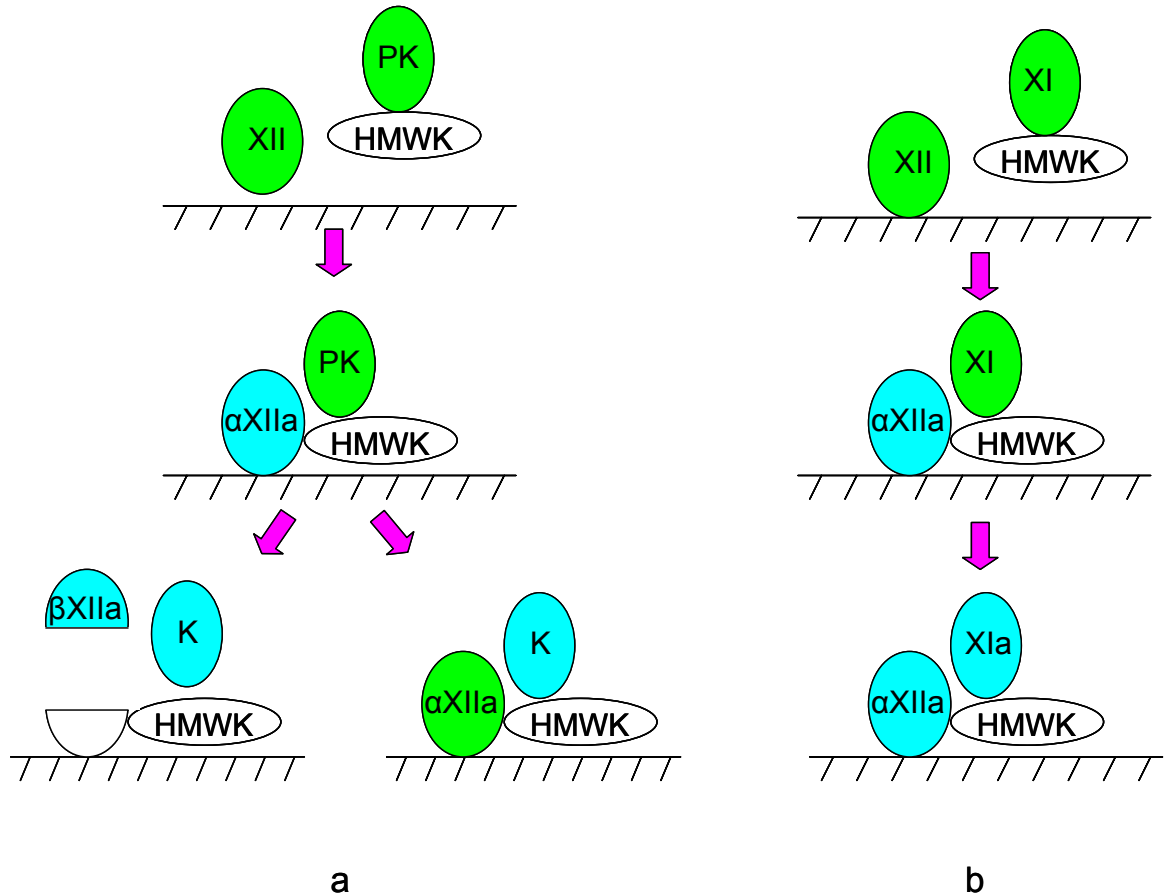


Fig. 1.2: Schematic representation of surface-dependent assembly of molecules responsible for contact activation (adapted from ref. [35]).

Human FXII, also known as Hageman factor [15], is thought to be the first factor activated during contact activation as a direct consequence of its ability to undergo autoactivation by contact with a material surface [13, 19, 36-38]. FXII is a single-chain glycoprotein with a molecular weight of approximately 80,000 [21] and is synthesized in

the liver and present in normal plasma at a concentration of 30ug/ mL [18]. FXII circulates in blood as a zymogen of a serine protease (FXIIa). Unlike most of the reactions in coagulation cascade, the reaction between FXII and surfaces does not require the presence of calcium ions.

After activation, FXII is transformed into serine protease α -FXIIa by a single proteolytic cleavage of the Arg373-Val374 peptide bond within a disulfide bond (as shown in Fig. 1.3) [18, 23]. α -FXIIa is a two chain molecule that is created by a split of a peptide bond. The light chain with the active site has a molecular weight of 26,000. The N-terminal heavy chain has a molecular weight of 54,000. The main part of the heavy chain is easily split off, forming a low molecular weight (28,000) active enzyme (β -FXIIa). This additional cleavage results in two fragments, an amino-terminal portion (MW 52,000) and a carboxy terminal portion (MW 28,000) [38, 39]. The 28,000 fragment is designated as β -FXIIa (FXII_f), which contains the active enzymatic site, but the surface binding property of FXII resides in the 52,000 component [37]. Both α -FXIIa (FXII_a) and β -FXIIa (FXII_f) are potent activators of prekallikrein, however, surface bound α -FXIIa is at least 100 times more active than β -FXIIa in the activation of FXI.

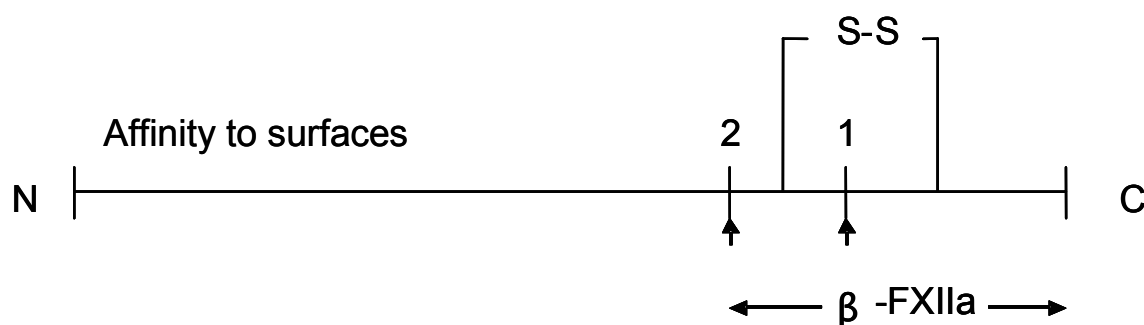


Fig. 1.3: Activation of FXII to 1. α -FXIIa and 2. β -FXIIa.

There are two main reactions that contribute to FXIIa formation: FXII autoactivation and kallikrein-dependent FXII activation [40]. FXII autoactivation is a process in which the zymogen FXII is activated by surface contact event. The cause of FXII autoactivation has been a controversial issue for a long time. Some researches suggest that binding to the negatively charged surfaces induces a conformation change of FXII that makes this protein more susceptible for cleavage [13, 19, 36-38].

It is inferred from the experimental data that FXII autoactivation occurs most efficiently on hydrophilic (water wettable) surfaces [41-44], with little or no FXII activation upon contact with hydrophobic (poorly water wettable) surfaces [41-44]. It has been shown that the propensity to activate the plasma coagulation cascade scales sharply with water wettability (surface energy) [42, 45, 46]. Data leading to this conclusion is compiled in Fig. 1.4 plotting propensity to contact activate the intrinsic pathway of blood plasma coagulation (measured by the relative index K_{ACT} , per unit area of procoagulant) as a function of procoagulant surface energy reported as water adhesion tension

$\tau^o = \gamma_{lv}^o \cos \theta$ (where γ_{lv}^o is water liquid-vapor interfacial tension and θ is the contact angle subtended by water on the procoagulant surface in either advancing or receding modes). Two types of procoagulant surfaces are represented; oxidized polystyrene film and self assembled monolayers (SAMs) supported on glass. Polystyrene procoagulants have mixed surface chemistry whereas SAM surfaces are well defined with identifying terminal functional groups. The trend line drawn through the data is identical for both polystyrene and SAM procoagulants and suggests an exponential-like increase in procoagulant efficiency with τ^o [42, 45, 46].

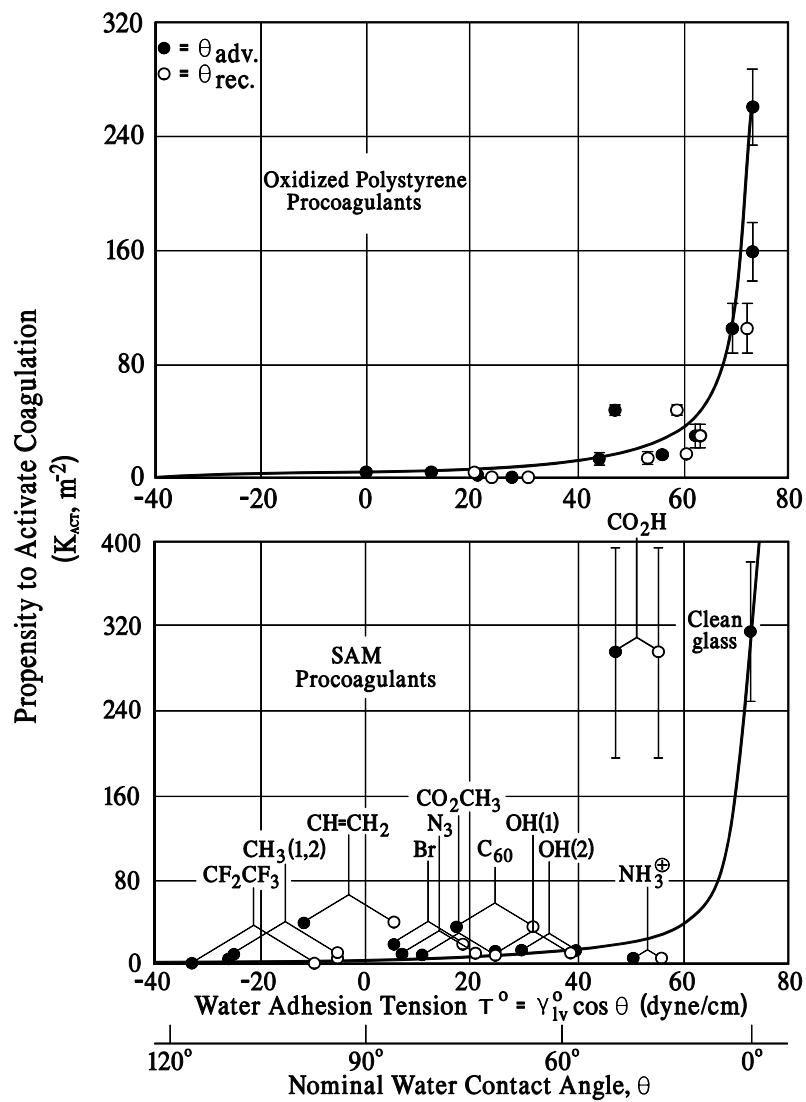


Fig. 1.4: Propensity to contact activate the intrinsic pathway of blood plasma coagulation as a function of procoagulant surface energy [47].

Based on this evidence obtained in whole plasma, it is clear that fully water wettable surfaces (high surface energy) exhibit higher catalytic potential than poorly water wettable surfaces (low surface energy). These findings are in general agreement with the expected dependence of catalytic potential on negatively-charged surface chemistry discussed above.

However, these results are somewhat puzzling when viewed from a surface-science perspective. It is generally accepted that the first event when blood comes into contact with a foreign surface is adsorption of blood protein onto that material [17]. And because adsorption/assembly of proteins of the activation complex onto a surface are the initial steps of contact activation [22], it is reasonable to expect that this would occur most efficiently at hydrophobic surfaces. But this is not observed. Indeed, just the opposite is observed: contact activation is most efficient at hydrophilic surfaces that are known to be less protein-adsorbent [41-43, 48, 49]. Important questions that arise in light of these findings are: (1) how do plasma proteins adsorb and assemble on hydrophilic surface and (2) why does adsorption on hydrophobic surface not lead to FXII autoactivation?

Answering these fundamental questions is the major objective of this thesis.

1.5 References

1. Williams, D., Definitions in biomaterials. Proceedings of a consensus conference of the european society for biomaterials. Vol. 4. March 3-5 1986, Chester, England: New York: Elsevier.
2. Ratner, B.D., A History of Biomaterials, in Biomaterials Science, B.D. Ratner, et al., Editors. 2004, Elsevier Academic Press: San Diego, California. p. 10-19.
3. Clark, A.E., Hench L.L., and Paschall H.A., The influence of surface chemistry on implant interphase histology: a theoretical basis for implant materials selection. *Journal of Biomedical Material Research*, 1976. 10: p. 161-177.
4. Jarcho, M. Tissue, cellular and subcellular events at a bone-ceramic hydroxylapatite interface. *Journal of bioengineering*, 1977. 1(2): p. 79-92.
5. Ratner, B.D., et al., Biomaterials Science. 2004, San Diego, California: Elsevier Academic Press.
6. Sundaram, S., et al., Modification of the Influence of Biomaterials on Contact Activation. *The International Journal of Artificial Organs*, 1991. 14(11): p. 729-731.
7. Luchtman-Jones, L., Broze Jr, G.J., The Current Status of Coagulation. *annals of medicine*, 1995. 27: p. 47-52.
8. Ratner, B.D., The Blood Compatibility Catastrophe. *J. Biomed. Mat. Res.*, 1993. 27: p. 283-287.

9. Grunkemeier J. M, Horbett T. A., Hemocompatibility of treated polystyrene substrates. *Journal of Biomedical Matererial Research*, 1998. 41(4): p. 657-70.
10. Rose, E.A., Gelijns, A.C., Moskowitz, A., Heitjan, D.F., Stevenson, L.W., Dembitsky, W., Long, J.W., Aschheim, D.D., Tierney, A.R., Levitan, T.G., Watson, J.T., Meier, P., Long-term Use of a Left Ventricular Assist Device for End-Stage Heart Failure. *N. Engl. J. Med.*, 2001. 345(20): p. 1435-1443.
11. Lavine, M., Roberts, M., Smith, O.,: *The Bionic Human*. Science, 2002. 295: p. 995-1032.
12. Ratner, B. D., *Characterization of Biomaterial Surfaces*. *Cardiovascular Pathology*, 1993. 2(3): p. 87s-100s.
13. Griffin, J. H., *Surface-dependent activation of blood coagulation*, in *Interaction of the blood with natural and artificial surfaces*, E.W. Salzman, Editor. 1981, MARCEL DEKKER, INC.: new york. p. 139-170.
14. Davie, E., Ratnoff, O., *Waterfall Sequence for Intrinsic Blood Clotting*. Science, 1964. 145: p. 1310.
15. Ratnoff, O.D., *Blood, Pure and Eloquent*, ed. e. M. M. Wintrobe. 1980, New York: McDraw-Hill. 601-607.
16. Mann, K.G., ed. *Prothrombin and Thrombin*. *Hemostasis and Thrombosis: Basic Principles and Clinical Practice*, ed. R.W. Colman, et al. 1994, J. B. Lippincott Company: Philadelphia. 277-300.
17. Sundaram, S., Irvine, L., Courtney, J. M., Lowe, G. D., *Modification of The Influence of Biomaterials On Contact Activation*. *The International Journal of Artificial Organs*, 1991. 14(11): p. 729-731.

18. Fuhrer, G., Gallimore, M. J., Heller, W., Hoffmeister, H. E., FXII. *Blut.*, 1990. 61(5): p. 258-66.
19. Silverberg, M., Dunn, J.T., Garen, L., Kaplan, A.P., Autoactivation of human Hageman factor. Demonstration utilizing a synthetic substrate. *J Biol Chem.*, 1980. 255(15): p. 7281-6.
20. Hantgan, R.R., Francis, C.W., Marder, U.J., Fibrinogen Structure and Physiology, in *Hemostasis and Thrombosis: Basic Principles and Clinical Practice*, R.W. Colman, et al., Editors. 1994, J.B. Lippincott Company: Philadelphia. p. 277-300.
21. Pixley, R.A., Colman, R.W., Factor XII: Hageman factor. *Methods in Enzymology*, 1993. 222: p. 51-65.
22. Colman, R.W., Scott, C.F., Schmaier, A.H., Wachtfogel, Y.T., Pixley, R.A., Edmunds JR, L.H., *Initiation of Blood Coagulation at Artificial Surfaces*. 1987.
23. Mitropoulos, K.A., High Affinity Binding of Factor FXIIa to an Electronegative Surface Controls the Rates of Factor XII and Prekallikrein Activation in vitro. *Thrombosis Research*, 1999. 94(2): p. 117-129.
24. Citarella, F., Willemin, W.A., Lubbers, Y.T., Hack, C.E., Initiation of Contact System Activation in Plasma is Dependent on Factor XII Autoactivation and not on Enhanced Susceptibility of Factor XII for Kallikrein Cleavage. *British Journal of Haematology.*, 1997. 99(1): p. 197-205.
25. Samuel, M., Pixley, P.A., Villanueva, M.A., Colman, R.W., Villanueva. G.B., Human Factor XII (Hageman factor) Autoactivation By Dextran Sulfate. Circular Dichroism, Fluorescence, and Ultraviolet Difference Spectroscopic Studies. *Journal of biological chemistry*, 1992. 267(27): p. 19691-7.

26. King, M.W., Blood Coagulation <http://web.indstate.edu/thcme/mwking/blood-coagulation.html>. 1996.
27. Colman, R.W. and, Contact System: A Vascular Biology Modulator With Anticoagulant, Profibrinolytic, Antiadhesive, and Proinflammatory Attributes. *Blood*, 1997. 90(10): p. 3819-3843.
28. Colman RW, Schmaier, A.H., Contact system: a vascular biology modulator with anticoagulant, profibrinolytic, antiadhesive, and proinflammatory attributes. *Blood*, 1997. 90(10): p. 3819-43.
29. Anderson, N.L., Anderson, N.G., The Human Plasma Proteome: History, Character, and Diagnostic Prospects. *Molecular and Cellular Proteomics*, 2002. 1(11): p. 845-867.
30. Colman, R.W., Contact Activation Pathway: Inflammatory Fibrinolytic, Anticoagulant, Antiadhesive, and Antiangiogenic Activities, in *Hemostasis and Thrombosis: Basic Principles and Clinical Practice.*, M.V. Colman RW, Hirsh J, Clowes AW,, Editor. 2000, J.B. Lippincott Company: Philadelphia. p. 103-21.
31. Kaplan, A.P., Joseph, K., Shibayama, Y., Reddigari, S., Ghebrehiwet, B., Silverberg, M., The Intrinsic Coagulation/Kinin-Forming Cascade: Assembly in Plasma and Cell Surfaces in Inflammation. *Advances in Immunology*, 1997. 66: p. 225-272.
32. Saito, H., Ratnoff, O.D., Pensky, J., Radioimmunoassay of human Hageman factor (factor XII). *Journal of Laboratory and Clinical Medicine*, 1976. 88(3): p. 506-14.

33. Cochrane, C.G., Revak, S.D., Wuepper, K.D., Activation of Hageman Factor in Solid and Fluid Phases. *The Journal of Experimental Medicine*, 1973. 138: p. 1564-1583.
34. Colman, R.W., Schmaier, A.H., Contact System: A Vascular Biology Modulator With Anticoagulant, Profibrinolytic, Antiadhesive, and Proinflammatory Attributes. *Blood*, 1997. 90(10): p. 3819-43.
35. Griffin, J.H., Recent advances in the understanding of contact activation reactions. *Seminar of Thrombosis and Hemostasis*, 1979. 5(254-273).
36. Revak, S.D., Cochrane, C.G., Johnston, A.R., Hugli, T.E., Structural Changes Accompanying Enzymatic Activation of Human Hageman Factor. *Journal of Clinical Investigation*. 1974 Sep;54(3):619-27., 1974. 54(3): p. 619-27.
37. Revak, S.D., Cochrane, C.G., The Relationship of Structure and Function in Human Hageman Factor. The Association of Enzymatic and Binding Activities With Separate Regions of The Molecule. *Journal of Clinical Investigation*. 1974 Sep;54(3):619-27., 1976. 57(3): p. 852-860.
38. Revak, S.D., Cochrane, C.G., Griffin, J.H., The Binding and Cleavage Characteristics of Human Hageman Factor During Contact Activation. A Comparison of Normal Plasma With Plasmas Deficient in Factor XI, Prekallikrein, or High Molecular Weight Kininogen. *Journal of Clinical Investigation*. 1974 Sep;54(3):619-27., 1977. 59: p. 1167-1175.
39. Revak, S.D., et al., Structural changes accompanying enzymatic activation of human Hageman factor. *Journal of Clinical Investigation*. 1974 Sep;54(3):619-27., 1974. 54(3): p. 619-27.

40. Saito, H., Kojima, T., Factor XII, Prekallikrein, and High-Molecular-Weight Kininogen, in *Molecular Basis of Thrombosis and Hemostasis*, K.A. High, Roberts, H.R., Editor. 1995, Marcel Dekker: New York. p. 269-85.
41. Vogler, E.A., Graper, J.C., Sugg, H.W., Lander, L.M., Brittain, W.J., Contact Activation of the Plasma Coagulation Cascade.2. Protein Adsorption on Procoagulant Surfaces. *J. Biomed. Mat. Res.*, 1995. 29: p. 1017-1028.
42. Vogler, E.A., Graper, J.C., Harper, G.R., Lander, L.M., Brittain, W.J., Contact Activation of the Plasma Coagulation Cascade.1. Procoagulant Surface Energy and Chemistry. *J. Biomed. Mat. Res.*, 1995. 29: p. 1005-1016.
43. Vogler, E.A., Nadeau, J.G., Graper, J.C., Contact Activation of the Plasma Coagulation Cascade. 3. Biophysical Aspects of Thrombin Binding Anticoagulants. *J. Biomed. Mat. Res.*, 1997. 40(1): p. 92-103.
44. Zhuo, R., et al., Procoagulant Stimulus Processing by the Intrinsic Pathway of Blood Plasma Coagulation. *Biomaterials*, 2004. in press.
45. Zhuo, R., Miller, R., Bussard, K.M., Siedlecki, C.A., Vogler, E.A., Procoagulant Stimulus Processing by the Intrinsic Pathway of Blood Plasma Coagulation. *Biomaterials*, 2005. 26: p. 2965-73.
46. Zhuo, R., Colombo, P., Pantano, C., Vogler, E.A., Silicon Oxycarbide Glasses for Blood Contact Applications. *Acta Biomaterialia*, 2005. 1: p. 583-9.
47. Vogler, E.A., et al., Contact Activation of the Plasma Coagulation Cascade.1. Procoagulant Surface Energy and Chemistry. *J. Biomed. Mat. Res.*, 1995. 29: p. 1005-1016.

48. Vogler, E.A., Structure and Reactivity of Water at Biomaterial Surfaces. *Adv. Colloid and Interface Sci.*, 1998. 74(1-3): p. 69-117.
49. Vogler, E.A., Water and the Acute Biological Response to Surfaces. *Journal of Biomaterials Science Polymer Edition*, 1999. 10(10): p. 1015-45.

Chapter 2

Materials and Methods

2.1 Materials

2.1.1 General Reagents

Water was obtained from a Millipore Simplicity 185 system. This system produces water virtually free of organic and inorganic contaminants: ≤ 5 ppb of total organic content (TOC), ≤ 1 cfu/ml of micro-organisms, and 18.2 M Ω ·cm resistivity at 25°C).

0.01M phosphate buffered saline (PBS, 140Mm NaCl, 0.0027M KCl, Ph=7.4 at 25°C, Sigma) is obtained by dissolving into 1 liter of Millipore water. 2-propanol and chloroform were all reagent grade (VWR). Octadecyltrichlorosilane (OTS, United Chemical Technologies, Inc.) and 3-aminopropyltriethoxysilane (APS; United Chemical Technologies, Inc.) were used as received. 15×75 mm polystyrene tubes (VWR) were washed by Millipore water for three times and air-dried prior to use. All glassware was cleaned by 3X serial rinses in 18 M Ω water, 2-propanol, and chloroform (reagent grade,

VWR) followed by air-plasma treatment (plasma cleaner, Harrick Plasma). The principal of plasma cleaner is as following: when a gas under sufficiently low pressure is subjected to a high frequency oscillating electromagnetic field, the accelerated ions collide with the gas molecules, ionizing them and forming plasma. Then the ionized gas in the plasma interacts with solid surfaces placed in the same environment. The high energy plasma particles can remove organic contamination by combining with the contaminant on the surface to form carbon dioxide or methane. And the chemical reaction occurred between the plasma gas molecules and the surface can modify or enhance the physical and chemical characteristics of that surface.

In all assays used in this study, human plasma had been anticoagulated with the calcium chelator in order to keep them from clotting and extend their viability. So in order to allow the coagulation cascade to continue for this research, it is necessary to recalcify the plasma. CaCl_2 (Sigma) was chosen to be plasma recalcifying agent in this research. Based on the previous study, the optimal concentration of CaCl_2 was chosen to be 0.1M [1].

2.1.2 Human Platelet Poor Plasma

Platelet poor (citrate) plasma (PPP) is a proven experimental vehicle for investigating the coagulation cascade [2-4], both in traditional hematology (recalcified-citrate plasma is the preferred form of blood for aPTT (activated partial thromboplastin time (PTT) or PTT (partial thromboplastin time) testing [2] and in previous studies of coagulation/anticoagulation [5, 6]. Recalcified PPP is wholly coagulation competent,

requiring no additional proteins or phospholipids to recover clotting potential. Human platelet poor plasma (PPP, citrated) was prepared from outdated (within 2 days of expiration) lots obtained from the M.S. Hershey Medical Center Blood Bank. Plasma could be frozen and stored for up to one year. But once plasma was thawed, it had to be used within one week. Those thawed plasma that could not be used within one week are classified as “outdated”. It can not be used for human any more, but could be used in research. Plasma was aliquoted into 15 mL polypropylene tubes (Falcon, Becton Dickinson) and frozen at -20°C until use. Prior to use, plasma was warmed for about 40 minutes in 37°C water bath.

2.1.3 Human Platelet Poor FXII Deficient Plasma and FXI Deficient Plasma

Factor XII depleted plasma (12dPPP) with a dysfunctional contact activation system was used as received from George King Biomedical, Inc. It was prepared by the immunodepleting method using anti-FXII. 12dPPP was received in 1 mL aliquots and stored at -80°C . In some experiments, 12dPPP was optionally reconstituted with variable FXII concentrations (R12dPPP). FXI deficient plasma (11dPPP) was used as received from Haematologic Technologies, Inc. (Essex Junction, VT). It was manufactured from normal, citrated human plasma, and was immunodepleted of FXI using anti-FXI. Each plasma was fully assayed to ensure the proper activity of the remaining factors ($>50\%$ activity), and was tested for fibrinogen, PT, aPTT, and clarity values. 11dPPP was received in 1mL vials and had a five-year expiration when stored continuously at -70°C .

2.1.4 Plasma Proteins

Human α -thrombin (Sigma) was obtained as a lyophilized product containing 350 National Institute of Health (NIH) units/mL. One NIH unit is defined as the amount of enzyme that hydrolyzes 1 mmol per minute at pH 8.4 and 37°C [7]. Thrombin solutions were freshly-prepared before each use by dissolution in phosphate buffer saline (PBS, Sigma-Aldrich) to 100 NIH unit/mL.

Human FXII and FXIIa were used as received from Haematologic Technologies, Inc. (Essex Junction, VT) and Enzyme Research Laboratories (South Bend, IN), respectively. FXIIa activity was specified by the vendor in traditional units of Plasma Equivalent Units (PEU/mL). FXI was obtained from Enzyme Research Laboratories and FXIa from Haematologic Technologies. FXIa was specified by the vendor in units of $\mu\text{g}/\text{mL}$, but the absolute activity of the preparation was unknown.

Other proteins used in the study are human IgM (Sigma), human IgG (Sigma), human FAF albumin, human FV albumin (Sigma), bovine albumin (Sigma). Desired amount of proteins was dissolved in PBS to get protein solutions.

2.1.5 Procoagulants

2.1.5.1 Clean and Silanized Glass Beads

Test glass beads applied in this work were 425-600 μm diameter glass beads (Sigma) in either cleaned or silanized form. Clean-glass procoagulants were prepared by

3X serial rinses in 18 M Ω water, 2-propanol, and chloroform, followed by air-plasma treatment of a single layer of washed-glass beads held in a 15 mm Pyrex glass petri dish (10 min. at 100 watts plasma; Herrick, Whippany NY). Clean glass beads were used within the same day of air-plasma treatment to assure the water-wetted condition. Silanized glass was obtained by either 1.5 hr. reaction with 5% octadecyltrichlorosilane (OTS in chloroform; United Chemical Technologies, Inc.) or by 5 min. reaction with 2% 3-aminopropyltriethoxysilane (APS in acetone; United Chemical Technologies, Inc.). Silanized beads were 3X rinsed in either chloroform or acetone, respectively, and dried in a vacuum oven at 110°C for 24 hr. Contact angles of glass-slide witness samples measured by Wilhelmy balance tensiometry (CDCA-100, Camtel Ltd.) typically yielded advancing/receding contact angles 0°/0°, 70°/40°, and 110°/90° for clean, APS, and OTS procoagulants, respectively, with no more than about 10° variation among batches. Contact angles cannot be read directly on glass beads but optical microscopy of the shape of the liquid meniscus of beads partly immersed in water on a microscope slide qualitatively confirmed that the treated beads were not different from the witness samples.

2.1.5.2 SiO_xC_y

All silicon carboxide were in powder form prepared by pyrolysis of precursor resins. Table **2.1** compiles sources and identities of thermosetting silicone resins (polysilsesquioxanes) used for preparation of test materials, along with sample identification applied herein. Total bulk-resin C content (from literature data [8] or

estimated using the rule of mixtures on the basis of the data reported in the cited literature) and the density of the SiO_xC_y glass samples (after pyrolysis at 1200°C in inert atmosphere) are also collected in Table 2.2. SiO_xC_y with X:Y ratios intermediate of those prepared from as-received resins were prepared from mixtures of SILRES 601 and SILRES 610. Weighed proportions were thoroughly mixed and melted together at 90 to 110°C , which is well above the glass transition temperature for both resins. The resulting mass was crushed using a mortar. These samples were labeled 25-SILRES and 50-SILRES, respectively. Several grams of the various powder samples were (partially) crosslinked by condensation of Si-OH groups by heating at 70°C for 24h in air and were then pyrolyzed by heating at 1200°C ($10^\circ\text{C}/\text{min}$ heating rate; 2h dwelling time; alumina crucibles) in inert atmosphere (N_2 99.99%, flow rate of $50 \text{ cm}^3/\text{min}$). The resulting black, glass powders were ground using a ball mill and sieved to produce powders with a controlled size of 425-600 μm . Surface composition of each of the specimens listed in Table 2.2 was altered by chemical etching in an alkaline solution containing Na_2CO_3 and NaOH (pH 12.3, prepared according to reference 14) at 80°C for 2 h.

Table 2.1: Polysilsequioxane Prepolymers Used in Preparation of SiO_xC_y Glasses

Sample Designation	Organofunctional Group	Total Carbon (wt %)	Total Carbon (atom %)	SiO _x C _y Glass Density (g/cm ³)
SILRES 610	Methyl	12.8	20.2	2.255 ± 0.001
SOC-A35	Methyl	13.7	21.6	2.228 ± 0.002
25 wt% SILRES 601 – 75 wt% SILRES 610*	Methyl-Phenyl	20.6**	29.6**	2.101 ± 0.002
50 wt% SILRES 601 – 50 wt% SILRES 610*	Methyl-Phenyl	28.4**	38.9**	1.974 ± 0.002
SR 355	Methyl-Phenyl	32.7	45.3	1.889 ± 0.002
H44	Methyl-Phenyl	39.1	52.6	1.894 ± 0.002
SILRES 601	Phenyl	44.0	57.6	1.799 ± 0.001
Reference glass	-	n.d.	n.d.	2.496 ± 0.001
Glass OTS-coated	-	n.d.	n.d.	2.496 ± 0.001

Notes: *Sample labeled 25-SILRES; *Sample labeled 50-SILRES; ** Estimate; n.d.= not determined

Test materials were analyzed using X-ray diffraction (Philips mod. PW1710, Cu $K\alpha$, operating at 40 kV and 30 mA, step of 0.05° every 4 s, Philips Analytical, Almelo, The Netherlands) and Scanning Electron Microscopy (mod. XL-20, Philips Analytical, Natick, MA). Surface composition was measured using X-ray photoelectron spectroscopy (XPS; a.k.a. ESCA) using a Model Axis Ultra spectrometer (Kratos Analytical, Wharfedale, Manchester, U.K.) with an monochromatic Al $K\alpha$ radiation source (1486.6 eV). C(1s), Si(2p), and O(1s) spectra were collected, with a step size of 0.1 eV and an energy of 40 eV per pass; the analyzed area was fixed at 700 x 350 μm . Binding energies were charge-referenced to the C(1s) peak at 284.6 eV. Quantification of the data involved calculating atomic percentages with sensitivity factors that were calibrated against a poly(dimethylsiloxane) (PDMS) standard. Curve fitting of the high-resolution spectra was conducted using a commercial software package [9]. Particle density was measured

using a gas pycnometer (mod. AccuPyc 1330, Micromeritics, Norcross, GA). Scanning electron microscopy (SEM) of prepared powders revealed irregular polyhedron-shaped particles for all SiO_xC_y glass compositions. Geometric area of particles used in coagulation tests was estimated by the following procedure. Particle axes lengths were measured from several SEM micrographs images from which an average surface area and volume was estimated. Given the actual particle volume used in coagulation tests (calculated from measured weights and densities), the total number of particles were computed by dividing by the average volume deduced from image analysis above. Total geometric area of particles used in each coagulation test was then calculated by multiplying by the average surface area from image analysis. This procedure is considered to give a better estimate of geometric surface area than obtained by simply assuming a spherical shape with a nominal diameter within the range 425 to 600 μm . But no way is found to independently verify accuracy of area estimates. However, it is noted that assumption of a polyhedral shape systematical underestimates actual area because particles have a higher fractile dimension. This area underestimate propagates into a systematic over estimate of procoagulation properties from coagulation tests. Thus, it is concluded that reported procoagulant properties of tested particles represent an upper-bound (worse case) assessment and that actual procoagulant properties are, in fact, better than suggested by this work.

Table 2.2: SiOxCy Glass Surface Composition Compared to SiOx Controls

Sample	Atom % Excluding Hydrogen							
	O	total C	Si	Si-C*	C-C+	C-O	C=O	CO ₂ H
As received SILRES 610	53.8	20.0	25.7	0.8	14.9	2.4	0.9	0.7
As received SOC- A35	50.1	22.8	27.1	3.3	14.3	3.2	1.2	0.8
As received 25- SILRES	51.6	23.1	24.4	0.9	14.8	3.6	0.8	1.5
As received 50- SILRES	33.8	56.0	8.7	0.0	40.0	8.1	2.9	3.6
As received SR355	46.6	38.3	14.4	1.4	28.8	4.1	2.00	2.00
As received H44	18.0	79.3	2.7	0.0	73.1	2.2	1.2	1.4
As received SILRES 601	35.9	48.0	16.1	1.3	36.7	5.7	2.6	1.8
SiOx (positive control)	58.8	24.9	15.7	0.0	22.1	2.2	0.6	0.4
Silanized SiOx (negative control)	13.2	77.9	8.9	0.0	75.7	2.2	0.0	0.0
Etched SILRES 610	53.5	23.7	22.9	2.0	15.8	3.2	1.2	1.0
Etched SOC-A35	55.7	17.5	26.8	1.0	11.8	2.9	0.8	0.8
Etched 25-SILRES	42.8	30.0	27.2	2.3	23.4	2.4	0.6	1.2
Etched 50-SILRES	41.8	36.5	21.7	0.0	34.6	1.2	0.2	0.5
Etched SR 355	57.3	17.9	24.8	0.0	13.1	2.5	0.7	0.4
Etched H44	22.4	65.5	12.1	0.0	65.5	0.0	0.0	0.0
Etched SILRES 601	37.5	46.8	15.7	1.0	35.5	6.2	2.5	1.6
Notes: * Carbidic C; + Free C (turbostratic C in the SiOxCy glasses) plus adventitious C (BE = 284.6 ev).								

2.1.5.3 Pyrolytic carbon

Pyrolytic carbon in the form of 10X10X0.1 mm rectangles obtained from Minerals Technologies Inc. (New York) were solvent rinsed (as described above) and air

dried but were not subjected to plasma treatment. PC specimens thus prepared were suitable only for qualitative comparison to procoagulants in powder form due to poor mixing of thin PC films with PPP. For this purpose, 1,2,3,4, 5, and 10 PC rectangles were added to each of six tubes used in the coagulation assay.

2.2 Methods

2.2.1 Coagulation-Time Assays

The basic protocol for coagulation-time assays used in this work has been described in detail in previous work [5, 6] and applied in this work in several variations: surface-area titrations (SAT), thrombin titration (TT), surface-area/FIIa co-titrations (COT), FXIIa titration, and FXIa titration. In each variation, 0.5 mL of thawed plasma equilibrated with ambient temperature was transferred into 15×75 mm polystyrene tubes (VWR) and diluted with sufficient PBS to bring the final total liquid volume to 1 mL; including all additives which varied according to the assay. In SAT and COT experiments, tubes containing varying amount of solid procoagulant between 0 – 300 mg (as measured on an electronic balance to within 0.1 mg) were prepared before liquid ingredients were added. In COT and TT experiments, serially-increasing volumes between 0 and 50 μ L of FIIa (100 NIH unit/mL in PBS) were added to each tube in the titration series. FXIIa and FXIa titration experiments are described in detail in section **2.2.5**. In all cases, coagulation was induced by recalcification with 0.1mL of 0.1 M

CaCl₂ and contents were mixed on a slowly-turning hematology mixer (Roto-shake Genie, Scientific industries, Inc.). Coagulation time *CT* after recalcification was noted by a distinct change in fluid-like rheology to gel formation, allowing determination of the end point of the coagulation process to within 10 s or so [5]. These simple, yet highly sensitive, recalcification-time assays eliminated extraneous contributions to coagulation associated with many modern instrumented tests (*e.g.* activating surfaces of stirrers and tubing) and yielded smooth dose-response curves that varied with procoagulant properties (surface chemistry and energy) or enzyme concentration.

2.2.2 Multiple Activation of Plasma Coagulation

A single 12 X 75 mm glass tube was cleaned according to the protocol described above for clean glass bead procoagulants, including air-plasma-discharge treatment. 0.1 mL of 0.1 M CaCl₂ and 0.4 mL of PBS buffer was added to 0.5 mL plasma and time to coagulation was measured while the tube was turned on a hematology mixer as described above. After coagulation, clot was removed by draining liquid contents, shaking-out solid contents, and rinsing 3X with ~ 5 mL PBS. An additional 1 mL PBS was added to the tube and the contents turned for 2 hr on a hematology mixer after which the wash was replaced with fresh citrated PPP, PBS, and CaCl₂. This process was repeated 5X for each of 3 separate trials employing a single glass tube, achieving an average coagulation time of 6.9±0.7 min (N= 3X5=15).

2.2.3 Mathematical Methods of Thrombin Titration

Models of plasma coagulation applied here were basically extensions of previously-published work [5, 6]. The core idea behind these models are as follow: surface activation of plasma coagulation was proposed to occur in some proportion to procoagulant surface area that led to production of a hypothetical activated fibrin monomer F^* . F^* subsequently entered into rate-limiting oligomerization (measured by a rate constant k_p with min^{-1} units) into a fibrin mesh that ultimately caused plasma to coagulate. A key premise was that coagulation did not occur until a fixed fraction of fibrinogen α had been converted into F^* , independent of procoagulant surface properties, and the rate of F^* production controlled coagulation time CT . Thus, surface-activated coagulation was compared to a negative control (typically time to coagulation in the absence of any activator CT^o), leading to an analytical solution for CT in terms of ratios of unknown rate constants:

$$CT = -\left(\frac{1}{k_p}\right) \ln\left[\frac{K_{act}^{SAT} A + e^{-k_p CT^o}}{(K_{act}^{SAT} A + 1)}\right] \quad \mathbf{2.1}$$

Where A represented procoagulant surface area and K_{act}^{SAT} a ratio of rate constants that measured the ‘catalytic potential’ of the procoagulant surface under study. Eq. **2.2** was used exactly as previously described, including assignment of an arbitrary value to the unknown k_p fixed by a two-parameter fit of Eq. **2.1** to experimental CT data

obtained using a positive-control standard. In this case, clean glass beads were positive controls for which $k_p = 0.54 \pm 0.10 \text{ min}^{-1}$ was obtained (average \pm std. dev for $N = 3$ separate trials; compare to $0.70 \pm 0.09 \text{ min}^{-1}$ for porcine plasma). Thus, K_{act}^{SAT} measured activation potential relative to this internal standard and is not to be interpreted as a quantitative characteristic of procoagulants studied herein. Likewise k_p should not be regarded as representative of human PPP in general.

The FIIa-titration model used herein was described in ref. [6]. The essential idea underlying this theory was that an exogenous FIIa spike was instantaneously (relative to the timeframe of coagulation) partitioned between free and bound forms. As in the surface-activation model discussed above, it was assumed that FIIa hydrolysis of fibrinogen led to production of F^* and that the fraction of free thrombin was vanishingly small (mole fraction $X_{TF} \rightarrow 1$; see ref. [5] for details). Elaboration of this model led to an analytical relationship between observed CT and FIIa-spike concentration $[T^o]$ in (NIH unit/mL as applied herein):

$$CT = \frac{\alpha[F^o]}{k_3[T^o]} + \frac{1 - e^{-k_p CT}}{k_p} \quad \mathbf{2.2}$$

Where the term $\frac{\alpha[F^o]}{k_3}$ was an unknown constant treated as a single variable parameter. Recognizing that Eq. **2.2** cannot be explicitly solved for CT without additional simplifying assumptions, a commercial engineering-equation-solver software package (F-Chart Software, Madison, WI) was used to obtain the best-fit statistical

solution to experimental FIIa-titration data (observed CT at various $[T^o]$) using $k_p = 0.54 \pm 0.10 \text{ min}^{-1}$ as discussed above in reference to SAT.

The COT model was a simple extension of Eq. **2.2** wherein it was assumed that activation of the intrinsic cascade produced a bolus concentration of endogenous FIIa (measured by the parameter Θ with dimensions of NIH unit/mL) that directly added to the exogenous FIIa spike, such that:

$$CT = \frac{\alpha[F^o]}{k_3([T^o] + \Theta)} + \frac{1 - e^{-k_p CT}}{k_p} \quad \mathbf{2.3}$$

Thus, under conditions of this assumption, Eq. **2.3** permitted extraction of Θ by fitting to COT data, again obtained by use of engineering-equation-solver software mentioned above in reference to TT.

2.2.4 Pyrolytic Carbon

Pyrolytic carbons in the form of 10X10X0.1 mm rectangles obtained from Minerals Technologies Inc. (New York) were solvent rinsed (as described above) and air dried but were not subjected to plasma treatment. PC specimens thus prepared were suitable only for qualitative comparison to procoagulants in powder form due to poor mixing of thin PC films with PPP. For this purpose, 1,2,3,4, 5, and 10 PC rectangles were added to each of six tubes used in the coagulation assay.

2.2.5 Surface Activation of Activation of FXII in Neat-Buffer Solution and Plasma

The basic experimental strategy to compare FXII activation in neat-buffer-solution (no proteins other than FXII and activation products) and human-blood plasma is illustrated in Fig. **2.1**. Test solutions were either purified FXII in PBS buffer at physiological concentration of 30 $\mu\text{g}/\text{mL}$ [10] [11] or citrated platelet-poor plasma (Panel A). Two sources of plasma were used; one prepared from blood collected from normal donors (PPP) and the other was a commercial Factor XII-deficient plasma (12dPPP) with a dysfunctional contact-activation system that served as a negative control. In the latter instance, 12dPPP was optionally reconstituted to normal physiological FXII concentration (R12dPPP) with the same FXII used to prepare neat-buffer solutions. Putative FXIIa produced by 30 min. contact with hydrophilic or hydrophobic procoagulant surfaces was either released into solution (free) or remained associated with activating surfaces (bound). Supernate containing free FXIIa was separated from surface-bound FXIIa by decantation (Fig. **2.1**, Panel B).

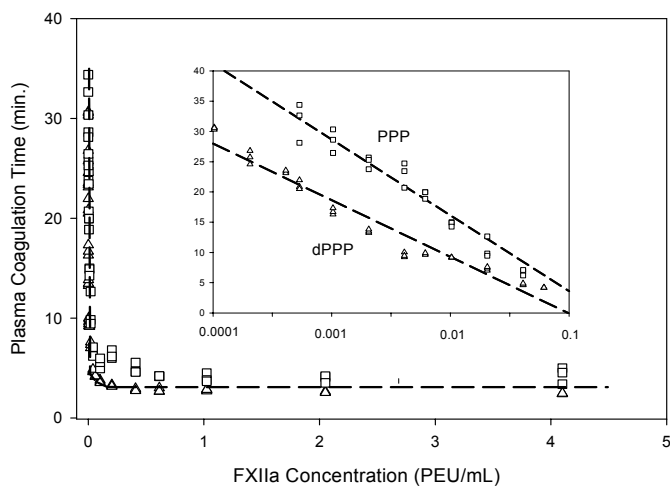
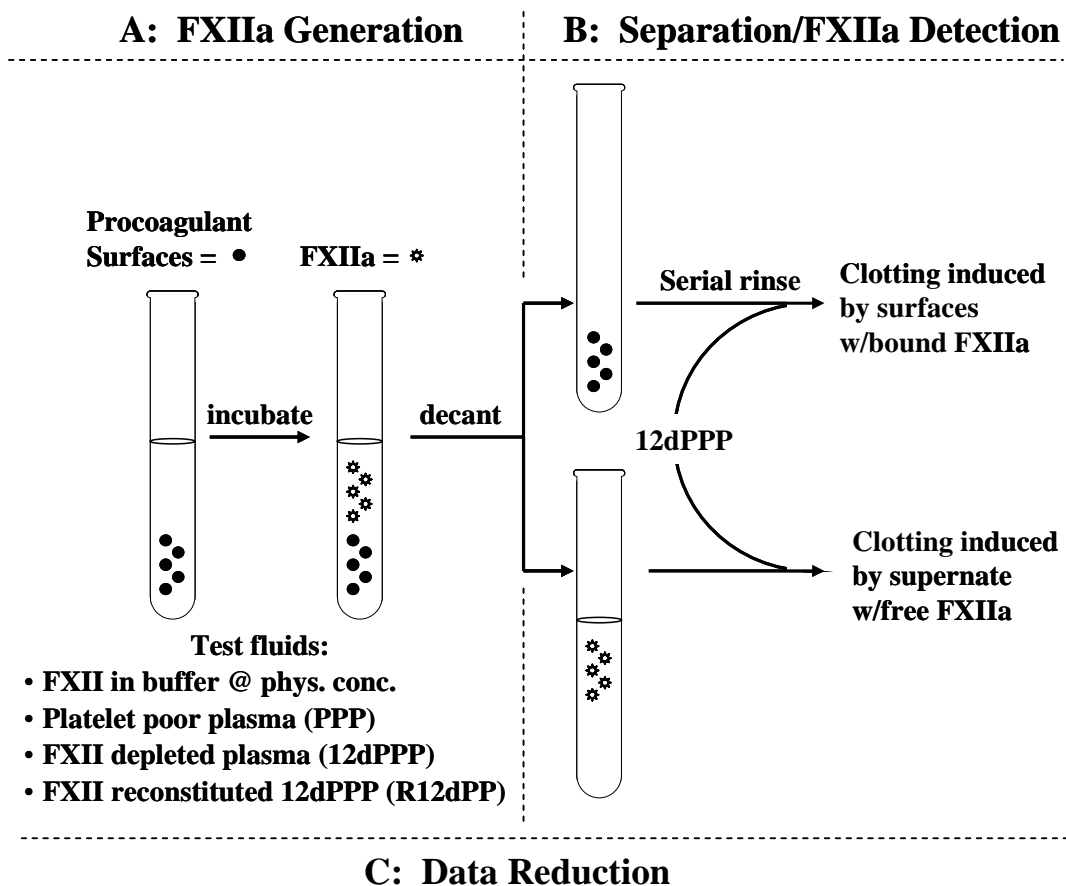
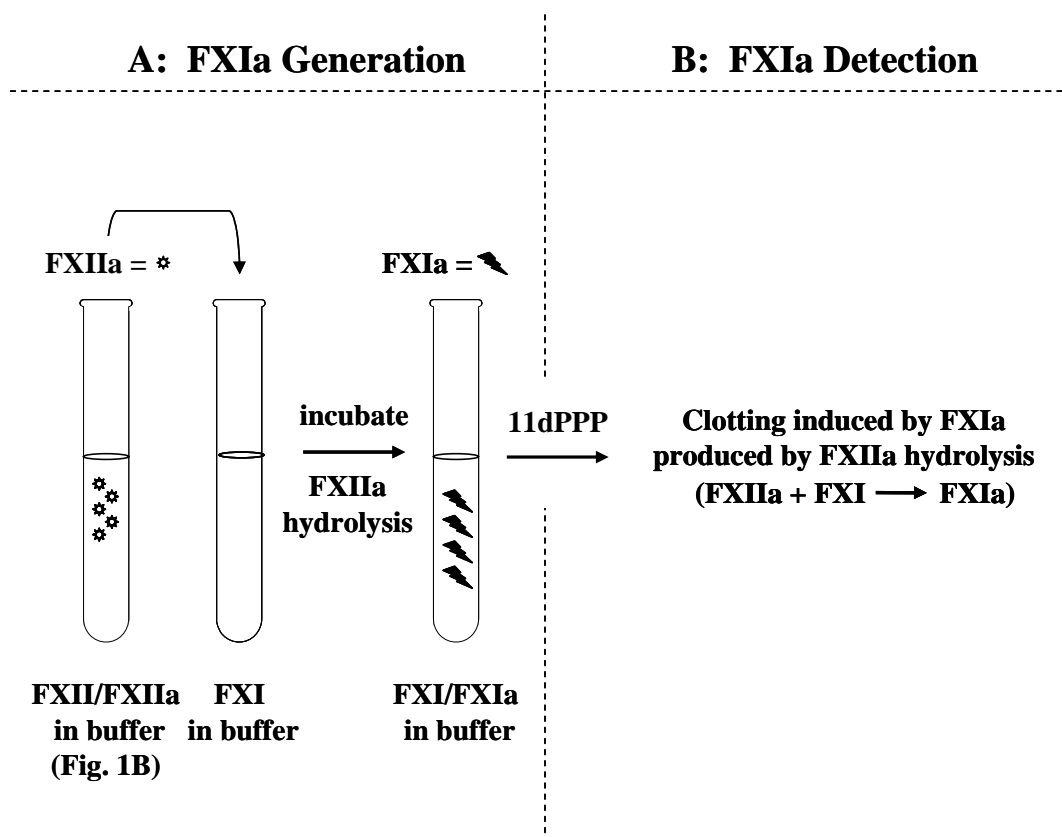


Fig. 2.1: Schematic experimental outline for detection of FXIIa produced by contact with procoagulant surfaces.

Free and bound FXIIa activities were quantified by measuring reduction in coagulation time of 12dPPP upon addition of supernate or activating surfaces, respectively, with reference to a FXIIa titration curve (Fig. **2.1**, Panel C inset). FXIIa activity in PPP was quantified by measuring PPP coagulation time directly, again by referring to a FXIIa titration curve. FXIIa titration curves in 12dPPP and PPP happen to provide a reasonably linear calibration curve when scaled on a logarithmic concentration axis (Fig. **2.1** Panel C). It is emphasized that appealing to a coagulation-time calibration curve was a purely pragmatic approach to measuring FXIIa and not based on enzyme-kinetic analysis. No special effort was made to resolve procoagulant-associated FXIIa into loosely- or tightly-bound FXIIa fractions, other than to rinse procoagulants 3X in 1 mL serial washes and check for FXIIa activity remaining on procoagulant particles and in the third-serial- rinse solution.



C: Data Reduction

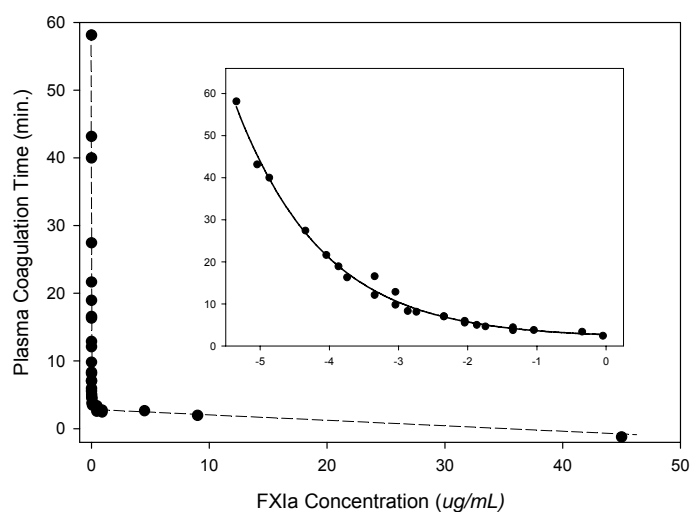


Fig. 2.2: Schematic experimental outline for detection of FXIa produced by hydrolysis of FXI by products of FXII activation.

2.2.6 FXI Hydrolysis by Surface Activated FXII

Fig. 2.2 outlines the experimental plan used to measure FXI hydrolysis to FXIa by putative FXIIa ($FXI \xrightarrow{FXIIa} FXIa$) in surface-activated FXII solutions obtained from Fig. 2.1, Panel B. Incubation with FXI solutions ($5 \mu\text{g} / \text{mL}$) were either for fixed times (30 min.) or varied over $0 < t \leq 30$ in 2-to-5 min. intervals. Putative FXIa was detected by measuring reduction in coagulation time of 11dPPP upon addition of FXI solution, with reference to a FXIa titration curve (Fig. 2.2, Panel C). In this instance, the FXIa titration curve was not linear when scaled on a logarithmic concentration axis, as was the case with FXIIa described above. Rather, CT response to serially-increasing $[FXIa]$ was curvilinear and was fit to an arbitrary four-parameter logistic equation (smooth curve through data of Fig. 2.2 Panel C; $R^2 = 99.4\%$) which was used as a calibration curve that permitted estimation of unknown $[FXIa]$ from experimentally-measured CT . It is emphasized that appealing to a coagulation-time calibration curve was a purely pragmatic approach to measuring FXIa and not based on enzyme-kinetic analysis.

As shown in Fig. 2.2, Panel A incubates supernate of Fig. 2.1B with FXI solution whereupon putative activated FXII fragments (i.e. FXIIa) hydrolyze FXI to FXIa ($FXI \xrightarrow{FXIIa} FXIa$). Panel B detects FXIa by measuring coagulation time of FXI-depleted plasma (11dPPP). Panel C is a calibration curve (obtained by exogenous FXIa titration of 11dPPP) that relates observed plasma coagulation time to FXIa concentrations. The line through data of Panel C is a guide to the eye whereas the line

through data of the inset is the result of least-squares fit of an arbitrary four-parameter logistic equation through the data interval shown ($R^2 = 99\%$).

2.2.7 Chromogenic Assay

The amidolytic activity of FXIIa was measured using a chromogenic substrate s-2302 (H-D-Pro-Phe-Arg-pNA· 2HCl, MW = 611.6 used as received from Diapharma Group Inc., Columbus, OH). A 4.0 mM stock solution of the chromogen was prepared in 18 MΩ water (obtained from a Millipore Simplicity Unit) and stored at 2-8°C for no more than 6 months. A 0.4 mM working solution was prepared by diluting the stock solution 10-fold with buffer (0.05M Tris/Hcl, 0.012 M NaCl, 0.003M EDTA, PH 7.8). The actual FXIIa assay was performed by mixing 450 μL of working solution with 150 μL of test solution in a ultra-microcuvette (VWR) held in the chamber of an automatically-recording UV-VIS spectrophotometer (DU® Series 500, Beckman Coulter, Inc., Fullerton, CA). Absorbance change at 405 nm was recorded for 5 min. to determine the initial velocity of color development.

2.3 References

1. Bussard, K.M., Interactions of Model Biomaterials and Enzymes in Contact Activation of the Blood Plasma Coagulation Cascade, in Bioengineering. 2002, Pennsylvania State University: Hershey, PA. p. 35-37.
2. Brown, B., Hematology: Principles and Procedures. 3 ed. 1980, Philadelphia: Lea and Febiger. 113-119.
3. Mitropoulos, K.A., High Affinity Binding of Factor XIIa to an Electronegative Surface Controls the Rates of Factor XII and Prekallikrein Activation in Vitro. Thrombosis Research, 1999. 94: p. 117-129.
4. Mitropoulos, K.A., The Levels of FXIIa Generated in Hyman Plasma on an Electronegative Surface are Insensitive to Wide Variation in the Concentration of FXII, Prekallikrein, High Molecular Weight Kininogen or FXI. Thromb. Haemost., 1999. 82: p. 1033-40.
5. Vogler, E.A., Graper, J.C., Harper, G.R., Lander, L.M., Brittain, W.J., Contact Activation of the Plasma Coagulation Cascade.1. Procoagulant Surface Energy and Chemistry. J. Biomed. Mat. Res., 1995. 29: p. 1005-1016.
6. Vogler, E.A., Nadeau, J.G., Graper, J.C., Contact Activation of the Plasma Coagulation Cascade. 3. Biophysical Aspects of Thrombin Binding Anticoagulants. J. Biomed. Mat. Res., 1997. 40(1): p. 92-103.

7. Hemker, H.C., *The Handbook of Synthetic Substrates (For The Coagulin and Fibrinolytic System)*. 1983: Martinus Nijhoff Publisher.
8. Scheffler, T., Kaschta, J., Muensted, H., Buhler, P., Greil, P., Pyrolytic decomposition of preceramic organo polysiloxanes. *Innovative Processing and Synthesis of Ceramics, Glasses, and Composites IV: Ceramic Transactions*, 2000. 115: p. 239-250.
9. C. Öneby, Silicon Oxycarbide Formation on SiC Surfaces and at the SiC/SiO₂ Interface. *J. Vac. Sci. Technol.*, 1997. 15(3): p. 1597-1602.
10. Anderson, N.L., Anderson, N.G., *The Human Plasma Proteome: History, Character, and Diagnostic Prospects*. *Molecular and Cellular Proteomics*, 2002. 1(11): p. 845-867.
11. Saito, H., Ratnoff, O.D., Pensky, J., Radioimmunoassay of human Hageman factor (factor XII). *Journal of Laboratory and Clinical Medicine*, 1976. 88(3): p. 506-14.

Chapter 3

Procoagulant Stimulus Processing by the Intrinsic Pathway of Blood Plasma Coagulation

Potential of the intrinsic pathway of human blood plasma coagulation in vitro by contact with a solid procoagulant surface leads to bolus release of thrombin (FIIa) in concentration proportion to the intensity of activation as measured by procoagulant surface area or energy (water wettability). This rather remarkable finding is confirmed using two different assays: one triggering coagulation substantially through the intrinsic pathway alone and the second triggering coagulation through the intrinsic pathway in the presence of exogenous FIIa spikes. Similarity of experimental outcomes of these assays strongly suggests that endogenous FIIa production through the intrinsic pathway is independent of the absolute amount of FIIa present in plasma. Furthermore, we corroborate previous work indicating that procoagulant surfaces remain activating after repeated use and are not poisoned or denatured in the process of activating plasma coagulation. It is concluded that the sharp control mechanism that gives rise to bolus-production of FIIa from the intrinsic pathway must occur between surface activation of FXII and the FII \rightarrow FIIa step, is not related to inhibition by FIIa, and does not involve deactivation of procoagulant surfaces.

3.1 Introduction

Perioperative bleeding and thrombosis are significant barriers to the development and implementation of advanced in-dwelling blood pumps and ventricular assist devices [1, 2]. Indeed, thrombosis remains a risk in the application of ordinary biomedical devices such as catheters, now used in the tens-of-millions annually in various nosocomial procedures [3]. Thrombosis can usually be traced to adverse blood-biomaterial interactions that lead to the formation of emboli. Bleeding, on the other hand, is frequently associated with excessive anticoagulation employed to prevent thrombosis. Thus, blood-contact phenomena persists as one of the more important facets of biomaterials surface science and development of truly hemocompatible materials remains a largely unrealized objective [3, 4]. Future advances in the surface-engineering of blood-contacting biomaterials [4, 5] are critically dependent on a detailed understanding of how blood “processes” presence of an artificial material at a molecular level. Toward this understanding, This study have focused on the blood-plasma coagulation cascade in vitro as a highly simplified, yet very informative, experimental system that can be used to probe surface-contact events that trigger platelet-poor plasma (PPP) coagulation in a manner that is substantially (but not wholly) independent of cellular interactions [6, 7]. The general expectation is that this information will provide guidance to the design of materials with improved hemocompatibility.

The classical biochemistry of the intrinsic pathway suggests that a “procoagulant stimulus” originating in the exposure of plasma to a test surface (herein also referred to as

a dose), potentiates a cascade of zymogen-enzyme conversions (a response) that culminate in the release of the protease thrombin (FIIa). Individual steps of this cascade have been the subject of intense scrutiny over the last few decades, resulting in a quite complete characterization of the biochemistry of separated/purified reactions, especially for the extrinsic cascade that is partly responsible for hemostasis of circulating whole blood *in vivo*. However, much less is known about the holistic operation of the intrinsic cascade that is activated by contact with foreign materials [7] beyond that inferred from the classical tests of coagulation [8]: partial prothrombin time (PTT), and activated prothrombin time (aPTT) (see ref. [9] and citations therein). PTT and aPTT protocols purposely saturate the coagulation cascade with procoagulant dose (thromboplastin or thromboplastin mixed with a high surface area silica or kaolin, respectively) to evoke maximum response (minimum coagulation time) from the so-called extrinsic and intrinsic pathways of plasma coagulation, respectively. These tests effectively side-step the question of “dose processing” that we seek to more fully understand by carefully controlling the kind/intensity of dose as an experimental variable (esp. surface area, chemistry, and energy) and relating this to the observed response (coagulation time or release of enzyme intermediates) using mathematical models of plasma coagulation.

Modeling kinetics of a series of interconnected zymogen-enzyme conversions in which the product of a preceding reaction is the enzyme of a subsequent reaction is a rather complicated affair, especially when self-amplifying loops and feedback inhibition are taken fully into account. Early efforts [10-14] have led to informative computational models of the extrinsic pathway [14-27] but, as already mentioned, much less work has been dedicated to modeling the intrinsic pathway that is activated by contact with

material surfaces [28, 29]. No doubt a limitation has been a dearth of fundamental information relating procoagulant surface properties to the extent that the intrinsic pathway is potentiated [6] and the proportions between dose (surface area, chemistry, energy) and response (release of activated enzyme, coagulation time). It is these structure-property relationships that the current research seeks for the purpose of developing biomaterials with improved hemocompatibility.

As an alternative to developing a manifold of differential equations representing individual enzyme reactions expressed in terms of a number of rate constants and activation efficiencies (related to procoagulant surface properties) that have been derived under conditions that may or may not be entirely relevant to whole-plasma coagulation *in vitro*, we have adopted the “phenomenological” approach used in traditional hematology that abstracts the cascade into functional compartments grouping related multi-step enzyme reactions. This engineering method is especially useful in modeling the holistic behavior of a complex *in vitro* experimental vehicle such as PPP [6, 7] for which all sources and sinks of enzyme or surface activities may not be clearly known or identified. A significant goal is to derive simplified analytical relationships between dose and response written explicitly in terms of rate parameters (typically ratios of rate constants) that measure an effective compartment potentiation. This strategy has the decided advantage over purely computational models in that derived analytical expressions can be statistically fit to experimental data using rate parameters as adjustable factors of the fit. In turn, fitted-rate parameters (with error estimates derived from least-squares statistics) can be scaled against dose characteristics to induce or infer how dose is processed by the cascade. Although this sort of modeling will not typically yield kinetic information about

the individual enzyme-mediated reactions comprising the coagulation compartment under investigation and thus cannot supplant/replace detailed computational kinetics, it has been shown to provide useful insights into how the *intact* cascade is activated [6] and deactivated [7] in whole plasma. Importantly, this information quantitatively links material properties to the coagulation of whole plasma.

Herein this study applies human PPP as an experimental system, coagulation time as the measured response, and phenomenological modeling to demonstrate that procoagulant stimulus originating in contact with surfaces with varying water wettability (surface energy) propagates through the cascade in a manner that releases a bolus of FIIa in remarkable concentration-proportion to procoagulant surface area. This work extends and corroborates previous work that used porcine plasma as a test system, suggesting that the classical mechanism of the intrinsic cascade of blood coagulation requires some revision or upgrading to fully account for the details of surface activation.

3.2 Thrombin Titration of Human Plasma

Sensitivity and reproducibility of human PPP coagulation from outdated blood (see Methods and Materials) was tested by ‘thrombin titration’ (TT) experiments in which coagulation time CT of recalcified plasma induced by increasingly-concentrated exogenous-bolus spikes of human α -thrombin $[T^o]$ was observed. Fig. 3.1A collects results of a number of FIIa titrations performed on one batch of plasma on different dates spanning approximately 1 year of experimentation. As can be readily appreciated from

this plot, CT was approximately sigmoidal on a $\log_{10} [T^o]$ (unit/mL) scale, with a very noisy low-concentration asymptote near 46 min and more consistent high-concentration limit near 0.5 min. Thus, the TT working range appeared to be approximately two decades in $[T^o]$, lying between $1 \times 10^{-2} < [T^o] < 1$ unit/mL. Fig. **3.1 B** redraws data of Fig. **3.1A** falling within this working range on $1/[T^o]$ scale, consistent with Eq. **2.2** of Methods and Materials. Line through the data is best fit of Eq. **2.2**, with $R^2=89.3\%$ using $k_p=0.54$ and yielding $\frac{\alpha[F^o]}{k_3} = 0.24 \pm 0.09$.

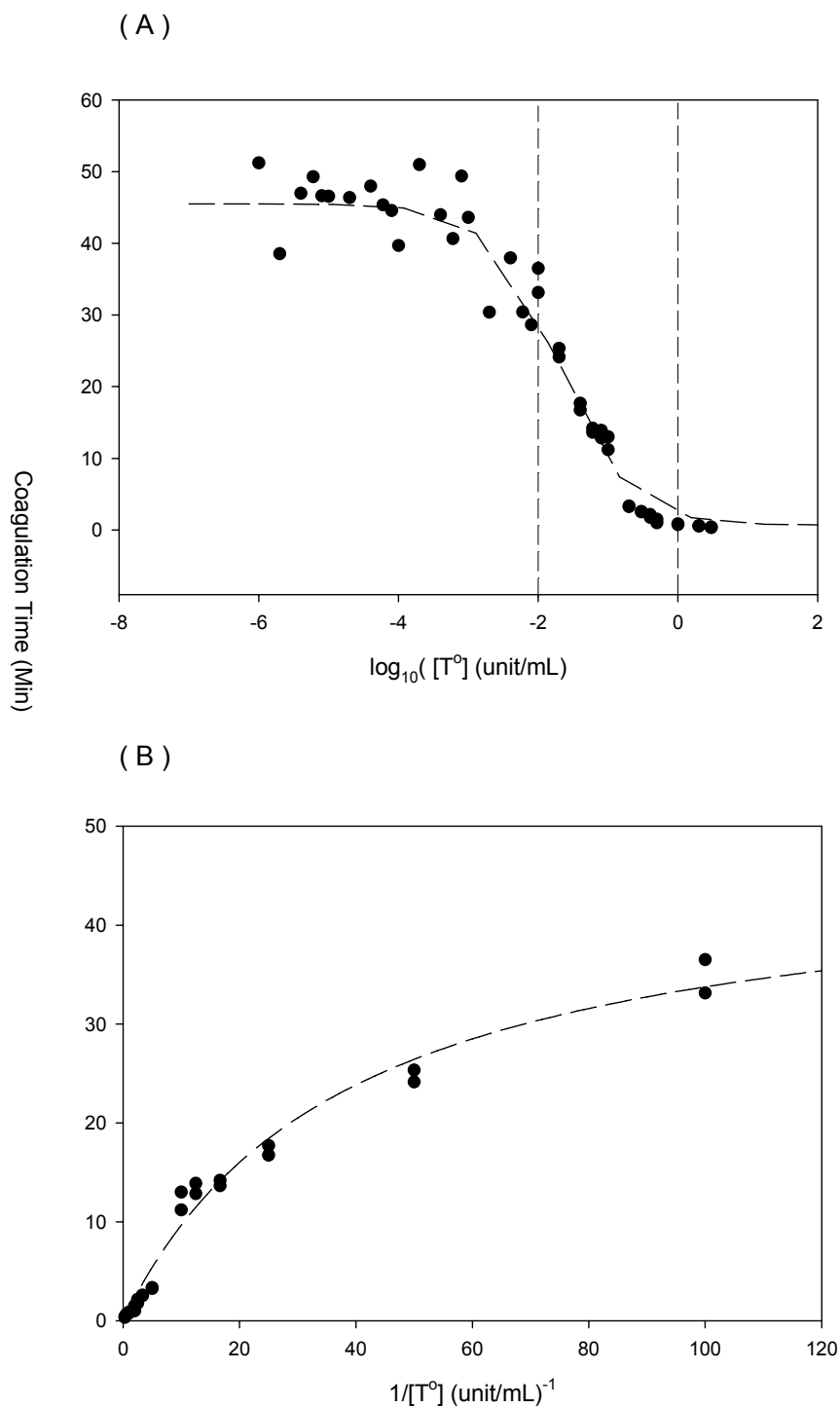


Fig.3.1: (A) Thrombin titrations (TT) plotted on a $\log_{10}[T^o]$ axis.

(B) TT on $1/[T^o]$ coordinates consistent with Eq. 2.1 of Method and Materials.

3.3 Surface Area Titration (SAT) of Human Plasma

Fig. 3.2 collects results of human PPP activation by serially-increasing surface area of solid procoagulants with different surface chemistry/energy obtained by silanizing clean glass beads with APS or OTS. Significant effort was invested in the clean-glass SAT curve, especially at low surface area, to verify the trend suggested by Eq. 2.1 applied to human PPP and to confidently establish a value for k_p (see Methods and Materials). Much less effort was expended in the low surface-area regime for APS and OTS, focusing instead on higher-surface area for the purpose of establishing a confident value for K_{act}^{SAT} as the single adjustable parameter in non-linear least-square fitting to Eq. 2.1 with $k_p = 0.54 \text{ min}^{-1}$ (see Methods and Materials). Smooth lines drawn through the data of Fig. 3.2 represent the best fitted curves. Table 3.1 collects results for the three procoagulants studied in this work where the error estimate given for K_{act}^{SAT} represents standard error of regression through pooled data of three separate SAT experiments for each procoagulant. Evidently, the SAT model represented by Eq. 2.1 adequately simulated experimental data, corroborating previous studies of porcine PPP coagulation [7] using a much broader array of polymer and self-assembled monolayer (SAM) test procoagulant surfaces. K_{act}^{SAT} values in Table 3.1 will be discussed further in the discussion section.

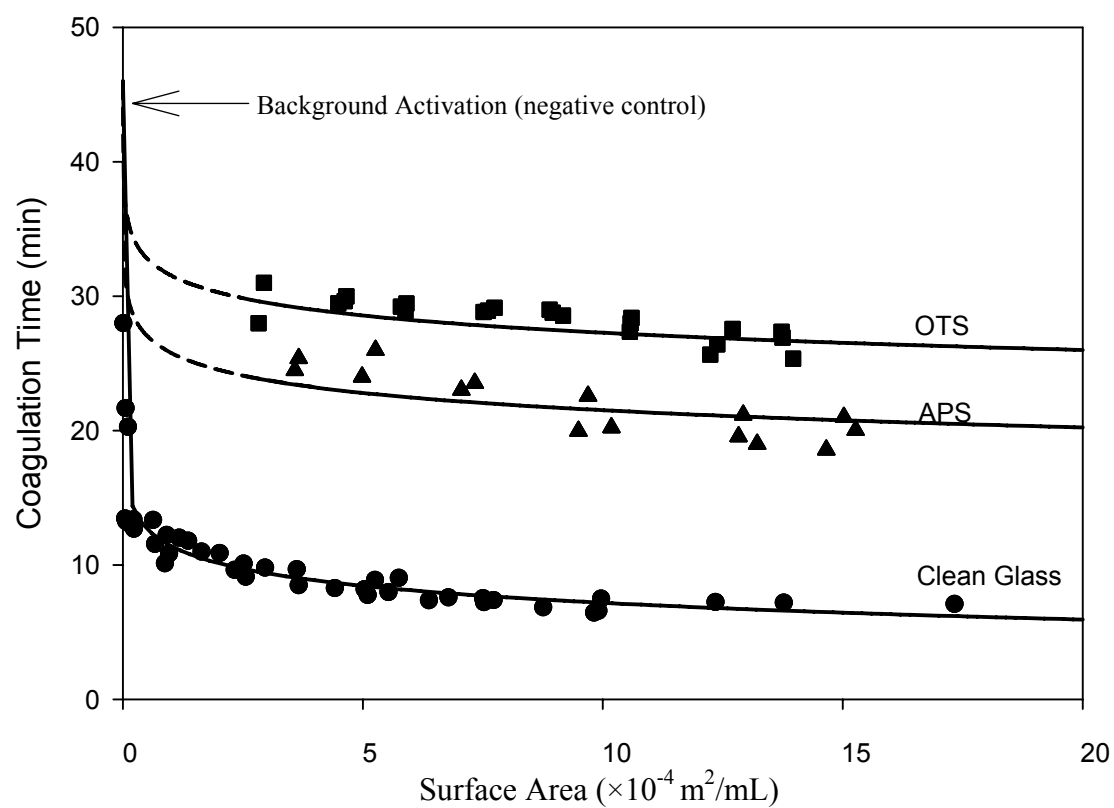


Fig. 3.2: Surface area titration with glass beads bearing different surface chemistries plotting observed coagulation time CT as a function of procoagulant surface area per mL test solution.

Table 3.1: Procoagulant Catalytic Activities

Procoagulant	Norminal Contact Angle (adv. / rec.)	K_{act}^{SAT} from SAT (mL/m ²) N=3	K_{act}^{COT} from COT (unit/m ²) N=2
Clean Glass	0°/0°	21.1±2.1	35.7±3.7
APS Treated Glass	70°/40°	$(9.0±1.7)×10^{-3}$	4.0±0.8
OTS Treated Glass	110°/90°	$(4.0±1.7)×10^{-4}$	2.8±0.5

Fig. 3.3 collects representative results from FIIa titration of human PPP in the presence of varying surface areas of water-wettable glass spheres. Smooth lines drawn through the data of Fig. 3.3 were obtained by non-linear least-square fitting to Eq. 2.3 with $k_p = 0.54$ (as discussed above in reference to SAT) and $\frac{\alpha[F^0]}{k_3} = 0.24$ (as discussed above in reference to TT). Evidently, the COT model represented by Eq. 2.3 adequately simulated experimental data for all cases up-to-and-including $4.7×10^{-4}$ m²/mL surface area clean glass procoagulant beads. Co-titration results obtained with more hydrophobic procoagulants (not shown) were similar except that the difference between co-titration (surface activation of FXII in the presence of FIIa) and FIIa titration (with no added solid procoagulant) was much less pronounced. Table 3.2 collects fitted values of variable

Θ for clean and silane-treated glass procoagulants performed in duplicate. Fig. 3.4 plots Θ as a function of surface area A showing a strong linear relationship ($R^2 \geq 96\%$) for all three test procoagulants with a slope K_{act}^{COT} that measures the amount of endogenous FIIa released per-unit-area procoagulant. Thus, K_{act}^{COT} is a measure of the catalytic power of the procoagulants that is similar to K_{act}^{SAT} . In Fig. 3.4, range on the mean of duplicate trials (N=2) collected in Table 3.2 is approximated by symbol size. Note that the Θ axis is scaled by 10^{-n} with n values listed in figure annotations on the left side of the figure. Fig. 3.5 and Table 3.2 compare K_{act}^{COT} and K_{act}^{SAT} values for the test procoagulants. As shown in Fig. 3.5, Procoagulant catalytic potential derived from SAT (K_{act}^{SAT} , left axis, circles) and COT (K_{act}^{COT} , right axis, triangles) coagulation assays scaled as a function of procoagulant surface energy expressed as water adhesion tension $\tau^o = \gamma_{lv}^o \cos \theta$, where the 'o' superscript denotes pure PBS buffer with interfacial tension $\gamma_{lv}^o = 72$ dyne/cm at 25 °C, exhibiting contact angles θ on test surfaces measured in both advancing (filled symbols) and receding modes (open symbols). Uncertainty indicated by error bars represent standard deviation of mean for K_{act}^{SAT} (N=3) and range for K_{act}^{COT} (N =2). Note that K_{act}^{SAT} and K_{act}^{COT} are two different measures of procoagulant catalytic activity with two different dimensions. Each suggests an exponential-like dependence on procoagulant surface energy as measured by τ^o .

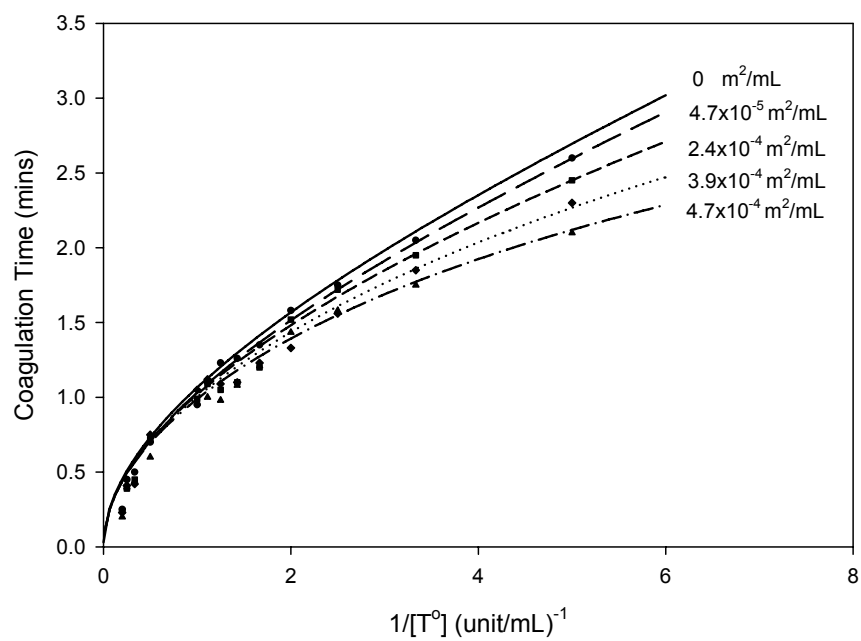


Fig. 3.3: Representative thrombin titration curves in the presence of varying surface area of fully-water-wettable glass procoagulants.

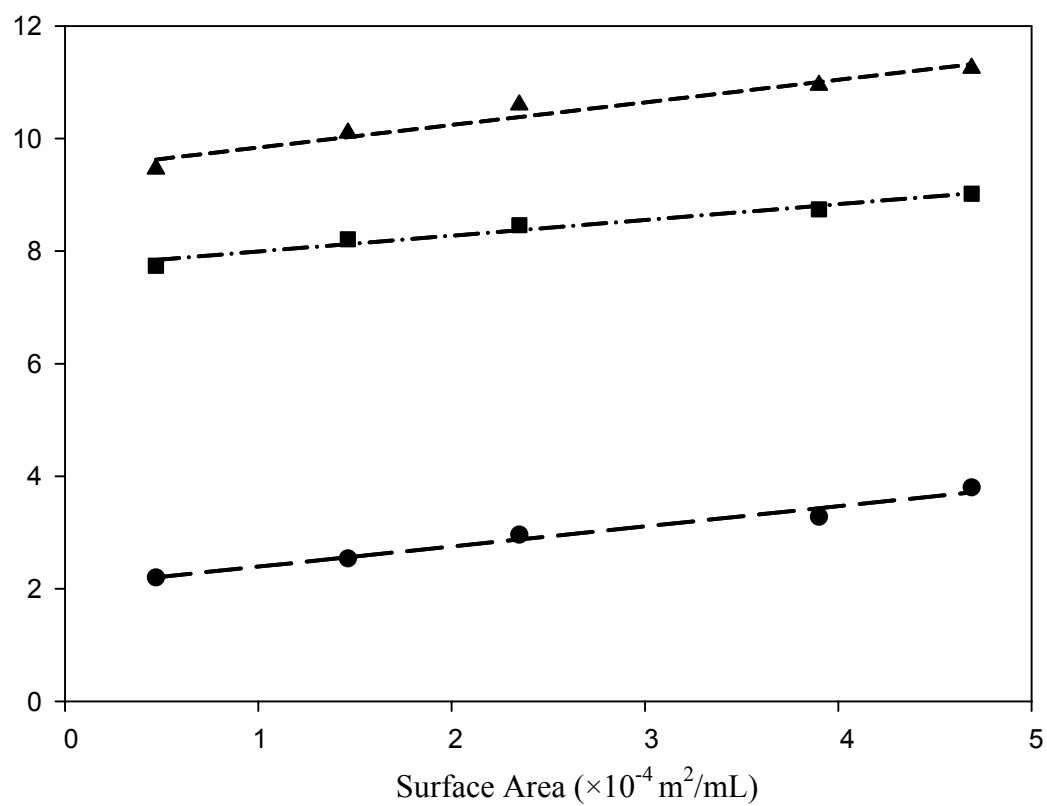


Fig. 3.4: Bolus thrombin concentration Θ produced by varying surface area of glass-sphere procoagulants with different surface chemistries (\bullet clean glass, \blacktriangle APS treated glass, \blacksquare OTS treated glass).

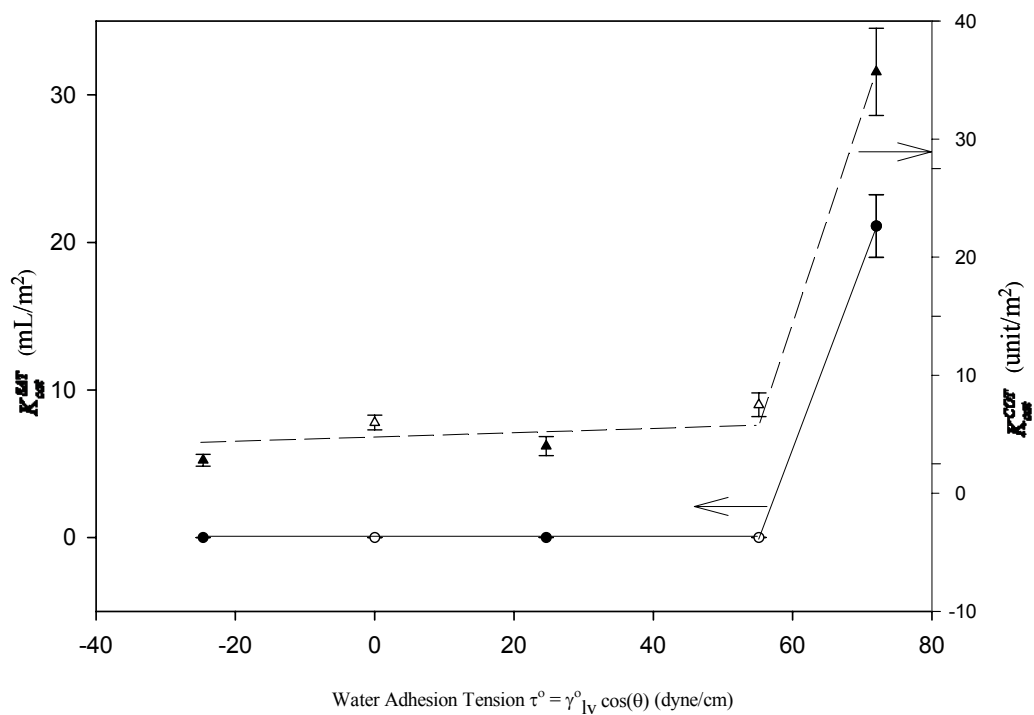


Fig. 3.5: Procoagulant catalytic potential derived from SAT (K_{act}^{SAT} , left axis, circles) and COT (K_{act}^{COT} , right axis, triangles) coagulation assays scaled as a function of procoagulant surface energy expressed as water adhesion tension.

Table 3.2: Endogenous FIIa Production

Surface Area of Procoagulants ($10^{-4} \times \text{m}^2/\text{mL}$)	Trial Number	Clean Glass Θ ($10^{-2} \times \text{unit}/\text{mL}$)	APS Treated Glass Θ ($10^{-3} \times \text{unit}/\text{mL}$)	OTS Treated Glass Θ ($10^{-3} \times \text{unit}/\text{mL}$)
0.47	1	2.10	9.37	7.67
	2	2.31	9.56	7.80
1.5	1	2.55	10.2	8.20
	2	2.43	10.0	8.02
2.4	1	3.06	10.5	8.46
	2	2.87	10.6	8.37
3.9	1	3.40	10.9	8.81
	2	3.27	11.0	8.66
4.7	1	3.61	11.3	8.94
	2	3.98	11.5	9.10

3.4 Retention of Procoagulant Catalytic Potential

Fig. 3.6 collects results of repeated coagulation assays in a single, clean glass tube following the protocol outlined in the Methods and Materials section. As shown in

Fig. 3.6, coagulation time (CT , min) of plasma in a single clean glass tube used in multiple coagulation assays does not vary significantly, implying that procoagulant surfaces remain activating throughout the course of plasma-coagulation experiment (see Methods and Materials for protocol). Uncertainty indicated by error bars represent standard deviation of the mean of three separate trials ($N=3$). Mean and standard deviation of three replicate tubes indicated that no single trial could be confidently distinguished from the average of 6.9 ± 0.7 min. These results corroborate previous studies with porcine PPP [6, 30] and demonstrate that repeated activation of plasma coagulation does not measurably affect the procoagulant potential of a surface exposed to whole plasma.

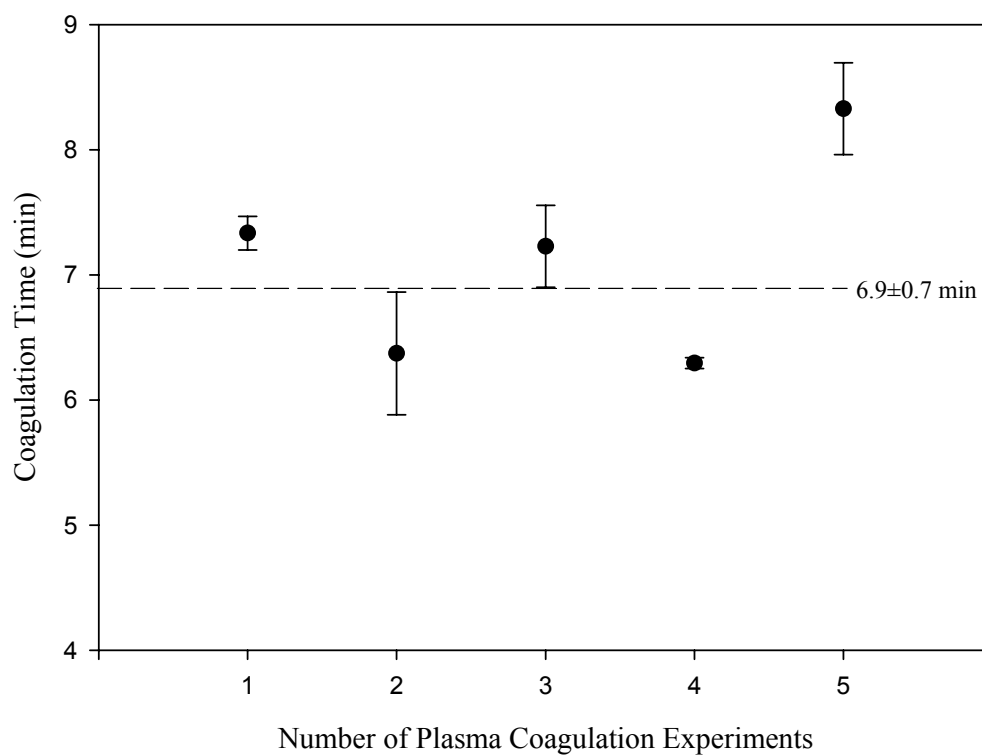


Fig. 3.6: Coagulation time (CT , min) of plasma in a single clean glass tube used in multiple coagulation assays.

3.5 Discussion

Smooth and reproducible results obtained by thrombin titration (TT), surface-area titration (SAT), and thrombin-surface-area co-titration (COT) coagulation assays applied to human PPP verify that re-calcified plasma is a reproducible, robust test system for the investigation of enzyme and surface-activated coagulation in vitro. Quality of the

fit of the SAT, TT, and COT models represented by Eq. 2.1 to 2.3 of the Methods and Materials section to experimental data strongly suggests that simplifying assumptions underlying theory were reasonable approximations of reality and the parameters of these models are important controlling factors. When scaled to procoagulant surface properties, these parameters provide insights into the hemocompatibility of materials; at least from the perspective of platelet poor plasma that is substantially depleted of cellular contributions to coagulation.

SAT curves (Fig. 3.2) obtained using clean glass beads, APS, and OTS silane-modified glass beads formed nested, nearly parallel curves on the same axes, giving visual testimony to the conclusion drawn from studies of porcine PPP that procoagulants have variable, surface-energy-dependent catalytic potential [6, 7, 30]. Fit of the SAT model (Eq. 2.1 of Materials and Methods) K_{act}^{SAT} quantifies this procoagulant catalytic potential and Fig. 3.5 suggests that K_{act}^{SAT} scales sharply with procoagulant surface energy (as measured by water adhesion tension) in a manner similar to that observed with porcine PPP; although this work explored a much more limited selection of procoagulant surfaces than previous work.

Co-titration is an interesting extension of SAT experiments in which the intrinsic cascade is activated to produce endogenous FIIa in the presence of increasingly-concentrated exogenous FIIa spikes. Fig. 3.3 shows that endogenous FIIa produced by serially-increasing surface area of clean glass procoagulant adds to the exogenous thrombin spike used in the titration experiment (compare also to Fig. 3.1B noting differences in $[T^o]^{-1}$ scaling). Interpreted in terms of the COT model of Eq. 2.3,

endogenously-produced FIIa adds to the exogenous spike in a manner dependent on both surface area and surface energy of the solid procoagulant. Smooth lines through the data of Fig. 3.3 result from the fit of Eq. 2.3 to the data, yielding an estimate of the amount of endogenous FIIa produced, as measured by the fitted parameter Θ . Fig. 3.4 shows that Θ scales linearly with procoagulant area with a slope K_{act}^{COT} that is a measure of procoagulant catalytic potential to produce endogenous FIIa. Thus K_{act}^{COT} is analogous to K_{act}^{SAT} obtained from SAT curves in that both measure the propensity of a surface to potentiate the intrinsic pathway. It is important to stress, however, that these two different parameters were obtained from two completely different assays are based on two different models of coagulation, and have different dimensions (unit/m² compared to mL/m², respectively). However, as shown in Fig. 3.5, these independent measures of procoagulant catalytic potential yield similar trends with procoagulant surface energy, suggesting that there is indeed a sharp dose-response relationship between surface energy and procoagulant catalytic potential, similar to that observed in porcine PPP[6, 30]. Firm functional relationships between procoagulant catalytic potential and procoagulant surface energy for human PPP awaits similar studies embracing a greater selection of surface types.

An important assumption underlying both SAT and COT models was that FIIa is produced by activation of the intrinsic cascade of plasma coagulation as a bolus concentration, as opposed to continuous production of FIIa by the continuous presence of procoagulant surface area. Quality of fit of these models to experimental data suggests this assumption was reasonable and that FIIa was produced in bolus-concentration

proportion to the intensity of activation as measured by procoagulant surface area or energy (water wettability). It is noted that this conclusion is consistent with direct measurement of FIIa generation by chromogenic assays in which it was observed that FIIa concentration rises sharply with time in contact with Ti alloys and remains relatively constant throughout the coagulation reaction [31]. Results also corroborate conclusions based on thrombin-aptamer titration of endogenous thrombin produced by activation of the intrinsic cascade [7]. However, results reported herein seem inconsistent with FIIa-burst kinetics reported to occur in whole blood [24, 32, 33] where FIIa generation occurs predominately on and within cells [33]. Furthermore, burst intensity in proportion to surface activation appears to be inconsistent with a self-amplifying mechanism of FIIa production mediated by cofactors (FVa and FVIIIa) assembled on cell membranes.

It is of interest to speculate how this rather remarkable production of FIIa in bolus-concentration proportion to the intensity of procogulant activation occurs. The control mechanism must lie between surface activation of FXII and FIIa generation – the two points of cascade activation explored in this work. Apparently, biochemistry of the intrinsic cascade is effectively turned off in the continuous presence of an activating procoagulant surface since experiments summarized in Fig. 3.6 show that strongly-activating procoagulant surfaces remain activating through multiple applications, discounting the possibility of procoagulant poisoning or deactivation by fouling with plasma proteins; at least for the clean-glass procoagulants studied herein. Suggestion that FXI is activated by FIIa in plasma [34, 35] seems inconsistent with results reported herein because this would presumably lead to continuous amplification of procoagulant activation rather than punctuated deactivation. Rather, work of Mitropolous *et al.* [36],

showing that FXIIa inhibits the $\text{FXII} \rightarrow \text{FXIIa}$ appears to be a more likely process that could lead to a self-termination reaction that effectively sends an activating pulse down the coagulation cascade, culminating in discontinuous production of FIIa in proportion to the originating stimulus.

3.6 Summary

Human plasma has been shown to be a robust experimental system for studies of the surface activation of coagulation in vitro. Three different coagulation assays provide a measure of the dynamic range of coagulation time that can be explored using exogenous thrombin (FIIa) spikes (thrombin titration, TT) and/or surface activation of the intrinsic pathway of coagulation (surface area titration, SAT or thrombin-surface area titration, COT). Mathematical models of TT, SAT, and COT assays predicated on the idea that FIIa is available as a bolus concentration (either as an exogenous spike as in TT or an endogenous bolus produced by the intrinsic cascade in SAT) give excellent fit to experimental data, strongly suggesting that simplifying assumptions underlying theory were reasonable approximations of reality and that model parameters are important controlling factors.

Results of SAT and COT assays strongly suggest that endogenous FIIa is produced by potentiation of the intrinsic pathway of plasma coagulation in bolus concentration-proportion to the intensity of procoagulant activation, as measured by surface area and surface energy. The control mechanism leading to bolus FIIa production apparently lies between FXII activation and FIIa generation, is shown not to be inhibited

or limited by the absolute concentration of FIIa in plasma, and is not consistent with cell-mediated thrombin-burst kinetics observed in whole blood. Furthermore, experimental results show that procoagulant surfaces remain activating throughout the coagulation process, suggesting that the cascade must somehow be deactivated or ‘turned off’ soon after being activated or ‘turned on’, as opposed to continuous FIIa generation by a continuously-activated intrinsic cascade. The FXII→FXIIa reaction itself seems a likely point of control, as has been suggested previously, but the exact surface-mediated steps involved are not apparent from this work. In any event, the traditional biochemistry of surface activation to the plasma coagulation cascade appears to require elaboration/modification to account for bolus production of thrombin in a strict concentration-proportion to the activating procoagulant dose.

3.7 References

1. Rose E.A., Gelijns A.C., Moskowitz A., Heitjan D.F., Stevenson L.W., Dembitsky W., et al. Long-term Use of a Left Ventricular Assist Device for End-Stage Heart Failure. *N. Engl. J. Med.* 2001;345(20):1435-1443.
2. Lavine M., Roberts M., Smith O. Bodybuilding: The Bionic Human. *Science* 2002;295:995-1032.
3. Ratner B.D. Blood Compatibility-A Perspective. *J. Biomat. Sci. Polym. Ed.* 2000;11(11):1107-1119.
4. Ratner B.D. The Blood Compatibility Catastrophe. *J. Biomed. Mat. Res.* 1993;27:283-287.
5. Pappas N.A, Langer R. New Challenges in Biomaterials. *Science* 1994;263:1715-1719.
6. Vogler E.A, Graper J.C, Harper G.R, Lander L.M, Brittain WJ. Contact Activation of the Plasma Coagulation Cascade.1. Procoagulant Surface Energy and Chemistry. *J. Biomed. Mat. Res.* 1995;29:1005-1016.
7. Vogler E.A, Nadeau J.G, Graper J.C. Contact Activation of the Plasma Coagulation Cascade. 3. Biophysical Aspects of Thrombin Binding Anticoagulants. *J. Biomed. Mat. Res.* 1997;40(1):92-103.
8. Brown B. Hematology: Principles and Procedures. 3 ed. Philadelphia: Lea and Febiger; 1980.

9. Kogan A.E., Kardakov D.V., Khanin M.A. Analysis of the Activated Partial Thromboplastin Time Test Using Mathematical Modeling. *Thromb. Res.* 2001;101:299-310.
10. Martorana F, Moro A. On the Kinetics of Enzyme Amplifier Systems with Negative Feedback. *Mathematical Biosciences* 1974;21:77-84.
11. Martorana F. Some considerations on the Enzyme Amplifier System: the Blood Clotting. *J. Nuclear Med. and Allied Sci.* 1978;22(4):181-183.
12. Levine S.N. Enzyme Amplifier Kinetics. *Science* 1966;152:651-653.
13. MacFarlane R.G. An Enzyme Cascade in the Blood Clotting Mechanism and its Function as a Biochemical Amplifier. *Nature* 1964:498-499.
14. Khanin M.A, Semenov V.V. A Mathematical Model of the Kinetics of Blood Coagulation. *J. Theor. Biol.* 1989;136:127-134.
15. Kirchhofer D, Tschopp T.B, Baumgartner H.R. Active Site-Blocked Factors VIIa and IXa Differentially Inhibit Fibrin Formation in a Human Ex Vivo Thrombosis Model. *Arteriosclerosis, Thrombosis, and Vascular Biology* 1995;15:1098-1106.
16. Rand M.D, Lock J.B. Blood Clotting in Minimally Altered Whole Blood. In: Annual meeting of the American Society of Hematology; 1995; San Diego, California; 1995.
17. Peyrou V, Lormeau J.C, Herault J.P, Gaich C, Pflieger AM, Herbert JM. Contribution of Erythrocytes to Thrombin Generation. *Thrombosis Haemostasis* 1999;81:400-406.
18. Xu C.Q, Zeng Y.J, Gregersen H. Dynamic model of the role of platelets in the blood coagulation system. *Medical engineering & Physics* 2002;24:587-593.

19. Butenas S, Mann K.G. Evaluation of the Initiation Phase of Blood Coagulation Using Ultrasensitive Assays for Serine Proteases. *The Journal of Biological Chemistry* 1997;272(34):21527-21533.
20. Engelmann B, Luther T, Muller I. Intravascular tissue factor pathway - a model for rapid initiation of coagulation within the blood vessel. *Thrombosis Haemostasis* 2003;89(1):3-8.
21. Jesty J, Beltrami E, Willems G. Mathematical analysis of a proteolytic positive-feedback loop: Dependence of lag time and enzyme yields on the initial conditions and kinetic parameters. *Biochemistry* 1993;32:6266-6274.
22. Beltrami E, Jesty J. Mathematical analysis of activation thresholds in enzyme-catalyzed positive feedbacks: Application of the feedbacks of blood coagulation. *Proceedings of the National Academy of Sciences of the United States of America* 1995;92:8744-8748.
23. Hockin M.F, Jones K.C, Everse S.J, Mann K.G. A Model for the Stoichiometric Regulation of Blood Coagulation. *The Journal of Biological Chemistry* 2002;277(21):18322-18333.
24. Jones K.C, Mann K.G. A Model for the Tissue Factor Pathway to Thrombin. *The Journal of Biological Chemistry* 1994;269(37):23367-23373.
25. Lawson J.H, Kalafatis M, Stram S, Mann K.G. A Model for the tissue factor pathway to thrombin I. An Empirical Study. *The Journal of Biological Chemistry* 1994;269(37):23357-23366.

26. Pohl B, Beringer C, Bomhard M, Keller F. The quick machine - a mathematical model for the extrinsic activation of coagulation. *Haemostasis* 1994;24(6):325-337.
27. Kuharsky A.L, Fogelson A.L. Surface-Mediated Control of Blood Coagulation: The Role of Binding Site Densities and Platelet Deposition. *Biophysical journal* 2001;80:1050-1074.
28. Ataullakhanov F.I, Molchanova D.A, Pokhilko A.V. A simulated mathematical model of the blood coagulation system intrinsic pathway. *Biofizika* 1995;40(2):434-442.
29. Gregory G, Basmadjian D. An Analysis of the Contact Phase of Blood Coagulation: Effects of Shear Rate and Surface Are Intertwined. *Annals of Biomedical Engineering* 1994;22:184-193.
30. Mitropoulos K.A. The Levels of FXIIa Generated in Human Plasma on an Electronegative Surface are Insensitive to Wide Variation in the Concentration of FXII, Prekallikrein, High Molecular Weight Kininogen or FXI. *Thromb. Haemost.* 1999;82:1033-1040.
31. Vogler E.A, Graper J.C, Sugg H.W, Lander L.M, Brittain W.J. Contact Activation of the Plasma Coagulation Cascade.2. Protein Adsorption on Procoagulant Surfaces. *J. Biomed. Mat. Res.* 1995;29:1017-1028.
32. Ishitoya H, Kawamura M, Linneweber J, Motomura T, Ichikawa S, Nishimura I, et al. Titania gel reduces thrombin generation. *Artificial Organs* 2002;26(11):959-963.

33. Narayanan S. Multifunctional roles of thrombin. *Annals of Clinical & Laboratory Science* 1999;29(4):275-280.
34. Fenton J.W. Thrombin. In: Waltz DA, Fenton JW, Shuman MA, editors. *Bioregulatory Functions of Thrombin*. New York: The National Academy of Sciences; 1986. p. 5-15.
35. PA vdB, Meijers J, Bouma B. Feedback activation of factor XI by thrombin in plasma results in additional formation of thrombin that protects fibrin clots from fibrinolysis. *Blood* 1995;86(8):3035-3042.
36. Gailani D, Broze G.J. Factor XI activation in a revised model of blood coagulation. *Science*. 1991;253(5022):909-912.
37. Mitropoulos K.A. High affinity binding of factor XIIa to an electronegative surface controls the rates of factor XII and prekallikrein activation in vitro. *Thrombosis Research* 1999;94:117-129.

Chapter 4

Silicon Oxycarbide Glasses for Blood-Contact Applications

Silicon oxycarbide (SiO_xC_y) glass compositions are shown to exhibit a variable propensity to contact activate coagulation of whole human blood plasma that depends on X:Y surface stoichiometry. SiO_xC_y exhibit activation properties similar to pyrolytic carbon (PC) over a broad range of X:Y ratios. Surface composition of SiO_xC_y glass powders prepared by pyrolysis of thermosetting polysilsequioxanes roughly correlated with total carbon concentration of precursor resins and could be significantly modified by etching in alkaline solutions. Results suggest that SiO_xC_y may offer unique properties as a substitute for PC in medical-device applications demanding excellent tribological properties, such as artificial heart valves.

4.1 Introduction

Hard biocompatible materials exhibiting excellent tribological (friction and wear) properties are of considerable value in a wide variety of medical-device applications ranging from dentistry to orthopedics to reconstructive surgery. Pyrolytic carbon (PC), either in monolithic form or applied as a coating, has been a material of choice for such applications for more than 50 years [1], offering a bioadhesive surface [2, 3] with good hemocompatibility [4, 5]. In particular, PC has been widely applied in heart-valve

applications and is successfully used in a number of commercial products [5]. However, PC physical properties can be a limitation for applications demanding long-term mechanical stability under applied stress. Herein we report development of silicon oxycarbide (SiO_xC_y) glass compositions that may find biomedical applications as an alternative for PC.

Silicon oxycarbide (SiO_xC_y) glasses are novel amorphous materials in which carbon is substituted for oxygen within the Si-O matrix, greatly strengthening the molecular structure of the resulting glass network. Silicon is thus simultaneously bonded to carbon and oxygen in a configuration that can be controlled by the synthesis procedure [6, 7]. Carbon content can be as high as 70 mol%, depending on precursor materials used or the processing approach adopted [8]. SiO_xC_y glasses have tailorable physical properties that strongly depend on the microstructure (presence of phase separation and bonding state of carbon) and composition (carbon content). SiO_xC_y glasses exhibit remarkable mechanical properties including: elastic modulus, bending strength, hardness; chemical durability superior to conventional silicate glasses in aggressive environments; and resistance to oxidation at high temperature, devitrification, and creep. These unique properties strongly correlate with the increase in the average coordination number in the glass network [9-14]. SiO_xC_y can be fabricated by pyrolysis of suitable organosilane precursors at a temperature $> 800^\circ\text{C}$ [6-14], by Chemical Vapor Deposition (CVD) [15], or by reactive sputtering. The use of organosilane precursors permits fabrication of variously shaped (monolithic) ceramic objects (bulk or porous components [1, 16, 17], fibers [18], micro tubes [19], coatings [20] – provided that the substrate can withstand processing at moderate-to-high temperatures). Plasma and sputter deposition methods

permit formation of SiO_xC_y glass layers on a variety of substrata, especially including polymers with a relatively low-process-temperature window.

In this chapter, it is reported that the structure-property relationships connecting SiO_xC_y composition with the propensity to activate coagulation in whole human blood plasma. Results show that activation of the intrinsic pathway of the plasma coagulation cascade by contact with SiO_xC_y powders scales with oxygen content X. SiO_xC_y formulations with narrow range of X:Y ratios were developed that exhibited activation properties as low as hydrophobic silane-treated glass and it was found that a relatively broad range of X:Y ratios exhibited activation properties similar to PC. Results thus suggest that SiO_xC_y has utility in blood-contacting medical-device applications.

Table 4.1: Procoagulant Activity of SiO_x and SiO_xCy Glasses

Samples	K_{act}^{COT} (mL/m ²)
SiO _x	21±2
Silanized SiO _x	$(4.0±1.7)×10^{-4}$
Pyrolytic Carbon	0.5±0.1
SILRES 610	4.0±0.6
SiOC-A35	1.8±0.6
25-SILRES	3.5±0.6
50-SILRES	2.2±0.7
SR355	1.8±0.7
H44	0.9±0.3
SILRES 601	2.3±0.2
Etched SILRES 610	3.6±0.2
Etched SiOC-A35	6.3±0.3
Etched 25-SILRES	3.6±0.2
Etched 50-SILRES	2.4±0.2
Etched SR 355	1.8±0.8
Etched H44	0.21±0.03
Etched SILRES 601	2.2±0.1

4.2 SiO_xC_y Glasses

Pyrolysis at 1200 °C converted all silicone resins to an amorphous SiO_xC_y ceramic material with 75-85% yield (weight ratio of the ceramic residue to the starting material). X-ray diffraction (Fig. 4.1) showed that the resulting ceramic was completely amorphous. XPS surface composition collected in Table 2.1 showed that the total surface carbon roughly correlated with the carbon composition of starting materials (Table 2.1). However, samples H44 and 50-SILRES had a much higher surface C composition than in the bulk, whereas surface carbon for samples 25-SILRES, SR355 and SILRES 601 was lower. Variations among starting precursors possibly reflect variable stability of glass compositions to high-temperature carbothermal reduction [21]. Alkaline etching of ceramic powders reproducibly modified surface composition but in a manner seemingly uncorrelated with starting composition.

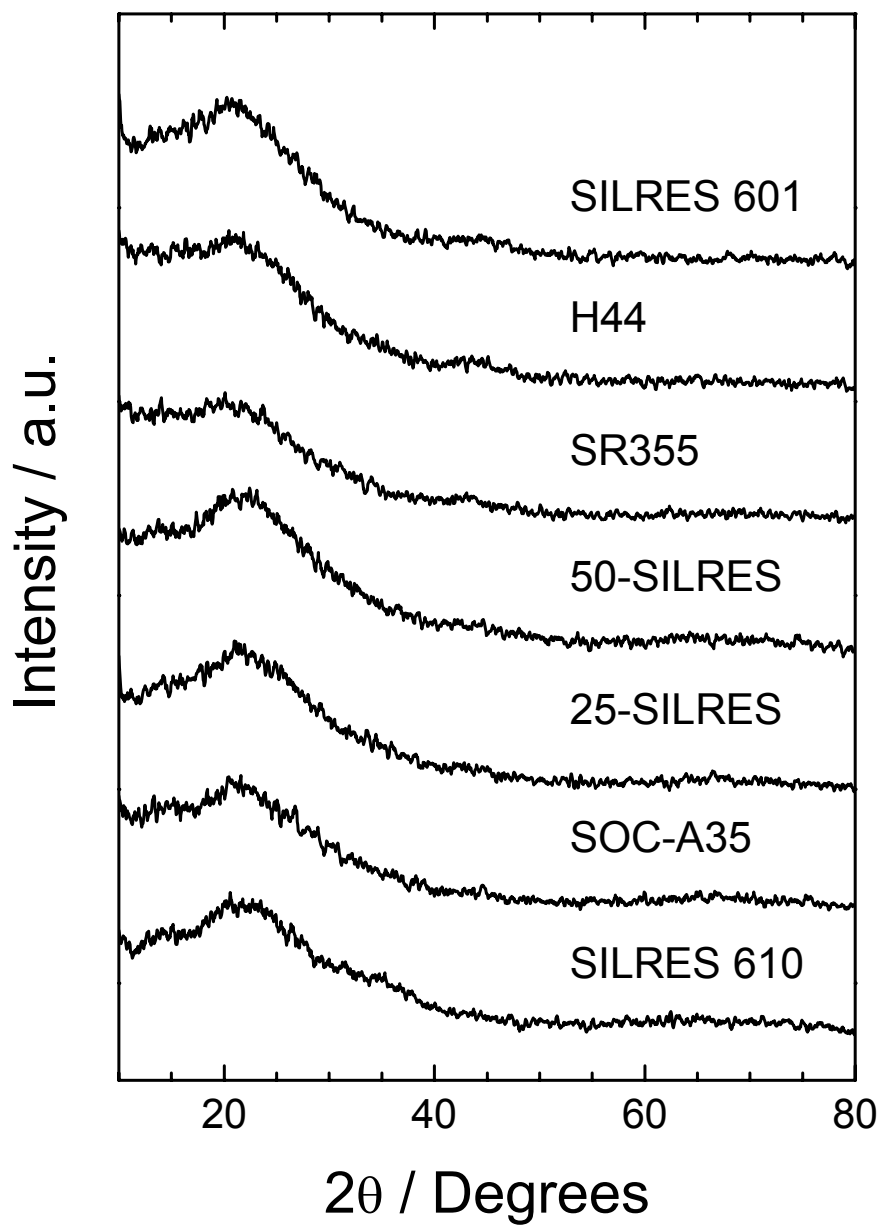


Fig. 4.1 X-ray diffraction pattern of the SiO_xC_y glasses prepared by pyrolysis of polysilsequioxanes.

4.3 Plasma Activation

Contact activation of human platelet poor plasma (PPP) coagulation was used as a measure of SiO_xC_y hemocompatibility. This assay measures only propensity to activate the homoral phase of blood coagulation and does not assess platelet activation that would be required for a more rigorous measure of whole-blood contact properties. Reduction in PPP coagulation time (CT) with serially-increasing area of test procoagulant surface (surface area titration or SAT assay (see refs. [22-24]) was measured for SiO_xC_y formulations listed in Table 2.1 for comparison to hydrophobic (negative control) and hydrophilic glass beads (positive control). Fig. 4.2 graphically compares selected SiO_xC_y formulations, showing that SiO_xC_y activation properties fall broadly between the negative and positive procoagulant controls, depending on X:Y stoichiometry, and were generally comparable to the PC comparison specimen. SiO_xC_y activation properties were quantitatively ranked on an internally-consistent basis by statistical least-squares fitting of SAT data like that illustrated in Fig. 4.2 to Eq. 2.1 of Methods and Materials, yielding an activation parameter K_{act}^{SAT} with dimensions of mL/m^2 . Procoagulants that strongly activate plasma coagulation on a per-unit-area basis have characteristically higher K_{act}^{SAT} values. Table 4.1 collects K_{act}^{SAT} values obtained for SiO_xC_y formulations listed in Table 2.1 along with positive/negative glass controls. Numerical ranking confirms visual comparison afforded by Fig. 4.2 in that SiO_xC_y was found to be a much less efficient procoagulant (better hemocompatibility) than clean glass controls but generally more

activating than silanized glass negative controls. Note that it was not possible to quantitatively compare SiO_xC_y to PC because PC film specimens were not amenable to quantitative SAT analysis. Evidently, however, SiO_xC_y and PC activation properties were qualitatively similar, as shown in Fig. 4.3. Previous work has shown that K_{act}^{SAT} scales sharply, almost discontinuously, with procoagulant water wettability [22-25]. Based on this trend, it is suggested that SiO_xC_y K_{act}^{SAT} correlates with atomic % oxygen measured by XPS, as shown by the arbitrary trend line drawn through the data of Fig. 4. (formulations with incrementally-increasing oxygen compositions within the 56<%O<60 range were unavailable to confirm the suggested trend).

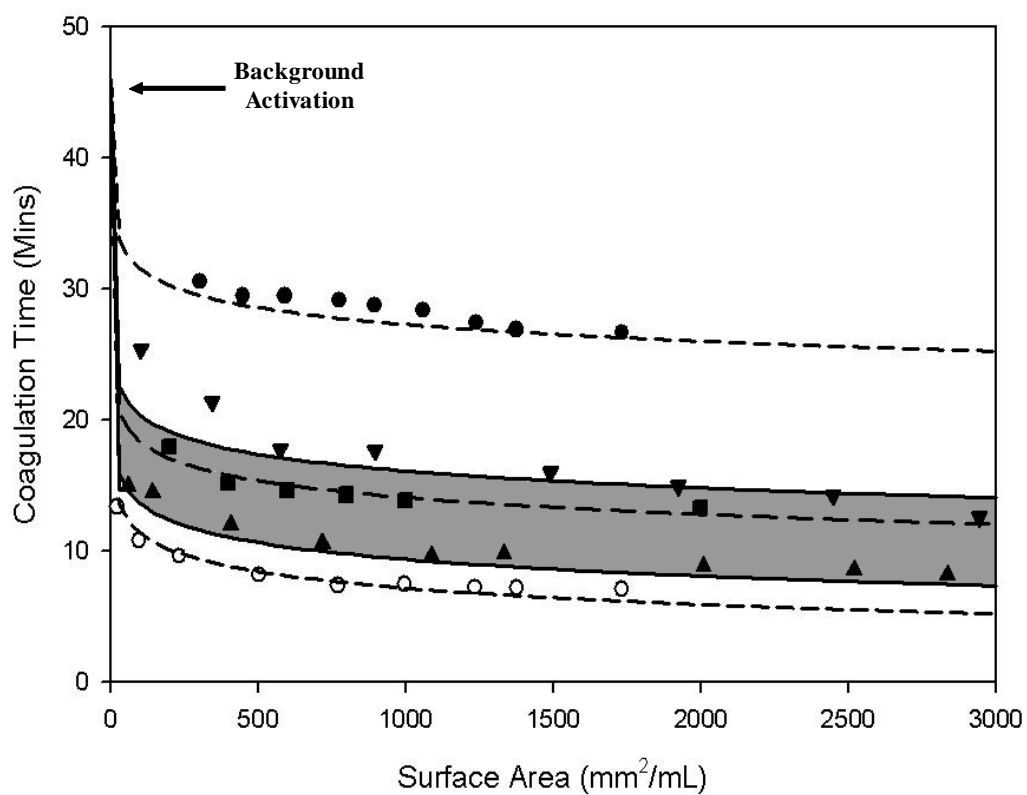


Fig. 4.2: Coagulation of human blood plasma coagulation induced by contact with variable surface area of SiO_xC_y glass powders compared to hydrophilic (water-wettable) SiO_x glass (open circles), hydrophobic silanized SiO_x glass (filled circles), and pyrolytic carbon (PC, filled squares).

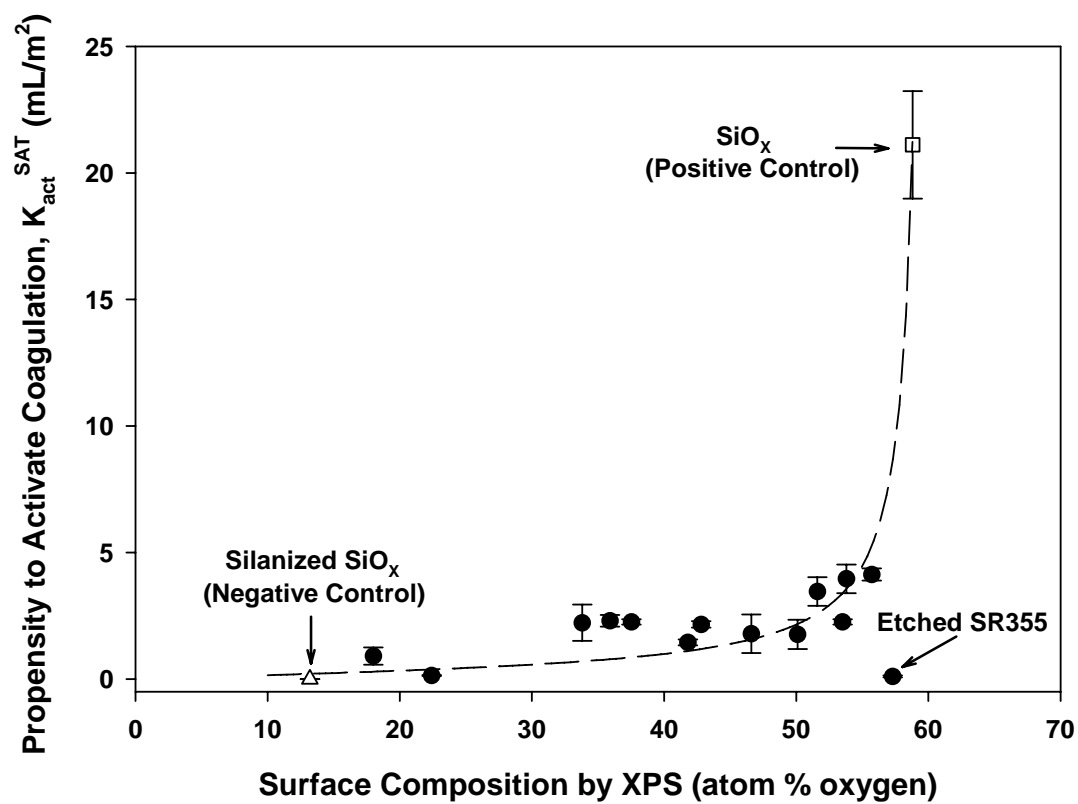


Fig. 4.3: K_{act}^{SAT} versus (surface) oxygen content for the various SiO_xC_y and reference samples. (● OTS treated glass, ○ clean glass, ▲ SiO_xC_y glass samples).

4.4 Discussion

Silicon oxycarbide (SiO_xC_y) glasses are novel amorphous materials for which physical properties such as modulus, durability, and resistance to hydrolysis/oxidation can be synthetically tailored by controlling the X:Y ratio. These glasses can be prepared in monolithic form or coated onto various materials, including polymers, using plasma deposition techniques for example. It has been found that the propensity of silicon oxycarbide glasses to activate blood plasma coagulation also depends on the X:Y stoichiometry. Inclusion of as little as 20 atom % carbon (as measured by XPS) greatly improves hemocompatibility of SiO_xC_y in this regard, relative to the SiO_x surface chemistry of ordinary soda-lime glass. In fact, SiO_xC_y activation properties were found to be comparable to pyrolytic carbon over a broad range of X:Y ratios and as inert as silanized glass (negative) controls at carbon compositions exceeding 60%. Ability to tailor physical properties combined with improved hemocompatibility suggests that silicon oxycarbide glasses may find use in medical applications requiring good tribological properties and blood compatibility, such as in mechanical heart valves. The data trend of Fig. 4.3 suggests that the ‘catalytic potential’ K_{act}^{SAT} of SiO_xC_y scales with surface oxygen composition Y, as measured by XPS. This trend is consistent with the finding that contact activation of plasma coagulation is a strong function of water wettability [22-25] because water wettability generally increases with surface oxygen composition [26] due to the commensurate increase in hydrogen-bonding surface sites.

Chemical etching was shown to alter surface composition. However, K_{act}^{SAT} of etched SiO_xC_y specimens fell within the same general trend in oxygen surface composition as unetched specimens, suggesting that chemical etching is a route to manipulate hemocompatibility independent of bulk properties.

4.5 Summary

Activation of the plasma phase of blood coagulation by silicon oxycarbide (SiO_xC_y) glass compositions varied with X:Y ratio and were comparable to a pyrolytic carbon standard over a broad range of compositions. Results of the human plasma coagulation activation assay employed to quantify hemocompatibility suggested that SiO_xC_y propensity to activate coagulation scales sharply with oxygen surface composition as measured by XPS, although formulations exhibiting surface oxygen within a relatively narrow 56<%O<60 range would be required to be definitive in this regard. In any event, it is clear that incorporation of as little as 20% carbon (as measured by XPS) sharply reduces plasma activation properties compared to the SiO_x composition of soda-lime glass (positive) controls. Activation properties of of higher-carbon-content SiO_xC_y (> 60%) were similar to non-activating, silanized glass (negative controls).

4.6 References

1. Haublod, A.D. and Shim H.S., Carbon in Biomedical Devices, in Biocompatibility of Clinical Implant Materials, D.F. Williams, Editor. 1979, CRC Press: Boca Raton, Fla. p. 3-24.
2. Cenni, E., et al., Adhesive Protein Expression on Endothelial Cells After Contact in vitro with Polyethylene terephthalate Coated with Pyrolytic Carbon. *Biomaterials*, 1995. 16: p. 1223-1227.
3. Stary, V., et al., Biocompatibility of the Surface Layer of Pyrolytic Carbon. *Thin Solid Films*, 2003. 433: p. 191-198.
4. Cenni, E., et al., Platelet and Coagulation Factor Variations Induced in vitro by Polyethylene terephthalate (Dacron) Coated with Pyrolytic Carbon. *Biomaterials*, 1995. 16: p. 973-976.
5. Gott, V.L., Alejo, D.E., and Cameron, D.E., Mechanical Heart Valves: 50 Years of Evolution. *Ann. Thorac. Surg.*, 2003. 76: p. S2230-S2239.
6. Corriu, R.J, Mutin, P.H., Vioux, A., Preparation and Structure of Silicon Oxycarbide Glasses Derived from Polysiloxane Precursors. 1997. 88: p. 327-330.
7. Pantano, C.G., Zhang, H., Silicon Oxycarbide Glasses. *J. Sol-Gel Sci.Tech.*, 1999. 14: p. 7-25.
8. Scheffler, M., Takahashi, T., Kaschta, J., Muensted, H., Buhler, P., Greil, P., Pyrolytic decomposition of preceramic organo polysiloxanes. *Innovative*

- Processing and Synthesis of Ceramics, Glasses, and Composites IV: Ceramic Transactions, 2000. 115: p. 239-250.
9. Eguchi, K., Silicon Oxycarbide Glasses Derived from Polymer Precursors. *J. Sol-Gel Sci. Tech.*, 1998. 13: p. 945-949.
 10. Turquat, C., Gregori, G., Walter, S., Sorarù, G.D., Transmission Electron Microscopy and Electron Energy-Loss Spectroscopy Study of Nonstoichiometric Silicon-Carbon-Oxygen Glasses. *J. Am. Ceram. Soc.*, 2001. 84: p. 2189-2196.
 11. Rouxel, T., Vicens, J., Creep Viscosity and Stress Relaxation of Gel-Derived Silicon Oxycarbide Glasses. *J. Am. Ceram. Soc.*, 2001. 84: p. 1052-1058.
 12. Rouxel, T., Keryvin, V., Sorarù, G.D., Surface Damage Resistance of Gel-Derived Oxycarbide Glasses: Hardness, Toughness, and Scratchability. *J. Am. Ceram. Soc.*, 2001. 84: p. 2220-2224.
 13. Walter, S., Brequel, H., Enzo, S., Microstructural and mechanical characterization of sol gel-derived Si-O-C glasses. *J. Europ. Ceram. Soc.*, 2002. 22: p. 2389-2400.
 14. Sorarù, G.D., Guadagnino, E., Colombo, P., Egan, J., Pantano, C.G., Chemical Durability of Silicon Oxycarbide Glasses. *J. Am. Ceram. Soc.*, 2002. 85: p. 1529-1536.
 15. Song, S.R., Chemical Vapor Deposition of Silicon Oxycarbide Thin Films by Oxy-Carbonization of $\text{SiH}_4\text{-CO}_2\text{-C}_2\text{H}_4$ Mixtures. Ph.D. Dissertation. Pennsylvania State University, University Park, PA., 1999.
 16. Greil, P., Polymer Derived Engineering Ceramics. *Adv. Eng. Mat*, 2000. 2: p. 339-348.

17. Colombo, P., Ceramic foams from preceramic polymers. *Mat. Res. Innovat.*, 2002. 6: p. 260-272.
18. Hu, Y., Preparation of silicon oxycarbide glass fibers from organically modified silicates. *J. Mater. Sci*, 2000. 35: p. 3155-3159.
19. Colombo, P., Bernardo, E., Capelletti, T., Maccagnan, G., Ceramic Microtubes from Preceramic Polymers. *J. Am. Ceram. Soc.*, 2003. 86: p. 1025-1027.
20. Takamura, N., Gunji, T., Abe, Y., Preparation of Silicon Oxycarbide Ceramic Films by Pyrolysis of Polymethyl- and Polyvinylsilsesquioxanes. *J. Sol-Gel Sci.Tech.*, 1999. 16: p. 227-234.
21. Sorarù, G.D., High Temperature Stability of Sol-Gel-Derived SiOC Glasses. *J. Sol-Gel Sci. Tech.*, 1999. 14: p. 69-74.
22. Zhuo, R., et al., Procoagulant Stimulus Processing by the Intrinsic Pathway of Blood Plasma Coagulation. *Biomaterials*, 2005. 26: p. 2965-2973.
23. Vogler, E.A., et al., Contact Activation of the Plasma Coagulation Cascade.1. Procoagulant Surface Energy and Chemistry. *J. Biomed. Mat. Res.*, 1995. 29: p. 1005-1016.
24. Vogler, E.A., et al., Contact Activation of the Plasma Coagulation Cascade.2. Protein Adsorption on Procoagulant Surfaces. *J. Biomed. Mat. Res.*, 1995. 29: p. 1017-1028.
25. Vogler, E.A., Structure and Reactivity of Water at Biomaterial Surfaces. *Adv. Colloid and Interface Sci.*, 1998. 74(1-3): p. 69-117.
26. Vogler, E.A., Interfacial Chemistry in Biomaterials Science, in *Wettability*, J. Berg, Editor. 1993, Marcel Dekker: New York. p. 184-250.

Chapter 5

Contact Activation of Blood Factor XII

Contact activation of blood factor XII (FXII, Hageman factor) in neat-buffer solution is shown not to be specific for anionic hydrophilic procoagulants as proposed by the accepted biochemistry of surface activation. Rather, FXII activation in the presence of plasma proteins leads to an apparent specificity for hydrophilic surfaces that is actually due to a relative diminution of the FXII→FXIIa reaction at hydrophobic surfaces. FXII activation in neat-buffer solution was effectively instantaneous upon contact with either hydrophilic (clean glass) or hydrophobic (silanized glass) procoagulant particles, with greater FXIIa yield obtained by activation with hydrophobic procoagulants. In sharp contrast, both activation rate and yield were found to be significantly attenuated at hydrophobic surfaces in the presence of plasma proteins. Putative FXIIa produced by surface activation with both hydrophilic and hydrophobic procoagulants was shown to hydrolyze blood factor XI (FXI) to the activated form FXIa ($FXII \xrightarrow{FXIIa} FXIIa$) that causes FXI-deficient plasma to rapidly coagulate.

Contact activation of blood factor XII by hydrophobic surfaces is shown to be inhibited by a competitive-protein-adsorption effect that appears to greatly reduce efficiency of the FXII-surface contact event. By contrast, no such inhibition was observed at hydrophilic (fully-water-wettable clean glass) surfaces, presumably because proteins

do not competitively adsorb to these surfaces and block FXII-surface contact. FXII-concentration-dependent rates of contact activation were measured at both surface types to compare-and-contrast dependencies. It is proposed that FXII adsorption, autoinhibition of FXII activation, and FXIIa desorption are three essential steps leading to contact activation of FXII and release of FXIIa into the solution phase.

5.1 Introduction

Activation of the blood zymogen factor XII (FXII, Hageman factor) into an active enzyme form, FXIIa, by contact with material surfaces is an important issue in the development of cardiovascular biomaterials. FXIIa is the central member of a self-amplifying activation complex that potentiates the intrinsic pathway of blood plasma coagulation. In turn, activation of the coagulation cascade can lead to formation of thrombus on the surface of biomaterials during the acute phase of blood contact [1]. Hence, this surface-catalyzed FXII→FXIIa reaction (also termed autoactivation in the hematology literature [2]) has been identified as an important cause of poor biomaterial hemocompatibility[3-8]. Indeed, thrombosis remains the significant barrier to development and implementation of advanced in-dwelling blood pumps and ventricular assist devices [9, 10] .

Contact activation of FXII occurs through a poorly-understood interaction of FXII with material surfaces [2, 8] that is a matter of continued investigation in the laboratories[11-15]. It has been long held that FXII activation occurs most efficiently in

contact with “anionic”[16-18] or “hydrophilic” (water wettable) procoagulants [12] [13-15], presumably due to a chemically-specific binding event between FXII and surface-resident negative charges. Technical reasons supporting this contention are many, perhaps originating in the routine hematology-laboratory observation that plasma clots relatively quickly in glass (hydrophilic) tubes but slowly in plastic (relatively hydrophobic) tubes [20]. Specificity for anionic hydrophilic surfaces thus explains that little-or-no FXII activation is observed in plasma brought in contact with hydrophobic procoagulants because these surfaces bear no anionic functional groups. Indeed, our previous work studying coagulation time of animal[14, 19] and human[12] plasma in contact with procoagulants bearing different oxidized surface chemistries concluded that procoagulants exhibit a surface-energy-dependent “catalytic potential” to induce FXII→FXIIa [11-13], in basic accord with the traditional view of FXII activation.

However, results of continued investigation into the details of FXII activation disclosed in this chapter show that FXII is activated in neat-buffer solution with nearly equal efficiency by contact with either hydrophobic or hydrophilic surfaces, discounting the specific-binding-event explanation for FXII activation. Moreover, It is found that both FXII activation rate and FXIIa yield in whole plasma brought in contact with hydrophobic procoagulants is significantly lower than at an equal surface area of hydrophilic procoagulant. Thus, FXII activation is neither specific to anionic hydrophilic procoagulants nor do these surfaces exhibit enhanced catalytic potential. Rather, FXII activation by hydrophobic surfaces immersed in whole plasma is significantly slower than at hydrophilic procoagulants, giving rise to the appearance of a surface-energy-dependent catalytic potential.

Further more, activation rate and yield was found to be significantly attenuated at hydrophobic surfaces in the presence of plasma proteins. Thus it is concluded that FXII activation in the presence of plasma proteins leads to an apparent specificity for hydrophilic surfaces that is actually due to a relative diminution of the FXII→FXIIa reaction at hydrophobic surfaces. It is speculated that this depressed activation rate/yield is due to an adsorption competition between FXII and a host of other plasma proteins [21] that substantially reduces efficiency of the FXII contact step at hydrophobic surfaces immersed in plasma.

It is report in this chapter that FXII activation rate and yield at hydrophobic procoagulant surfaces can be controlled by manipulating the protein composition of the fluid phase. Results confirm an important role of competitive-protein adsorption in the FXII activation process that is unrelated to enzymatic inhibition or allosteric regulation. Measurement of FXII activation rate-and-yield dependence on FXII concentration at hydrophilic and hydrophobic procoagulants leads to formulation of an FXII activation model invoking FXII adsorption, autoinhibition of FXII activation, and FXIIa desorption as three essential steps leading to the surface-mediated FXII→FXIIa reaction and release of FXIIa into the solution phase.

5.2 Surface Activation of FXII in Neat-Buffer Solution and Plasma

Data collected in Table 5.1 compiles results of 30 min. contact-activation experiments in terms of putative FXIIa generated in 12dPPP or PPP on a PEU-per-mL-supernate or PEU-per-unit-area-procoagulant basis. Serial-buffer rinses did not remove

putative FXIIa activity from either hydrophilic or hydrophobic surfaces (columns 4 and 7 of Table 5.1). Insignificant FXIIa activity was recovered in the third buffer rinse of hydrophobic procoagulants whereas a slight-but-significant amount of FXIIa was eluted from hydrophilic counterparts (columns 3 and 6 of Table 5.1). Fig. 5.1 compares kinetics of free FXIIa generated by contact with hydrophilic and hydrophobic procoagulants in both neat FXII solutions (Panel A) and PPP (Panel B). FXIIa production was effectively instantaneous in neat FXII solutions but the rate was slowed for both hydrophobic and hydrophilic procoagulants in PPP. Moreover, final FXIIa yield at hydrophobic procoagulants was reduced three-fold in PPP compared to neat FXII and the kinetics indicated a complex, multi-modal behavior (as suggested by the guide line drawn through the data of Fig. 5.1 B).

Table 5.1: Contact Activation of FXII by 30 min. Incubation with Hydrophilic and Hydrophobic Procoagulants

Test Solutions	Procoagulant Surface Type (500 mm ²)					
	Hydrophilic			Hydrophobic		
	Supernatant FXIIa/mL (PEU x 10 ⁻²)	3 RD Rinse of Bound FXIIa/mL (PEU x 10 ⁻²)	3X Rinsed Bound FXIIa/mm ² (PEU x 10 ⁻⁵)	Supernatant FXIIa/mL (PEU x 10 ⁻²)	3 RD Rinse of Bound FXIIa/mL (PEU x 10 ⁻²)	3X Rinsed Bound FXIIa/mm ² (PEU x 10 ⁻⁵)
dPPP	N.D.	N.D.	N.D.	N.D.	N.D.	N.D.
Neat FXII	1.85±0.10	0.84±0.39*	4.05±0.59	3.15±0.29	0.48±0.44	1.84±0.54
RdPPP	1.74±0.13	1.24±0.38*	3.56±0.31	0.80±0.63	0.08±0.08	1.42±0.62
PPP	2.24±0.07	0.72±0.43*	1.53±0.83	1.04±0.41	0.04±0.04	0.35±0.15

Notes: Autoactivation of FXII measured in terms of Lot # Equivalent Units (PEU) FXIIa after 30 min. incubation of test solution in contact with hydrophilic (gas discharge treated) or hydrophobic (silanized) glass-bead procoagulants (500 mm²/test); mean ± std. dev.; N=3, N.D = not detected (< 10⁻³ PEU /mL or < 10⁻⁶ PEU /mm² based on std. dev. of replicate FXIIa measurements) . * signifies mean is significantly greater than 0 at p ≤0.1. dPPP=FXII-depleted platelet poor plasma with a dysfunctional contact activation system; RdPPP=dPPP reconstituted with FXII with a functional contact activation system; PPP=platelet poor plasma from normal donors; FXII=phosphate buffer solution of FXII at 30 ug/mL.

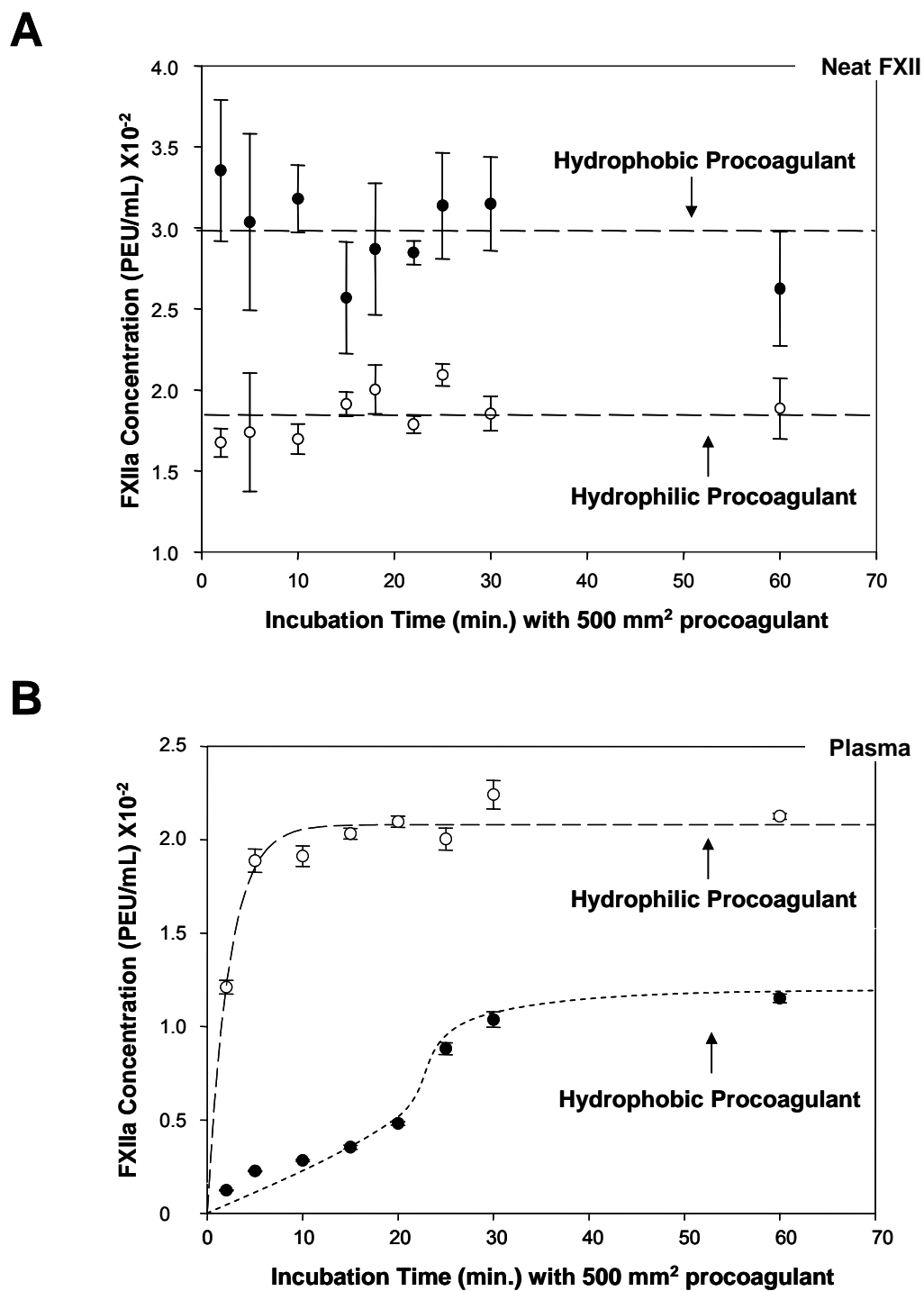


Fig. 5.1: Schematic experimental outline for detection of FXIIa produced by contact with procoagulant surfaces.

5.3 FXI Hydrolysis by Surface Activated FXII

Hydrolysis of FXI to FXIa by the products of FXII by surface activation ($FXI \xrightarrow{FXIIa} FXIa$; as outlined in Fig. 2.2) was used to confirm enzymic activity of activation products for FXI, an important component of the activation complex. Results are compiled in bar-graph form in Fig. 5.2 where the negative control was FXII solution incubated in a polystyrene tube with no added procoagulant. Bars compare supernate from 30 min. contact-activation experiments using hydrophilic or hydrophobic procoagulants, as shown in Fig. 5.2). The control is activation of FXII in a polystyrene tube with no added procoagulant particles. Error bars are the standard deviation of $N = 5$ replicate experiments. Results for hydrophilic and hydrophobic procoagulants were statistically identical (two-sample t test for $N=5$ at 95% confidence) and significantly different from control. The amount of FXIa produced by FXIIa hydrolysis did not significantly depend on the procoagulant type (hydrophilic or hydrophobic) used in the FXII activation step. Fig. 5.3 compares FXIa production kinetics induced by mixing FXI with FXII solutions after contact with either hydrophilic or hydrophobic procoagulants. Filled circles = supernate from FXII activation by hydrophilic procoagulants, filled squares = supernate from FXII activation by hydrophobic procoagulants (see Fig. 2.2). Error bars are the standard deviation of $N = 5$ replicate experiments (1σ). Slopes of the curves (from linear-least-squares regression) were statistically identical with null intercepts.

$$\text{Hydrophilic: } [FXIa] = (0.39 \pm 0.03)t - (0.46 \pm 0.52), R^2 = 97.4\%;$$

$$\text{Hydrophobic: } [FXIa] = (0.35 \pm 0.02)t - (0.44 \pm 0.45), R^2 = 97.8\%.$$

So Rates (slopes of least-squares best fit lines) were identical for hydrophilic and hydrophobic procoagulant cases.

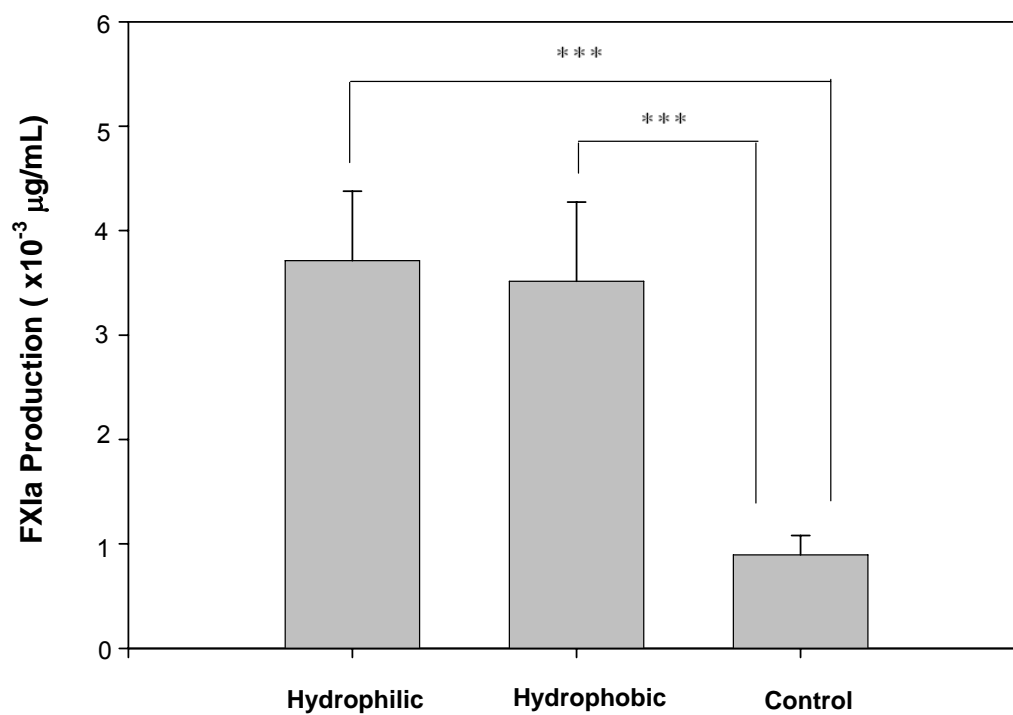


Fig. 5.2: FXIa produced by hydrolysis of FXI by products of FXII activation (30 min. incubation).

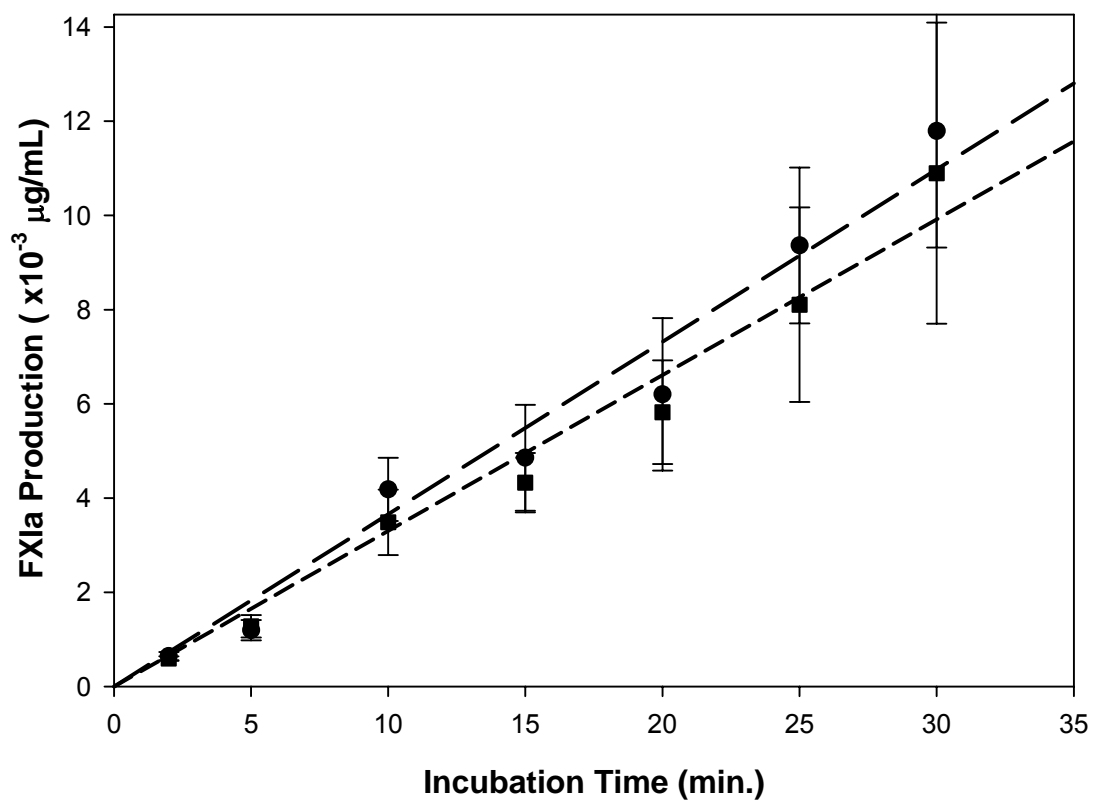


Fig. 5.3: Rate of FXIa hydrolysis by products of FXII activation.

5.4 Steady-State Surface Activation of FXII in Neat-Buffer Solution and a Protein Mixture

Fig. 5.4 compiles results of FXII activation experiments in which FXII solution concentration was varied over the range $0 \leq [FXII] \leq 30 \mu\text{g/mL}$ (physiological $[FXII] \sim 30 \mu\text{g/mL}$ or $0.4 \mu\text{M}$; also referred to as “1X” herein). Fig. 5.4 represents “steady state” activation (see kinetics discussed below) wherein FXII-containing solutions were contacted with hydrophilic or hydrophobic procoagulants. Results obtained in neat-buffer solution annotated “hydrophilic” and “hydrophobic” in Fig. 5.4 corroborate data shown in Fig. 5.1 that FXII activation is not specific to anionic hydrophilic surfaces, as proposed by the accepted biochemistry of surface activation. Rather, maximum steady-state FXIIa yield in contact with hydrophobic procoagulant was approximately 33% greater than that obtained at equivalent surface area hydrophilic procoagulant. A polystyrene (hydrophobic) tube containing no added procoagulant particles served as a kind of negative control. It is noted from Fig. 5.4 that activation from an “empty tube” contributes a small-but-measurable background to activation experiments. Results reported herein are not corrected for this background contribution.

Interestingly, when the solution phase was supplemented with 5 proteins unrelated to the plasma coagulation cascade, maximum steady-state FXIIa yield at hydrophilic procoagulants increased by approximately 65% and decreased by about 50% at hydrophobic procoagulants. These five proteins were human IgM (1000 kDa) and IgG (160 kDa) at 2 mg/mL each, human FAF and FV albumin (66 kDa) at 4 mg/mL each,

bovine albumin at 4 mg/mL; yielding a total of 16 mg/mL protein added to FXII. The only criteria for selection of these 5 proteins were (i) different protein types with (ii) size spanning 3 decades of MW and (iii) not being among proteins of the coagulation cascade.

The rate of FXIIa production exhibited an interesting $[FXII]$ dependence, asymptotically approaching maximum steady-state FXIIa yield through linear-like behavior over the $0 < [FXII] < 2 \mu\text{g} / \text{mL}$ range. Slope of the linear-like range (with units of PEU/ μg) was used to quantify initial rate of FXIIa production. Initial rate and maximum steady-state FXIIa yield are summarized in Table 5.2. Note that the initial phase for the empty tube control was more sigmoidal than linear in nature, possibly as a result of poor mixing of bulk solution with the tube wall.

Table 5.2: Maximum steady-state FXIIa yield and Initial Rate of FXII production

Condition	Maximum Steady-state Yield ($\times 10^{-2}$ PEU/mL)		Initial Rate ($\times 10^{-2}$ PEU/ μg)	
	Hydrophobic	Hydrophilic	Hydrophobic	Hydrophilic
Neat FXII	2.6 \pm 0.2	1.0 \pm 0.2	2.2 \pm 0.1	1.7 \pm 0.1
Neat FXII + 5 proteins	1.0 \pm 0.2	3.1 \pm 0.1	1.2 \pm 0.1	2.6 \pm 0.1

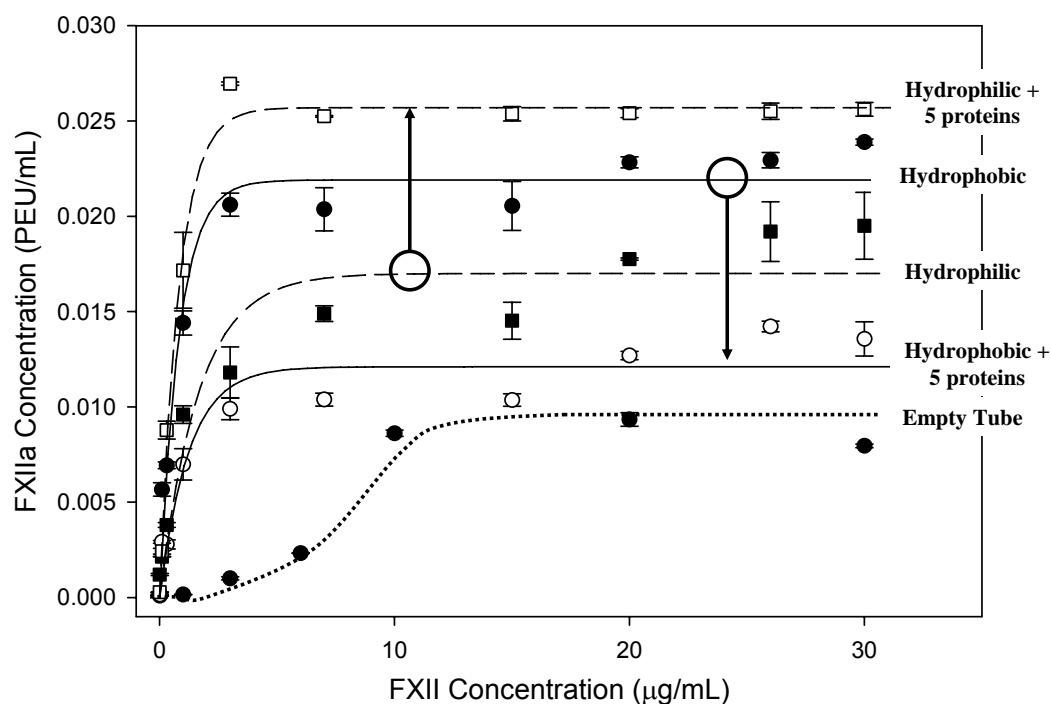


Fig. 5.4: FXII autoactivation in neat buffer solution optionally containing 8 mg/mL of 5 proteins unrelated to the plasma coagulation cascade.

5.5 FXII Activation Rate in Plasma

Fig. 5.5 compares FXII activation kinetics by hydrophilic (Panel A) and hydrophobic (Panel B) procoagulants (150 mm^2 nominal surface area) in plasma supplemented with exogenous spikes of FXII. Annotations of Fig. 5.5 A, B indicate FXII concentration in multiples of physiological concentration, wherein 1X = endogenous physiological concentration, no exogenous spike; 1.25 X = 25% exogenous spike; 1.5 X

= 50% exogenous spike, *etc.* Note that in all cases reported in Fig. 5.5 maximal FXIIa yield was reached well within 30 min. It is emphasized that activation-rate experiments reported in Fig. 5.5 reduced procoagulant surface area from 500 mm² used in steady-state activation studies to 150 mm² in an attempt to slow activation rate, especially for hydrophilic procoagulants.

With procoagulant surface area fixed at 150 mm², it is evident from data of Fig. 5.5 that serial increase in total plasma FXII concentration increased both rate and net production of FXIIa for hydrophilic and hydrophobic procoagulants. Fig. 5.6 plots both rate and maximum production of FXIIa as a function of $[FXII]$ expressed in multiples of physiologic concentration. Both parameters were directly proportional to $[FXII]$ for hydrophobic surfaces but appeared to saturate for hydrophilic procoagulants.

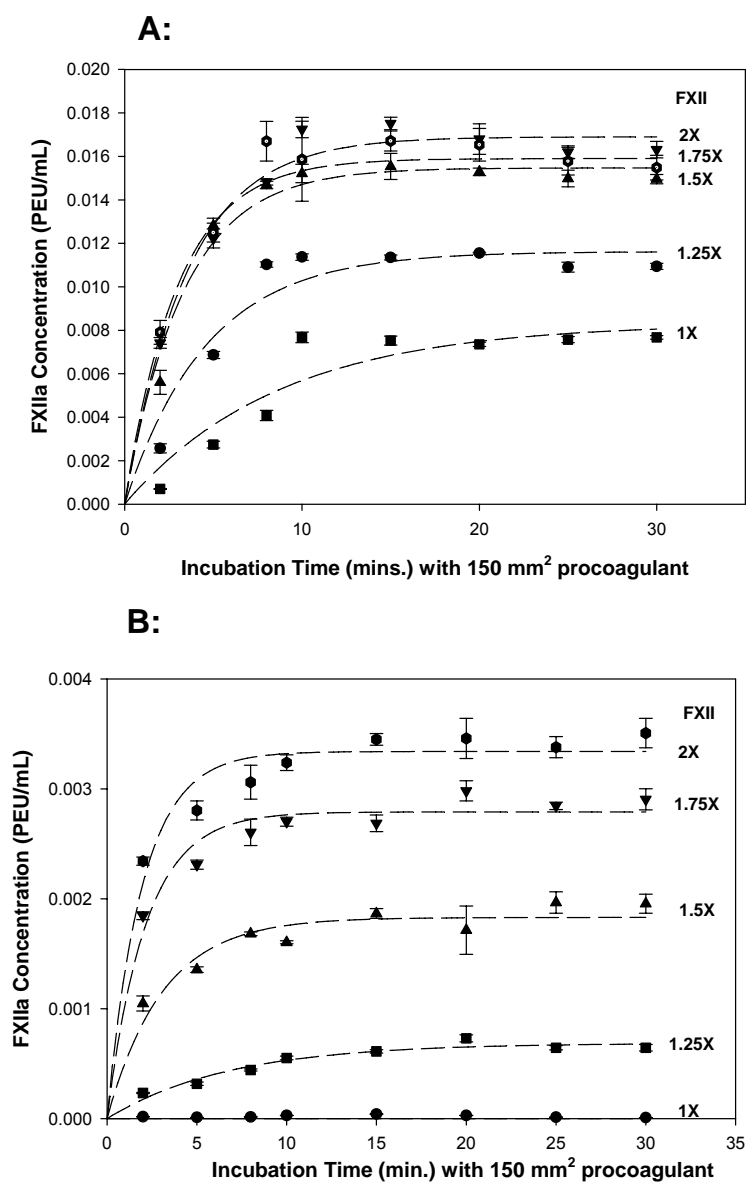


Fig. 5.5: FXII activation kinetics by hydrophilic (Panel A) and hydrophobic (Panel B) procoagulants (150 mm² nominal surface area) in plasma supplemented with exogenous spikes of FXII.

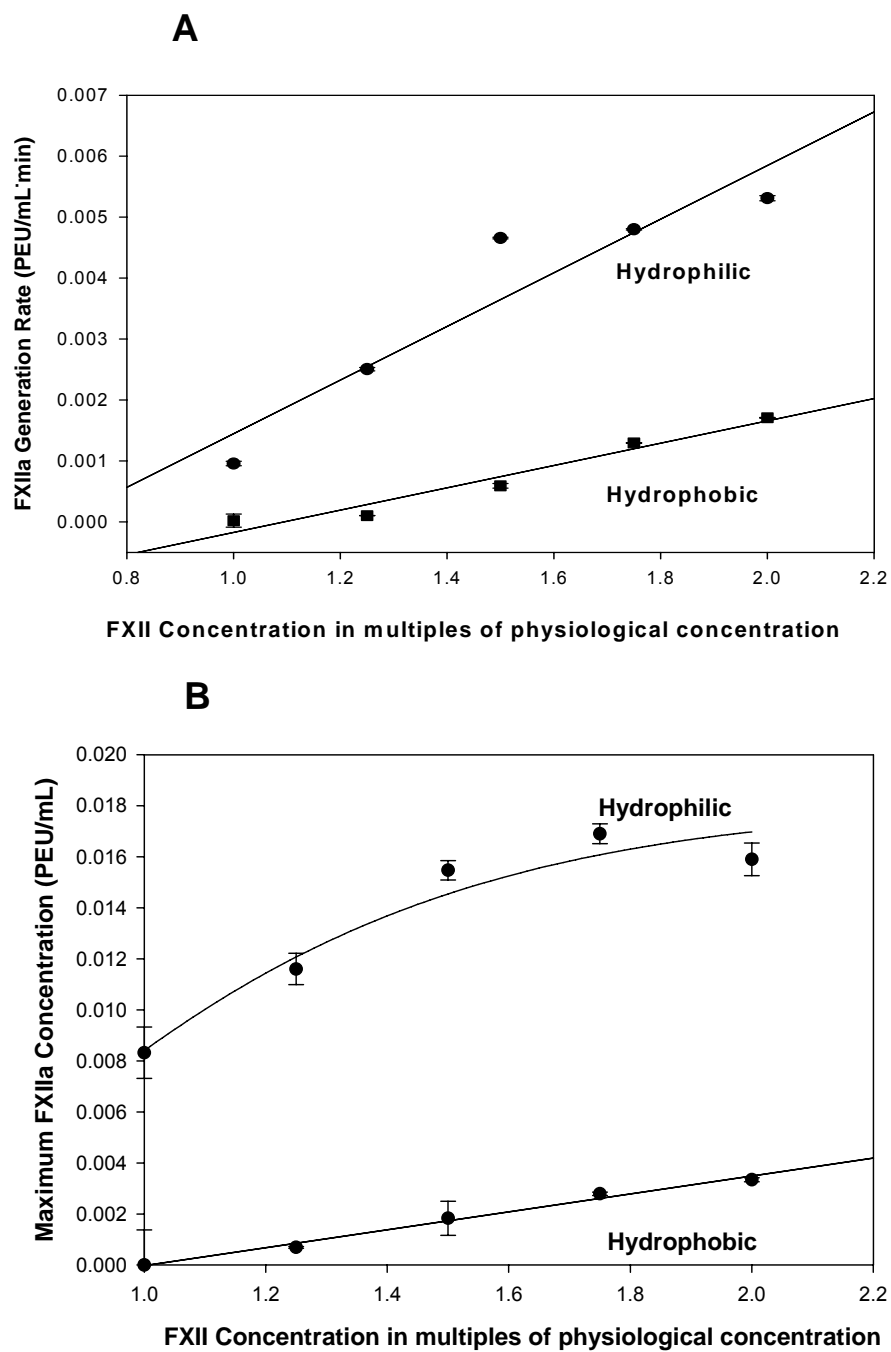


Fig. 5.6: Rate and net production of FXIIa as a function of $[FXII]$ expressed in multiples of physiologic concentration.

5.6 Discussion

Data collected in Table **5.1** shows that more FXIIa was produced by contact neat FXII in buffer with hydrophobic surfaces than by contact with hydrophilic surfaces (row 2). This observation stands in sharp contrast to the anticipated specificity of FXII activation for anionic hydrophilic surfaces. However, the opposite effect was observed in RdPPP and PPP (rows 3,4), which is in general accord with expectations based on accepted biochemistry. All taken together, data of Table **5.1** show that the activation biochemistry in presence of plasma proteins is quite different than that in neat FXII solution. Serial-buffer rinses did not remove putative FXIIa activity from either hydrophilic or hydrophobic surfaces (columns 4 and 7 of Table **5.1**). Insignificant FXIIa activity was recovered in the third-buffer rinse of hydrophobic procoagulants whereas a slight-but-significant amount of FXIIa was eluted from hydrophilic counterparts (columns 3 and 6 of Table **5.1**). These rinsing experiments suggest that FXIIa was more tenaciously bound to hydrophobic surfaces, in accord with the general expectation that proteins adsorb more tenaciously to hydrophobic surfaces than to hydrophilic surfaces. It is not clear from these simple rinsing experiments if FXIIa is irreversibly bound to either procoagulant surface.

Kinetics of Fig. **5.1** reveal that FXIIa production was effectively instantaneous in neat FXII solutions (Panel A) but the rate was significantly slowed for both hydrophobic and hydrophilic procoagulants in PPP. Moreover, final FXIIa yield at hydrophobic

procoagulants was reduced three-fold in PPP compared to neat FXII. These kinetic studies strongly suggest that the difference between FXII activation in neat-buffer solution and plasma noted in the data of Table 5.2 is a kinetic effect rather than due to specificity of the activation biochemistry for anionic hydrophilic surfaces. That is to say, it is the depression of activation rate and yield at hydrophobic procoagulant surfaces in the presence of plasma proteins that gives rise to an appearance of surface-energy-dependent catalytic potential. Or stated in another way, FXII activation in the presence of plasma proteins leads to an apparent specificity that is actually due to a relative diminution in the FXII→FXIIa reaction at hydrophobic surfaces immersed in plasma.

Hydrolysis of FXI to FXIa by the products of contact activation FXII presented in Fig. 5.2- Fig. 5.3 confirms that these products were indeed specific for FXI as anticipated for FXIIa. This evidence alone does not discount production of other FXII-related fragments (such as FXII_f, [2, 3, 6]) but does prove that some or all of these fragments exhibit procoagulation properties. No significant difference was observed for FXII solutions activated by hydrophilic or hydrophobic procoagulants, corroborating results discussed above showing that FXII activation in neat-buffer solution is not specific for hydrophilic surfaces.

Previous work has shown that coagulation time of animal[13] and human plasma[12] asymptotically decreases as a function of increasing procoagulant surface area to a minimum coagulation time characteristic of procoagulant surface chemistry/energy. It was further observed that this asymptotic coagulation time decreased monotonically with serially-increasing procoagulant surface energy (increasing hydrophilicity). These observations, and theoretical analysis thereof [12, 13, 19], led to

the conclusion that procoagulants exhibit a surface-energy-dependent “catalytic potential” to induce FXII→FXIIa [13]. Results reported herein suggest, however, that this catalytic potential is, in fact, independent of surface energy, with nearly equal activation observed at the extremes of surface energy. Apparently, it is the depression of activation rate and yield at hydrophobic procoagulant surfaces in the presence of plasma. It is suspected that this depressed activation rate/yield is due to an adsorption competition between FXII and a host of other plasma proteins [21] that substantially reduces efficiency of the FXII contact step at hydrophobic surfaces immersed in plasma. Adsorption competition does not occur in neat FXII solutions or at non-protein-adsorbent hydrophilic surfaces [14, 22], leading to efficient FXII contact and prompt activation. Thus, plasma coagulation time decreases with increasing procoagulant hydrophilicity presumably because protein adsorption and adsorption competition decreases with increasing surface energy. While the exact mechanism of FXII activation at procoagulant surfaces is not fully clarified, dependence of autoactivation rate and yield on the protein composition of the fluid phase must be included in any proposition aimed at augmenting or replacing the traditionally-accepted biochemistry of FXII surface activation.

The plasma coagulation cascade is characterized as an “enzyme-amplifier system” in which the product of a preceding reaction in a series of linked reactions is the catalytic enzyme of a subsequent reaction. Output and gain of such an enzyme amplifier is critically dependent on the intensity and temporal characteristics of the input. Early modeling [23] efforts have led to informative computational models of the so-called extrinsic pathway of plasma coagulation that is partly responsible for hemostasis *in vivo*. However, input to the extrinsic pathway is FVIIa resulting from tissue damage, not FXIIa

produced by contact with biomaterials. Much less work has been dedicated to modeling the intrinsic pathway that is activated by contact with material surfaces through FXII [24]. No doubt a limitation has been lack of fundamental information relating procoagulant surface properties to the production of FXIIa [13, 14]. Herein we have shown that FXII activation is independent of procoagulant surface energy but that activation rate and FXIIa yield at hydrophobic surfaces is significantly depressed in whole plasma. As a consequence, blood contact with hydrophilic surfaces gives rise to a sharp and intense input to the intrinsic cascade and coagulation observed in vitro is correspondingly prompt. By contrast, input to the intrinsic cascade induced by hydrophobic surfaces is more gradual and less intense leading to relatively sluggish clotting. Thus, the acute response of blood to material surfaces is not necessarily predictive of chronic exposure, rationalizing how it happens that biomaterials exhibit less than ideal hemocompatibility in vivo, even if seeming relatively inert to plasma coagulation in vitro.

Data of Fig. 5.4 corroborates the finding that FXII activation is not specific to anionic hydrophilic surfaces, as proposed by the accepted biochemistry of surface activation. Maximum static state FXIIa production dependence on $[FXII]$ is strongly suggestive of product inhibition operating in competition with autoactivation wherein increasing $[FXIIa]$ inhibits the $FXII \rightarrow FXIIa$. Indeed, autoinhibition has been suggested by Mitropoulos et al [12] [16] and implicated as a mediator of the contact activation of whole-plasma coagulation [12]. Alternatively, it may be suggested that maximum static state FXIIa production results from a precise balance between FXIIa supply and an unknown sink. The sink could be adsorption to surfaces (activator +

internal surface of test tubes) or FXIIa degradation into a form with no coagulation activity.

Data of Fig. 5.5 implicates an important role for plasma proteins in the activation process [12]. None of the 5 proteins used to supplement FXII solutions that caused a sharp increase in contact-activation properties of hydrophilic procoagulants and equally sharp decrease in activation properties of the hydrophobic procoagulants are directly involved in the coagulation cascade or are known inhibitors of proteases of the coagulation cascade. Inhibition of the $FXII \rightarrow FXIIa$ reaction by IgG and albumin has been suggested in the literature (see ref. [25] and citations therein), but little-or-no tangible biochemical explanation for inhibition has been offered. Indeed, data of Fig. 5.5 shows that the exogenous-protein mix was not exclusively inhibitory. Rather than attributing this added-protein effect to enhancement in the hydrophilic-procoagulant case and inhibition in the hydrophobic-procoagulant case, we propose that competitive-protein adsorption is responsible for mediation of FXII contacts. Adsorption competition between FXII and exogenous proteins substantially reduces efficiency of the FXII contact step at hydrophobic surfaces. Adsorption competition does not occur in neat FXII solutions or at non-protein-adsorbent hydrophilic surfaces [14], leading to efficient FXII contact and prompt activation.

5.7 Summary

FXII activation in neat buffer solution occurs with nearly equal efficiency (rate and FXIIa yield) at hydrophobic (poorly-water-wettable silanized glass) and anionic

hydrophilic (fully-water-wettable clean glass) procoagulant surfaces. This finding is strong evidence that the surface-mediated *FXII* → *FXIIa* reaction is not due to a chemically-specific-binding of FXII to anionic surfaces, as proposed by the traditional biochemistry of contact activation, because hydrophobic surfaces bear few, if any, such surface-bound oxidized functionalities. However, FXII activation in whole plasma occurs with significantly-greater efficiency at hydrophilic surfaces than at an equal surface area of hydrophobic procoagulant. Taken together, these experimental observations demonstrate an important role of plasma proteins in the activation process.

Furthermore, contact activation of FXII by hydrophobic surfaces is shown to be inhibited by a competitive-protein-adsorption effect that appears to greatly reduce efficiency of the FXII-surface contact event. By contrast, no such inhibition was observed at hydrophilic surfaces, presumably because proteins do not competitively adsorb to these surfaces and block FXII-surface contact. It is speculated that FXII adsorption, autoinhibition of FXII activation, and FXIIa desorption are three essential steps leading to contact activation of FXII and release of FXIIa into the solution phase.

Whatever the exact role of mechanism, it is evident that the standard paradigm of blood-plasma activation at biomaterial surfaces requires substantial revision. This mechanistic revision may lead to improved strategies for the surface engineering of cardiovascular materials.

5.8 References

1. Hanson, S.R., Harker, L.A., Blood Coagulation and Blood-Materials Interactions, in Biomaterials Science: An Introduction to Materials in Medicine, B.D. Ratner, Hoffman, A.S., Schoen, F.J., Lemons, J.E., Editor. 1996, Academic Press: San Diego.
2. Colman, R.W., Schmaier, A.H., Contact System: A Vascular Biology Modulator With Anticoagulant, Profibrinolytic, Antiadhesive, and Proinflammatory Attributes. *Blood*, 1997. 90(10): p. 3819-43.
3. Colman, R.W., Scott, C.F., Schmaier, A.H., Wachtfogel, Y.T., Pixley, R.A., Edmunds JR, L.H., Initiation of Blood Coagulation at Artificial Surfaces. 1987.
4. Cadena, R.A.D., Wachtfogel, Y.T., Colman, R.W., ed. Contact Activation Pathway: Inflammation and Coagulation. *Hemostasis and Thrombosis: Basic Principles and Clinical Practice*, ed. R.W. Colman, Marder, V.J., Salzman, E.W., Salzman, J., Hirsh, J. 1994, J. B. Lippincott Company: Philadelphia. 219-240.
5. Colman, R.W., Marder, V.J., Salzman, E.W., Hirsh, J., Overview of Hemostasis, in *Hemostasis and Thrombosis: Basic Principles and Clinical Practice*, R.W. Colman, Marder, V.J., Salzman, E.W., Hirsh, J., Editor. 1994: Philadelphia.
6. Colman, R.W., Contact Activation Pathway: Inflammatory Fibrinolytic, Anticoagulant, Antiadhesive, and Antiangiogenic Activities, in *Hemostasis and Thrombosis: Basic Principles and Clinical Practice*., M.V. Colman RW, Hirsh J, Clowes AW,, Editor. 2000, J.B. Lippincott Company: Philadelphia. p. 103-21.

7. Pokhilko, A.V., Ataulakhanov, F.I., Contact Activation of Blood Coagulation: Trigger Properties and Hysteresis Hypothesis Kinetic Recognition of Foreign Surfaces upon Contact Activation of Blood Coagulation: A Hypothesis. *J Theor Biol.*, 1998. 191: p. 213-9.
8. Samuel, M., Pixley, P.A., Villanueva, M.A., Colman, R.W., Villanueva. G.B., Human Factor XII (Hageman factor) Autoactivation By Dextran Sulfate. Circular Dichroism, Fluorescence, and Ultraviolet Difference Spectroscopic Studies. *Journal of biological chemistry*, 1992. 267(27): p. 19691-7.
9. Rose, E.A., Gelijns, A.C., Moskowitz, A., Heitjan, D.F., Stevenson, L.W., Dembitsky, W., Long, J.W., Ascheim, D.D., Tierney, A.R., Levitan, T.G., Watson, J.T., Meier, P., Long-term Use of a Left Ventricular Assist Device for End-Stage Heart Failure. *N. Engl. J. Med.*, 2001. 345(20): p. 1435-1443.
10. Lavine, M., Roberts, M., Smith, O., Bodybuilding: The Bionic Human. *Science*, 2002. 295: p. 995-1032.
11. Miller, R., Guo, Z., Vogler E.A., Siedlecki, C.A., Plasma Coagulation Response to Surfaces with Nanoscale Heterogeneity. *Biomaterials*, 2005. in press.
12. Zhuo, R., Miller, R., Bussard, K.M., Siedlecki, C.A., Vogler, E.A., Procoagulant Stimulus Processing by the Intrinsic Pathway of Blood Plasma Coagulation. *Biomaterials*, 2005. 26: p. 2965-73.
13. Vogler, E.A., Graper, J.C., Harper, G.R., Lander, L.M., Brittain, W.J., Contact Activation of the Plasma Coagulation Cascade.1. Procoagulant Surface Energy and Chemistry. *J. Biomed. Mat. Res.*, 1995. 29: p. 1005-1016.

14. Vogler, E.A., Graper, J.C., Sugg, H.W., Lander, L.M., Brittain, W.J., Contact Activation of the Plasma Coagulation Cascade.2. Protein Adsorption on Procoagulant Surfaces. *J. Biomed. Mat. Res.*, 1995. 29: p. 1017-1028.
15. Vogler, E.A., Nadeau, J.G., Graper, J.C., Contact Activation of the Plasma Coagulation Cascade. 3. Biophysical Aspects of Thrombin Binding Anticoagulants. *J. Biomed. Mat. Res.*, 1997. 40(1): p. 92-103.
16. Mitropoulos, K.A., High Affinity Binding of Factor FXIIa to an Electronegative Surface Controls the Rates of Factor XII and Prekallirien Activation in vitro. *Thrombosis Research*, 1999. 94(2): p. 117-129.
17. Mitropoulos, K.A., High Affinity Binding of Factor XIIa to an Electronegative Surface Controls the Rates of Factor XII and Prekallikrein Activation in Vitro. *Thrombosis Research*, 1999. 94: p. 117-129.
18. Mitropoulos, K.A., The Levels of FXIIa Generated in Hyman Plasma on an Electronegative Surface are Insensitive to Wide Variation in the Conventration of FXII, Prekallikrein, High Moleuclar Weight Kininogen or FXI. *Thromb. Haemost.*, 1999. 82: p. 1033-40.
19. Guo, Z., Bussard, K., Vogler, E.A., Siedlecki, C.A., Mathematical Modeling of Material-Induced Blood Plasma Coagulation. *Biomaterials*, 2006. 27: p. 796-806.
20. Vogler, E.A., Water and the Acute Biological Response to Surfaces. *Journal of Biomaterials Science Polymer Edition*, 1999. 10(10): p. 1015-45.
21. Anderson, N.L., Anderson, N.G., The Human Plasma Proteome: History, Character, and Diagnostic Prospects. *Molecular and Cellular Proteomics*, 2002. 1(11): p. 845-867.

22. Vogler, E.A., Structure and Reactivity of Water at Biomaterial Surfaces. *Adv. Colloid and Interface Sci.*, 1998. 74(1-3): p. 69-117.
23. Levine, S.N., Enzyme Amplifier Kinetics. *Science*, 1966. 152: p. 651-653.
24. Gregory, G., Basmadjian, D., An Analysis of The Contact Phase of Blood Coagulation: Effects of Shear Rate and Surface Are Intertwined. *Annals of Biomedical Engineering*, 1994. 22: p. 184-193.
25. Fuhrer, G., Gallimore, M.J., Heller, W., Hoffmeister, H.E., *FXII. Blut.*, 1990. 61(5): p. 258-66.

Chapter 6

Practical Application of a Chromogenic FXIIa Assay

Autohydrolysis of blood factor XII ($FXII + FXIIa \rightarrow 2FXIIa$) is found to be a significant reaction in neat-buffer buffer solutions of FXII but an insignificant reaction in the presence of plasma proteins. Autohydrolysis causes a chromogenic assay for FXIIa in buffer solution to strongly deviate from the traditional plasma-coagulation assay. Autohydrolysis can be accommodated by performing chromogenic detection of FXIIa as a rate assay in saturating concentrations of FXII. Rate-assay results performed in this way are shown to be in analytical agreement with the plasma-coagulation assay. Autohydrolysis can be used as a means of amplifying FXIIa produced by contacting neat-buffer solutions of FXII with biomaterials, suggesting a route to highly-sensitive measurement of biomaterial hemocompatibility.

6.1 Introduction

Adverse cell and protein interactions are major cause of failure of blood contacting biomaterials. Among these adverse protein-biomaterial interactions, surface-contact activation of blood Factor XII is important because this is the first step in a cascade of linked zymogen-enzyme conversions that ultimately leads to coagulation (clotting) of blood in the presence of artificial materials (the intrinsic pathway of blood-plasma coagulation). Thus, a full understanding of the surface biochemistry leading to FXII activation is critical to the prospective development of biomaterials with improved hemocompatibility.

Contact activation, also termed autoactivation in the hematology literature [1], occurs through a poorly-understood contact or binding step with procoagulant surfaces [1, 2] that is a matter of continued investigation in our laboratories [3-8]. Our work has substantially relied on a plasma-coagulation-time-assay [6, 9] to detect and quantify surface activation. Plasma can also be used to quantify FXIIa by using a calibration curve relating observed coagulation time (CT) to exogenously-added FXIIa concentrations (a.k.a. FXIIa titration). Although plasma coagulation offers a number of distinct advantages as a traditional-hematology assay for FXIIa (simple, reproducible, sensitive, biomedically relevant, *etc.*), it does not directly detect FXIIa but rather measures the response of the whole coagulation cascade to an exogenous FXIIa bolus that presumably includes kallikrein amplification [3]. Also, there is the unavoidable problem of lot-to-lot variability inherent in donated blood.

Commercial chromogenic assays, first introduced in the mid 1980's [10, 11], are an alternative to plasma coagulation that offer direct and specific detection of various coagulation factors such as FXIIa and FXII_f [12]. In the process of applying a chromogenic assay in our studies of FXII activation *in neat buffer solutions*, we discovered that autohydrolysis (FXII+FXIIa→2FXIIa) is an important contributor that must be properly accounted for to obtain agreement with traditional plasma-coagulation assays in which autohydrolysis is apparently insignificant. The outcome is an improved chromogenic-assay protocol that has utility in measuring activation properties of biomaterials [12-15].

6.2 FXIIa Titration of Human Plasma

Fig. 6.1 compares FXIIa titration of human platelet-poor plasma (PPP) and FXII-depleted platelet-poor plasma (12dPPP), illustrating how exquisitely sensitive plasma coagulation was to trace quantities of FXIIa (measured in PEU/mL; where PEU = Plasma Equivalent Units). Inset of Fig. 6.1 plots results on log-normal coordinates, revealing a useful calibration curve within the range $0.0001 < [FXIIa] < 0.1$ PEU/mL with good linearity and precision, where square brackets denote concentration

$$12dPPP: CT = (-9.36 \pm 0.35)[FXIIa] - (9.45 \pm 0.96); R^2 = 95.4\%;$$

$$PPP: CT = (-12.50 \pm 0.53)[FXIIa] - (8.95 \pm 1.22); R^2 = 95.7\% .$$

The curve drawn through the data of the main figure is a guide to the eye whereas lines through data of the inset are the result of linear-least-squares regression through the data interval shown.

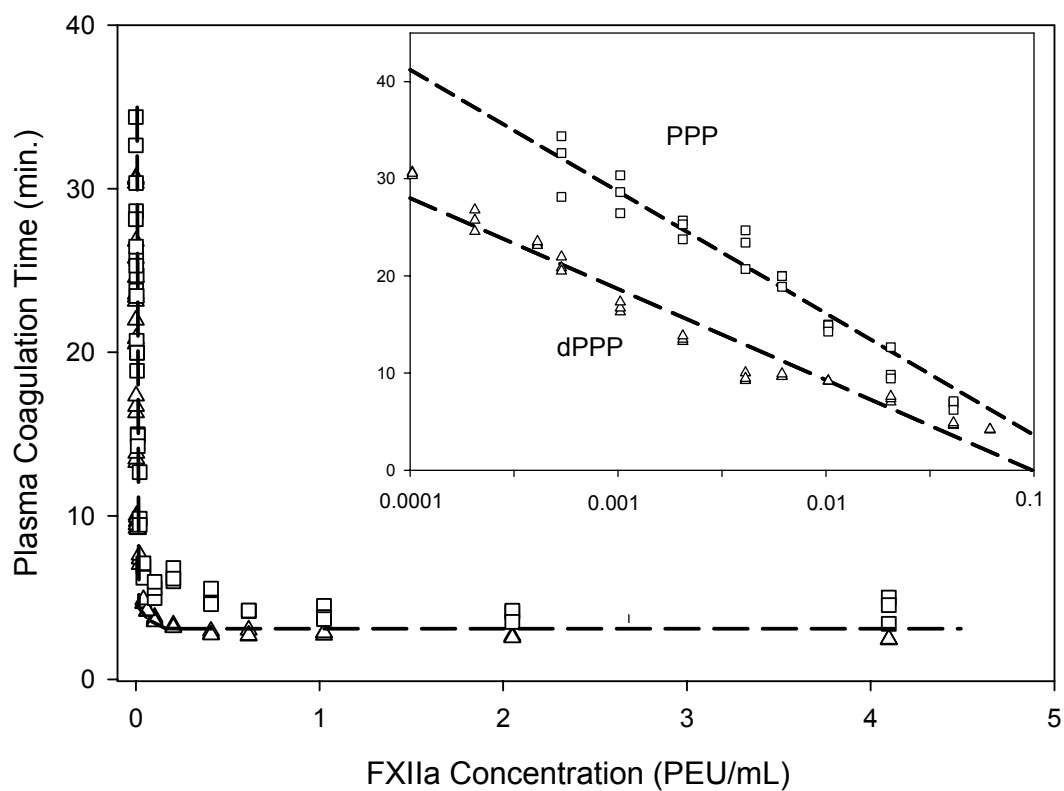


Fig. 6.1: FXIIa titration of normal platelet-poor plasma (PPP, squares) and FXII-depleted plasma (12dPPP, triangles). Inset plots results on log-normal coordinates within the range $0.0001 < [FXIIa] < 0.1$ PEU/mL

Fig. 6.2 shows slope of the FXIIa titration curve for FXII-depleted plasma (12dPPP; log-normal axes, see Fig. 6.1 inset) is not a function of exogenous FXII concentration, suggesting that autohydrolysis is not a significant reaction in the presence

of plasma. Error bars represent standard error in the slope of best-fit lines like that shown in Fig. 6.1 (inset).

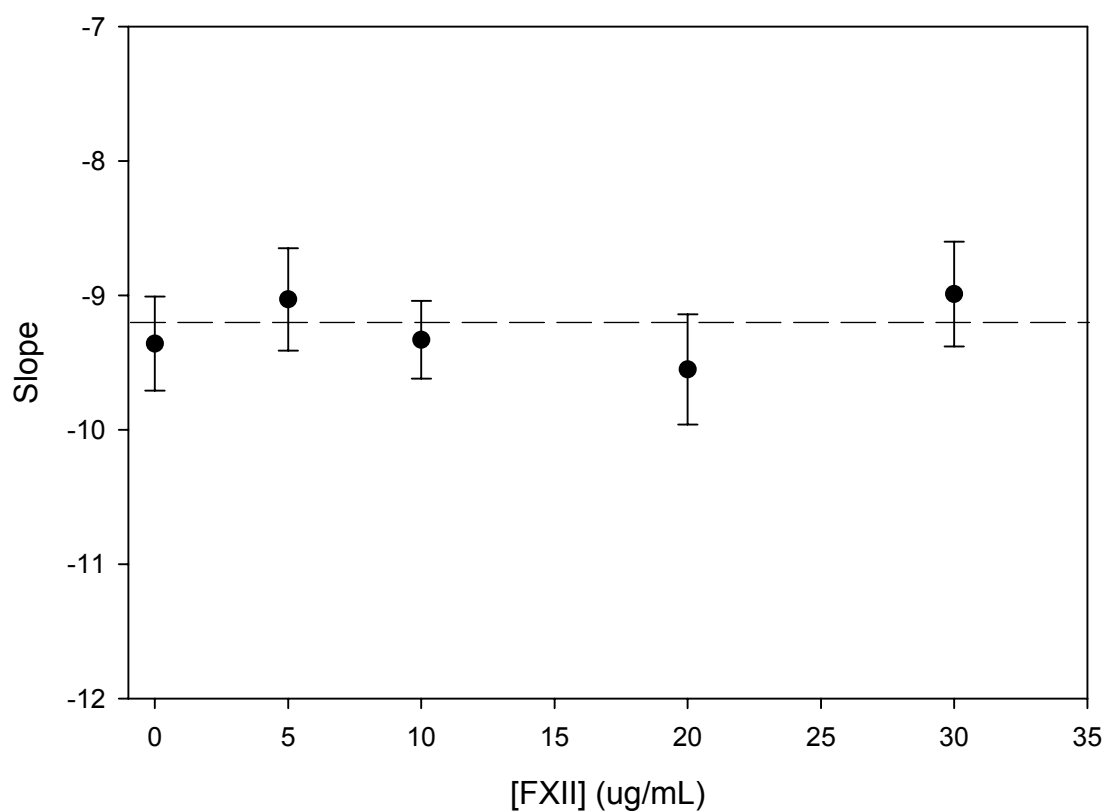


Fig. 6.2: Slope of the FXIIa titration curve for FXII-depleted plasma.

6.3 Chromogenic Assay for FXIIa in Buffer Solution

Fig. 6.3 plots color development (405 nm) kinetics for $[FXIIa] = 5 \times 10^{-3}$ PEU/mL dissolved in serially-increasing $[FXII]$ (annotations). It was observed that both

chromogen-development rate and absolute absorbance strongly depended on $[FXII]$ in the FXIIa analyte solution. Initial rates (in $\Delta A/\text{min}$; best fit lines drawn through the data on Fig. 6.3) at varying $[FXII]$ were found to systematically increase to a maximum rate V_{max} at swamping $[FXII] > 10 \mu\text{g/mL}$, as shown in Fig. 6.4 (see vertical line). In fact, a linear correlation between V_{max} and $[FXIIa]$ was observed, as shown in Fig. 6.5 (measured in $[FXII] = 20 \mu\text{g/mL}$ solution; $\Delta A/\text{min} = (0.744 \pm 0.17) [FXIIa]$; $R^2 = 96.5\%$). Fig. 6.5 thus served as a rate-assay calibration curve with good sensitivity and linearity over the dynamic range $0.005 < [FXIIa] < 0.1 \text{ PEU/mL}$).

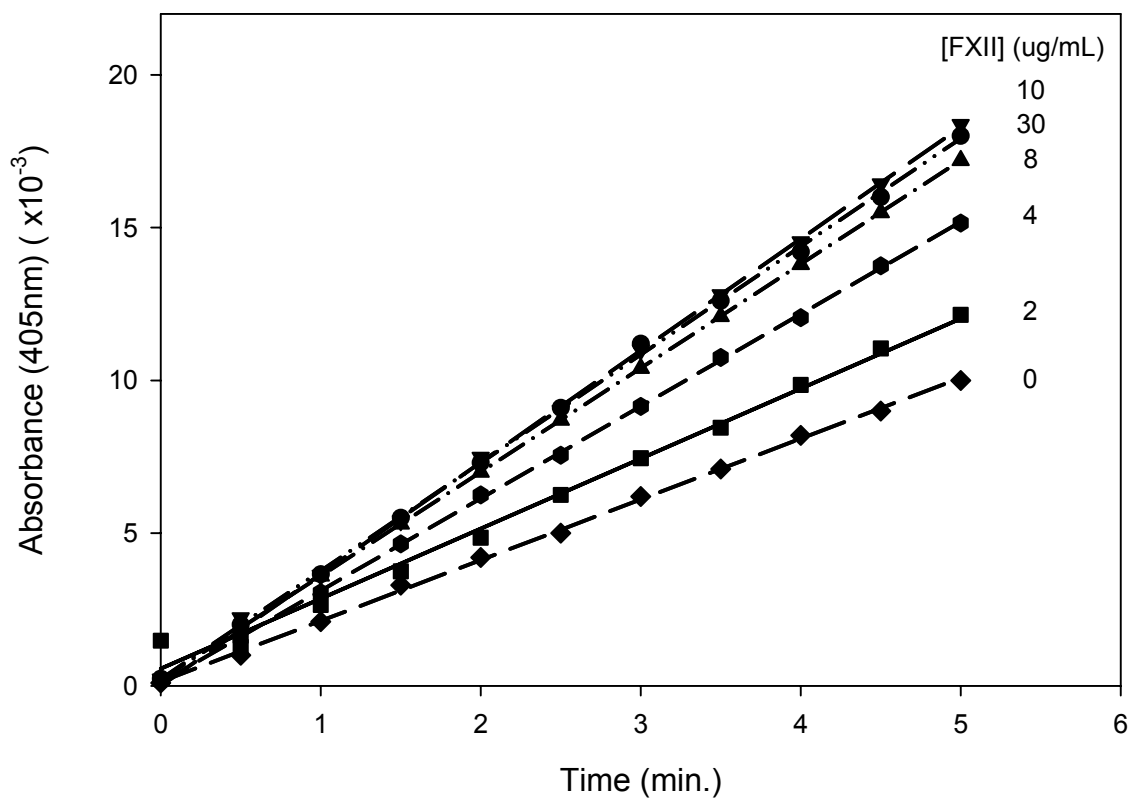


Fig. 6.3: Color development kinetics for a chromogenic FXIIa assay performed in neat-buffer solutions of FXII.

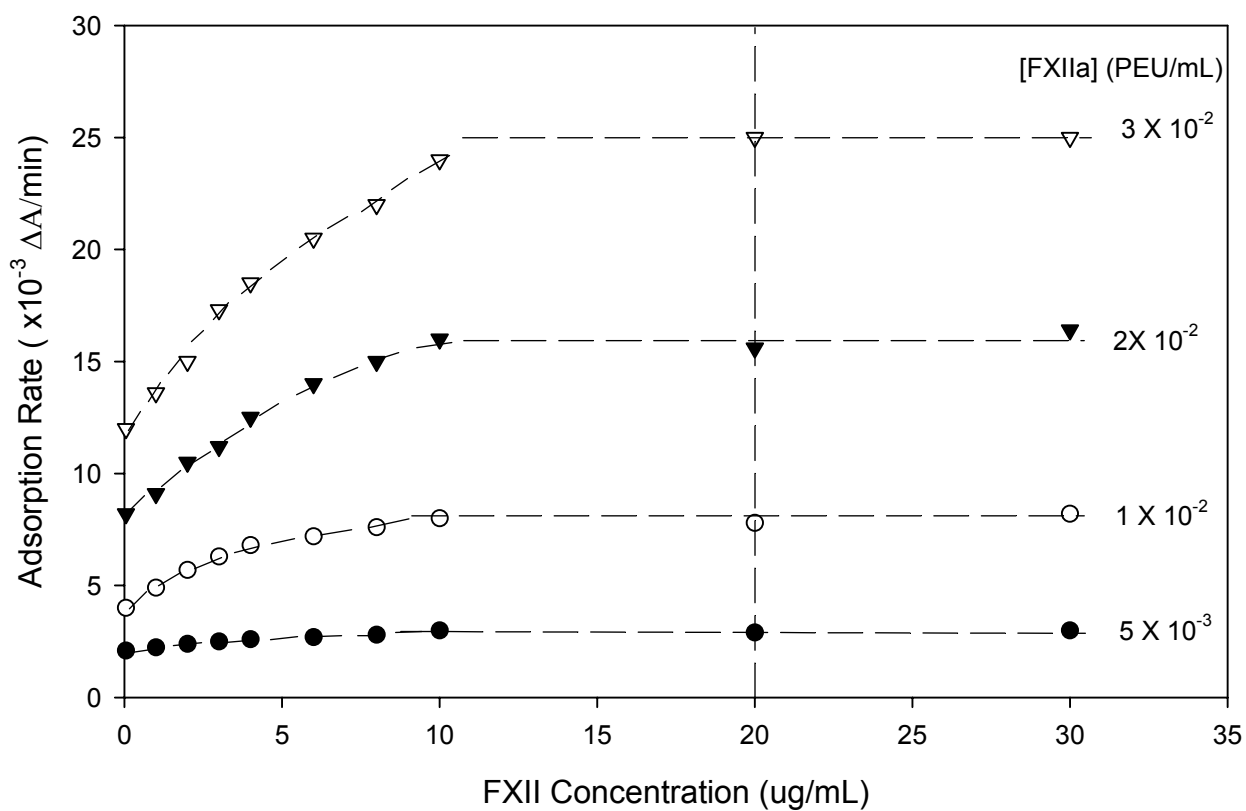


Fig. 6.4: Color-development rate ($\Delta A/\text{min}$ derived from best fit lines drawn through the data of Fig. 6.3) systematically increases to a maximum rate V_{max} at swamping $[FXII] > 10 \mu\text{g/mL}$ (see vertical line).

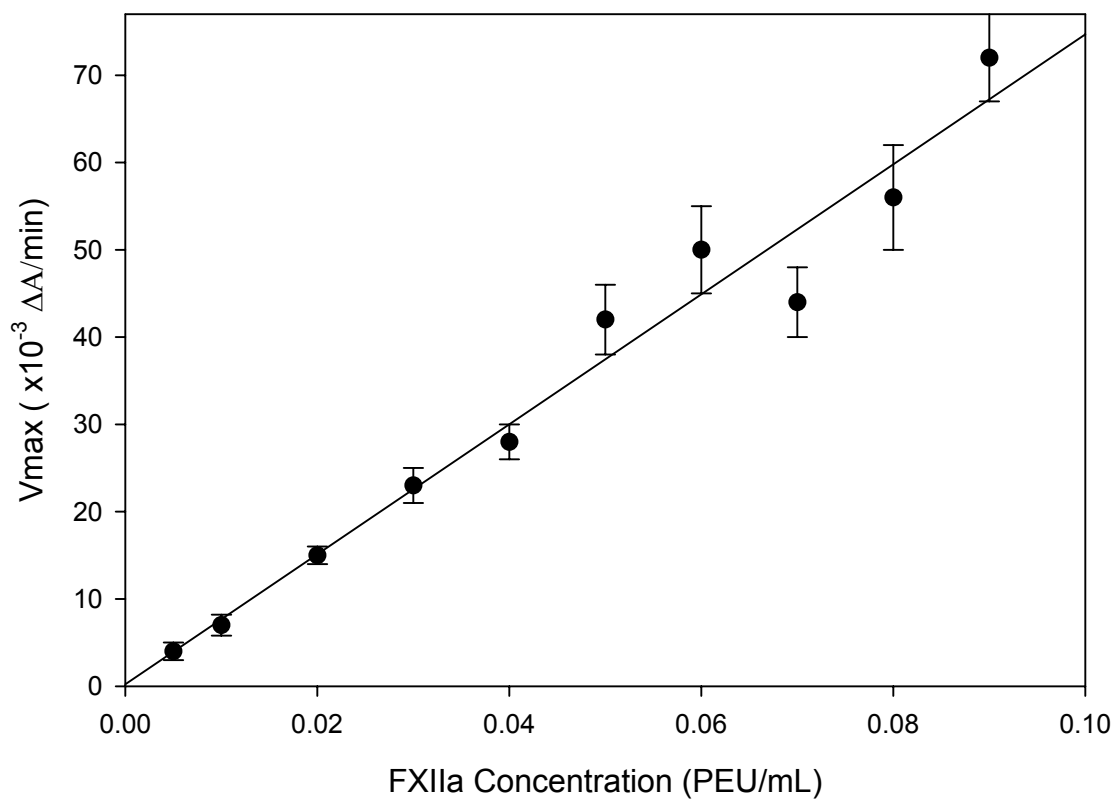


Fig. 6.5: Linear correlation between V_{\max} and $[FXIIa]$.

6.4 Correlation Between Plasma Coagulation and Chromogenic Rate Assay

Fig. 6.6 compares results of chromogenic and plasma coagulation assays for FXIIa by co-plotting results for the same FXIIa solutions prepared within the $0.005 < [FXIIa] < 0.1$ PEU/mL range in PBS. Chromogenic assay results were obtained using the V_{\max} calibration curve of Fig. 6.5, measuring FXIIa in a $[FXII] = 20$ $\mu\text{g/mL}$ solution in PBS. Plasma coagulation results were obtained using the PPP FXIIa titration curve of Fig. 6.1 with no FXII added to the FXIIa analyte solutions. Perfect correlation between these two FXIIa assays would fall on the diagonal with a unity slope and null intercept. The actual slope (1.13 ± 0.29) was not statistically different from unity and the intercept was not measurably different than zero (0.000 ± 0.001), demonstrating a high correlation ($R^2 = 97.0\%$) between these two assays. Fig. 6.7 is a plot of residuals about the fitted correlation line of Fig. 6.6, demonstrating that experimental error was randomly distributed over the entire $0.005 < [FXIIa] < 0.1$ PEU/mL range tested, and suggesting that slight differences between assays at any particular FXIIa concentration were not systematic.

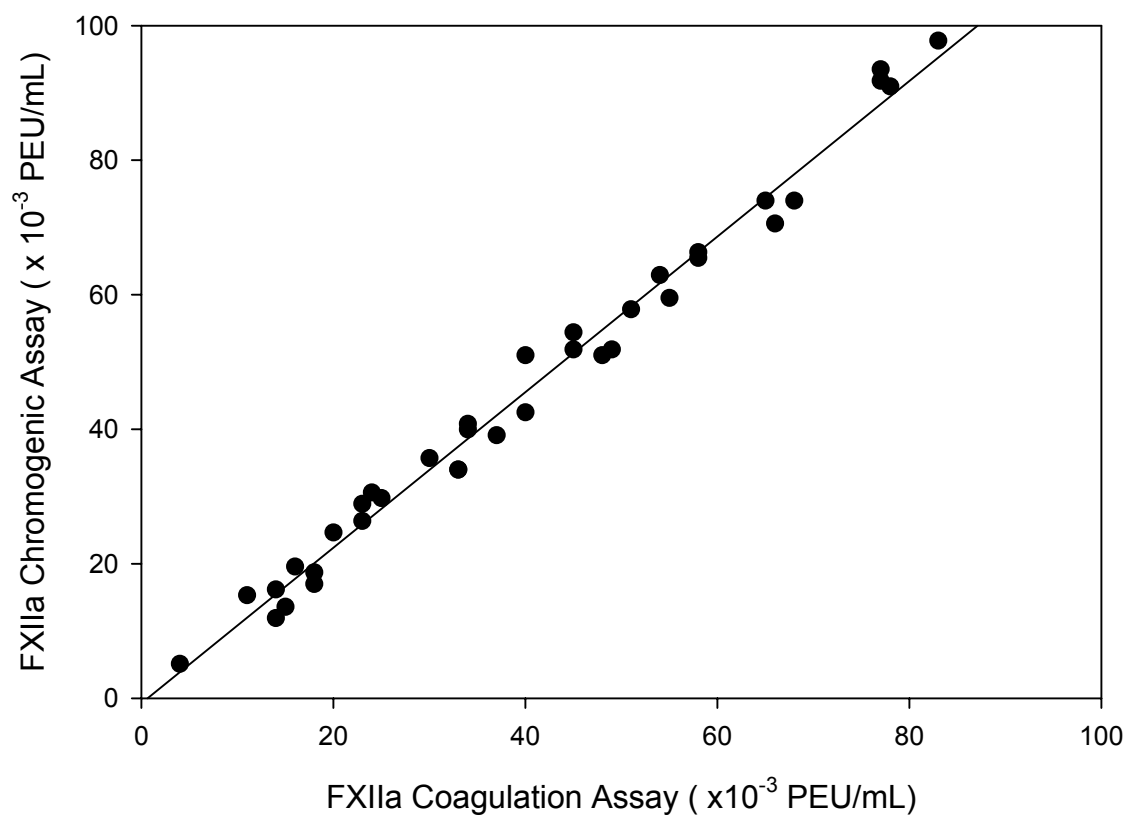


Fig. 6.6: Linear correlation between plasma-coagulation-time and chromogenic-rate assays for FXIIa.

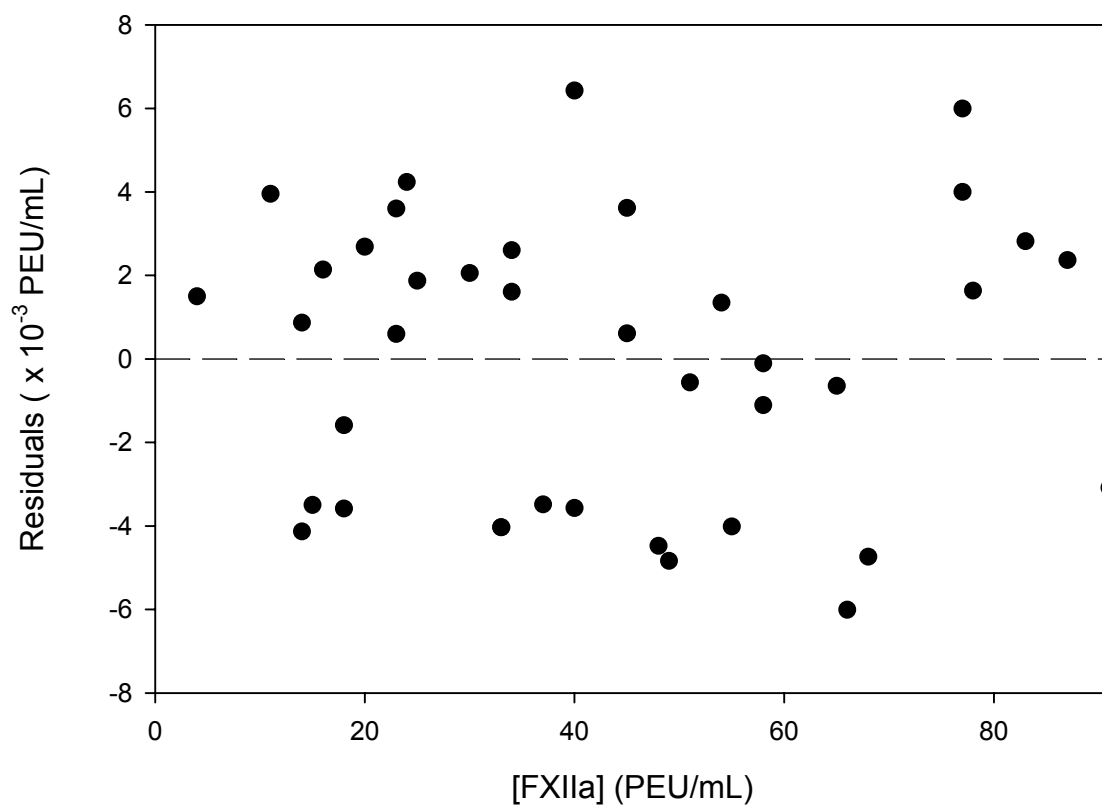


Fig. 6.7: Plot of residuals about the fitted correlation line of Fig. 6.6.

6.5 Discussion

Fig. 6.1 demonstrates that plasma is a very sensitive detector for FXIIa that can serve as the basis of a reliable FXIIa assay, as has been well appreciated in traditional hematology. Slopes of log-normal calibration curves (inset Fig. 6.1) were observed to be steeper for PPP than for 12dPPP for unknown reasons, possibly related to donor-to-donor differences in plasma or to the processing of normal plasma in the production 12dPPP. However, Fig. 6.2 demonstrates that the difference between PPP and 12PPP cannot be attributed to $[FXII]$ since the slope of the 12dPPP calibration curve was not a function of exogenous $[FXII]$ (FXIIa titration of RdPPP was not measurably different than 12PPP). This suggests that autohydrolysis in plasma is an insignificant reaction, as has been previously deduced from mathematical models of the intrinsic pathway of plasma coagulation [3]. It is of further interest to speculate in this regard that autohydrolysis in plasma is inhibited by rapid binding of FXIIa to coagulation proteins such as kallikrein or a specific inhibitor so that the free $[FXIIa]$ is always very low in plasma and autohydrolysis rate commensurately depressed. Of course, no such FXIIa binding is possible in neat-buffer solutions, possibly explaining why autohydrolysis is clearly observable in the absence of plasma proteins, as discussed further below.

Autohydrolysis of FXII ($FXII+FXIIa \rightarrow 2FXIIa$; where FXII is the substrate for the FXIIa enzyme) is a clearly observable reaction in buffer solutions containing both FXII and FXIIa that must be accounted for in chromogenic assays for FXIIa in purified-protein preparations. Based on the kinetics presented in Fig. 6.2 and Fig. 6.3, it is

apparent that autohydrolysis is a facile reaction that can amplify small quantities of FXIIa produced by contact activation of FXII with test biomaterials or even surfaces of containers (test tubes) in which FXIIa assays are performed. Although we did not detect procoagulant activity in the FXII preparations used in this work (FXII alone does not induce coagulation of recalcified 12dPPP, see Methods and Materials), we assume that putative FXIIa impurities in FXII solutions can be likewise be amplified by autohydrolysis. We estimate from Fig. 6.3 that as little as 5×10^{-3} PEU/mL FXIIa in a solution of 5 $\mu\text{g/mL}$ FXII in PBS can lead to measurable autohydrolysis. Presumably, FXIIa is not detected in FXII stock solutions because the container surface area/volume ratio is low and protein is always stored at low temperature.

Fig. 6.3-Fig. 6.5 show that the effect of autohydrolysis on chromogenic FXIIa assays can be accounted for by performing a rate assay in swamping concentrations of FXII. At $[\text{FXII}] \geq 20 \mu\text{g/mL}$ within the $0.005 < [\text{FXIIa}] < 0.1$ PEU/mL range, FXIIa is apparently saturated with substrate and proceeds at maximal velocity V_{max} directly proportional to $[\text{FXIIa}]$. Based on this evidence, we conclude that autohydrolysis in normal human plasma, if this reaction occurs at all, would also proceed at V_{max} because FXIIa concentrations would almost assuredly be saturated with FXII at physiologic concentrations near 30 $\mu\text{g/mL}$ [16, 17].

Excellent agreement between the chromogenic-rate and plasma-coagulation assays for FXIIa (Fig. 6.6) demonstrates that chromogenic substrates can be used to assay FXIIa in the presence of FXII in with high reliability. Randomly-distributed differences about the perfect-correlation line (Fig. 6.7) suggest that slight differences between assays

at any particular FXIIa concentration were not systematic. Unity slope means that both assay types have nearly equal sensitivity for FXIIa within the $0.005 < [FXIIa] < 0.1$ PEU/mL range. Hence, in this latter regard alone, there is no particular advantage of the chromogenic assay over the traditional plasma-coagulation assay. However, self-amplification of FXIIa through autohydrolysis in FXII solutions provides an opportunity for improving FXIIa detection limits beyond that available in plasma. This suggests a route to improved assessment of biomaterial hemocompatibility. Biomaterials immersed in pure FXII solutions creating an otherwise undetectable concentration of FXIIa by contact activation alone will, overtime (or elevated temperature), self-amplify FXIIa by autohydrolysis. Autohydrolysis can be used to bring total FXIIa up to measurable levels by either chromogenic or plasma coagulation assays, thereby increasing sensitivity.

6.6 Summary

It has been found that autohydrolysis of FXII ($FXII + FXIIa \rightarrow 2FXIIa$) is a clearly observable reaction in buffer solutions containing both FXII and FXIIa that must be accounted for in chromogenic assays for FXIIa in purified-protein preparations. It is reported herein a modification of standard protocols that corrects for autohydrolysis by measuring FXIIa production rate in swamping background concentrations of FXII (rate assay). Good correlation between this rate assay and the traditional plasma-coagulation measurement were obtained. Results suggest a route to improved assessment of biomaterial hemocompatibility.

6.7 References

1. Colman, R.W., Schmaier, A.H., Contact System: A Vascular Biology Modulator With Anticoagulant, Profibrinolytic, Antiadhesive, and Proinflammatory Attributes. *Blood*, 1997. 90(10): p. 3819-43.
2. Samuel, M., Pixley, P.A., Villanueva, M.A., Colman, R.W., Villanueva, G.B., Human Factor XII (Hageman factor) Autoactivation By Dextran Sulfate. Circular Dichroism, Fluorescence, and Ultraviolet Difference Spectroscopic Studies. *Journal of biological chemistry*, 1992. 267(27): p. 19691-7.
3. Guo, Z., Bussard, K., Vogler, E.A., Siedlecki, C.A., Mathematical Modeling of Material-Induced Blood Plasma Coagulation. *Biomaterials*, 2006. 27: p. 796-806.
4. Zhuo, R., Miller, R., Bussard, K.M., Siedlecki, C.A., Vogler, E.A., Procoagulant Stimulus Processing by the Intrinsic Pathway of Blood Plasma Coagulation. *Biomaterials*, 2005. 26: p. 2965-73.
5. Zhuo, R., Colombo, P., Pantano, C., Vogler, E.A., Silicon Oxycarbide Glasses for Blood Contact Applications. *Acta Biomaterialia*, 2005. 1: p. 583-9.
6. Vogler, E.A., Graper, J.C., Harper, G.R., Lander, L.M., Brittain, W.J., Contact Activation of the Plasma Coagulation Cascade.1. Procoagulant Surface Energy and Chemistry. *J. Biomed. Mat. Res.*, 1995. 29: p. 1005-1016.
7. Vogler, E.A., Graper, J.C., Sugg, H.W., Lander, L.M., Brittain, W.J., Contact Activation of the Plasma Coagulation Cascade.2. Protein Adsorption on Procoagulant Surfaces. *J. Biomed. Mat. Res.*, 1995. 29: p. 1017-1028.

8. Vogler, E.A., Nadeau, J.G., Graper, J.C., Contact Activation of the Plasma Coagulation Cascade. 3. Biophysical Aspects of Thrombin Binding Anticoagulants. *J. Biomed. Mat. Res.*, 1997. 40(1): p. 92-103.
9. Brown, B., *Hematology: Principles and Procedures*. 3 ed. 1980, Philadelphia: Lea and Febiger. 113-119.
10. Tripodi, A., Mannucci, P.M., Clinical Evaluation of a fully Automated Chromogenic Method for Prothrombin Time Compared with a Conventional Coagulation Method. *Clinical Chemistry*, 1984. 30(8): p. 1392-5.
11. Friberger, P., Synthetic Peptide Substrate Assays and Fibrinolysis and Their Application on Automates. *Seminars in Thrombosis and Hemostasis.*, 1983. 9(4): p. 281-300.
12. Van Der Kamp, K.W., Hauch, K.D., Feijen, J., Horbett, T.A., Contact Activation During Incubation of Five Different Polyurethanes or Glass in Plasma. *Journal of Biomedical Material Research*, 1995. 29(10): p. 1303-6.
13. Ziats, N.P., Pankowsky, D.A., Tierney, B.P., Ratnoff, O.D., Anderson, J.M., Adsorption of Hageman Factor (factor XII) and Other Human Plasma Proteins to Biomedical Polymers. *Journal of Laboratory and Clinical Medicine*, 1990. 116(5): p. 687-96.
14. Marata, B.M., Courtney, J.M., Sundaram, S., Determination of Contact Phase Activation by The Measurement of The Activity of Supernatant and Membrand Surface-adsorbed Factor XII (FXII): Its Relevance As A Useful Parameter for The In Vitro Assessment of Haemodialysis Membrane. *Journal of Biomedical Material Research*, 1996. 31: p. 63-70.

15. Grunkemeier, J.M., Tsai, W.B., Horbett, T.A., Hemocompatibility of Treated Polystyrene Substrates: Contact Activation, Platelet adhesion, and Procoagulant Activity of Adherent Platelets. *Journal of Biomedical Matererial Research*, 1998. 41(4): p. 657-70.
16. Anderson, N.L., Anderson, N.G., The Human Plasma Proteome: History, Character, and Diagnostic Prospects. *Molecular and Cellular Proteomics*, 2002. 1(11): p. 845-867.
17. Saito, H., Ratnoff, O.D., Pensky, J., Radioimmunoassay of human Hageman factor (factor XII). *Journal of Laboratory and Clinical Medicine*, 1976. 88(3): p. 506-14.

Chapter 7

Conclusions and Future Work

Plasma is the fluid phase of blood that contains all of the proteins necessary to cause blood to coagulate. Coagulation occurs through an elegant series of linked biochemical reactions known as the plasma coagulation cascade in which the product of a preceding reaction is the enzyme of a subsequent reaction. This cascade of self-amplifying zymogen-enzyme conversions can be potentiated by contact with biomaterials or by any of the enzymes of the coagulation cascade itself (procoagulants).

Human plasma has been shown to be a very sensitive and robust *in vitro* experimental system for studies of material surface activation of blood coagulation. An end-point-time assay measuring coagulation time of plasma induced by different procoagulants has been adapted to compare efficiency of activation at different points of intersection along the coagulation cascade: surface area titration (SAT) measuring activation properties of different test materials, thrombin titration (TT) measuring activation at the penultimate step in the coagulation cascade, thrombin-surface area co-titration (COT) measuring activation properties of different test materials in the presence of thrombin, and FXIIa titration measuring the effect of activated blood factor FXII on the cascade. These assays were used to improve understanding of the mechanism of biomaterial-induced coagulation of blood that is important in the development of cardiovascular biomaterials.

7.1 Contact Activation of Blood Plasma Coagulation by Model Surfaces

A previously-published model of surface contact activation of blood plasma coagulation [1-4] was improved and applied to understand activation of the plasma coagulation cascade by procoagulant surfaces. The resulting mathematical model (Eq. 2.1) related coagulation time to procoagulant surface area and was found to fit experimental SAT data very well, implying that the essential features of the model were generally descriptive of the plasma coagulation process. The model was reduced to a single adjustable parameter K_{act}^{SAT} that could be extracted from experimental data by statistical fitting. K_{act}^{SAT} was found to scale exponentially with surface energy, with low activation observed for poorly water wettable surfaces and very high activation for fully water wettable surfaces, corroborating previous studies.

7.2 Hemocompatibility of Silicon Oxycarbide Glasses

K_{act}^{SAT} was used as a measure of the hemocompatibility of various oxycarbide (SiOxCy) glasses of potential interest as blood-contacting biomaterials with excellent tribological properties. It was found that K_{act}^{SAT} of various SiOxCy formulations with different X:Y ratios were comparable to a pyrolytic carbon standard over a broad range of compositions. Results further suggest that SiOxCy propensity to activate coagulation scales sharply with oxygen surface composition as measured by XPS. Incorporation of as little as 20% carbon (as measured by XPS) sharply reduced plasma activation properties

compared SiO_x (soda-lime glass) controls. Activation properties of higher-carbon-content SiO_xCy (> 60%) were similar to non-activating, silanized glass. Results suggest that SiO_xCy glass might find application as a substitute for pyrolytic carbon in medical device applications that require excellent tribological properties, such as artificial heart valves.

7.3 Thrombin Production by Contact Activation of Plasma

Thrombin is a potent proteolytic enzyme of the plasma coagulation cascade that hydrolyzes blood fibrinogen into fibrin fragments that spontaneously oligomerize and cause plasma to clot. Three different coagulation assays (SAT, TT and COT assay) were used to explore thrombin production when plasma was activated by different procoagulants. Mathematical models were developed based on the assumption that thrombin was produced in a bolus manner. Excellent fit of these models to experimental data suggest that assumptions underlying theory were generally descriptive of the way thrombin is produced by activation of the plasma coagulation cascade and imply that thrombin is, in fact, produced by surface activation in proportion to the intensity of contact activation (as measured by surface area and surface energy). The control mechanism leading to bolus FIIa production apparently lies between FXII activation and FIIa generation, and was shown not to be inhibited or limited by the absolute concentration of FIIa in plasma. Experimental results further showed that procoagulant

surfaces were not deactivated by protein adsorption throughout the whole coagulation reaction.

7.4 Contact Activation of Blood Factor XII

The consensus opinion in biomaterials surface science is that hydrophilic or anionic “surfaces” are potent activators of the intrinsic pathway of blood plasma coagulation (materials such as glass, kaolin, celite, sulfatides, dextran sulfates, pyrophosphate, urate crystal, endotoxin, ellagic acid and other substances [5-7]). In sharp contrast to this widely held opinion, this work found that FXII activation in neat buffer solution occurred with nearly equal efficiency (rate and FXIIa yield) at hydrophobic and anionic hydrophilic procoagulant surfaces. However, FXII activation in whole plasma induced by hydrophilic surfaces was much more efficient than by hydrophobic surfaces. Furthermore, FXII activation by hydrophobic surfaces was shown to be inhibited by the presence of plasma proteins unrelated to the coagulation cascade whereas no such inhibition was observed at hydrophilic surfaces. These results suggest that competitive protein adsorption mediates contact activation of FXII. Results help explain why thrombus eventually forms on all materials exposed to blood and offer a new paradigm for the interpretation of hemocompatibility.

7.5 Autohydrolysis of Blood Factor XII

Autohydrolysis of FXII ($\text{FXII} + \text{FXIIa} \rightarrow 2\text{FXIIa}$) was shown to be a significant reaction in neat buffer solution that is apparently insignificant in whole plasma. Autohydrolysis was shown to significantly affect results of a chromogenic assay for FXIIa in neat buffer solutions. A modified protocol was developed that corrects for autohydrolysis and gave results in analytical agreement with the standard plasma coagulation time assay.

7.6 Future Work

The experiment data presented in this thesis shows that (i) autoactivation of FXII depends on FXII solution concentration and procoagulant surface area but is (ii) independent of procoagulant surface energy, and (iii) is moderated by the presence of proteins unrelated to the plasma coagulation cascade. A more thorough investigation of these experimental findings is required before a comprehensive biochemical mechanism of surface activation of blood plasma coagulation can be offered to replace existing paradigms that fail to account for these new results.

Firstly, in this work, only two procoagulant types were studied, representing surfaces at the extremes of surface energy (water wettability, termed hydrophobic and hydrophilic herein). In the future work, full range of surface energy should be explored, perhaps prepared by modern techniques of surface engineering employing self-assembled monolayers (such as silanes on glass and thiols on gold). Secondly, molecular biology techniques including electrophoresis, western blot and ELISAs should be used to expand

upon the relatively simple coagulation and chromogenic assays used in this work. In particular, it will be useful to fully characterize the autoactivation of FXII at surfaces using electrophoresis to separate various protein fragments that seem to accompany the FXII \rightarrow FXIIa reaction which might play different roles in blood coagulation. Finally, the role of competitive protein adsorption to procoagulant surfaces must be quantified to fully understand how autoactivation occurs in a multi-component solution such as whole plasma. No doubt mathematical models of autoactivation of FXII coupled to mass balance equations will be of great utility in this pursuit. Ultimately, a full understanding of contact activation of blood coagulation will permit engineering biomaterials with improved hemocompatibility for a wide variety of cardiovascular devices.

7.7 References

1. Vogler, E.A., Nadeau, J.G., Graper, J.C., Contact Activation of the Plasma Coagulation Cascade. 3. Biophysical Aspects of Thrombin Binding Anticoagulants. *J. Biomed. Mat. Res.*, 1997. 40(1): p. 92-103.
2. Vogler, E.A., et al., Contact Activation of the Plasma Coagulation Cascade.2. Protein Adsorption on Procoagulant Surfaces. *J. Biomed. Mat. Res.*, 1995. 29: p. 1017-1028.
3. Vogler, E.A., Graper, J.C., Harper, G.R., Lander, L.M., Brittain, W.J., Contact Activation of the Plasma Coagulation Cascade.1. Procoagulant Surface Energy and Chemistry. *J. Biomed. Mat. Res.*, 1995. 29: p. 1005-1016.
4. Zhuo, R., et al., Procoagulant Stimulus Processing by the Intrinsic Pathway of Blood Plasma Coagulation. *Biomaterials*, 2004. in press.
5. Colman RW, S.A., Contact system: a vascular biology modulator with anticoagulant, profibrinolytic, antiadhesive, and proinflammatory attributes. *Blood*, 1997. 90(10): p. 3819-43.
6. Samuel, M., Pixley, P.A., Villanueva, M.A., Colman, R.W., Villanueva. G.B., Human Factor XII (Hageman factor) Autoactivation By Dextran Sulfate. Circular Dichroism, Fluorescence, and Ultraviolet Difference Spectroscopic Studies. *Journal of biological chemistry*, 1992. 267(27): p. 19691-7.

7. Griffin, J.H., Surface-dependent activation of blood coagulation, in Interaction of the blood with natural and artificial surfaces, E.W. Salzman, Editor. 1981, MARCEL DEKKER, INC.: new york. p. 139-170.

VITA

EDUCATION

September 2001- Present, Ph. D. Candidate

Bioengineering, Pennsylvania State University, PA (Expected to graduate Fall 2006).

Advisor: Dr. Erwin A. Vogler.

September 1997- September 2001, B.S.

Biomedical Engineering, Shanghai Jiao Tong University, P.R.China

EXPERIENCE

Research Projects

- Biomaterials Surface Science Lab, Penn State University (Supervised by Dr. Erwin A. Vogler) Supported by Johnson & Johnson and the National Institute of Health

* **Autoactivation of Blood Factor FXII by Contact with Biomaterials** (July 2003 - Present)

* **Dose-response Relationship Connecting Biomaterial Surface Chemistry to Blood Coagulation** (July 2002 –July 2003)

* **Hemocompatibility of Silicon Oxycarbide Glasses** (July 2003 –July 2004)

Teaching Experience

Graduate Teaching Assistant (September 2002 – September 2003)

- The Huck Life Science Institute, Penn State University

PUBLICATIONS

- **Zhuo R**, Miller R, Bussard KM, Siedlecki CA, Vogler EA. Procoagulant Stimulus Processing by the Intrinsic Pathway of Blood Plasma Coagulation. *Biomaterials* 2005;26:2965-2973.
- **Zhuo R**, Colombo P, Pantano C, Vogler EA. Silicon Oxycarbide Glasses for blood-contact applications. *Acta Biomaterialia* 2005;1:583-589.
- **Zhuo R**, Vogler EA Contact Activation of Blood Factor XII Is Not Specific To Anionic Hydrophilic Surfaces, Accepted by *Biomaterials*.(2006)
- **Zhuo R**, Vogler EA Autoactivation of FXII on Surfaces, , In Review for *Biomaterials* (2006).
- **Zhuo R, Vogler EA** Role of Competitive Protein Adsorption in Contact Activation of Blood Factor XII, In preparation for *Biomaterials* (2006).